This work was presented at the Institute of Welding and Joining Technology

Comparison of different process variations in gas metal arc welding for wire arc additive manufacturing

Bachelor thesis

of João Francisco Wiggers

Head of institute: Univ. Prof. Dr. Ing. U. Reisgen

Supervisor: Dipl. Ing. A. Biber

Co-Supervisor: Univ. Prof. Dr. Ing. R.H.G. Silva

Aachen, im Februar 2024

RWTH Aachen University · ISF
Pontstraße 49 · 52062 Aachen · Germany
office@isf.rwth-aachen.de
www.isf.rwth-aachen.de
fon +49 (0)241-80 93870/71
fax +49 (0)241-80 92170

Abstract

Additive manufacturing is becoming more and more present in the industry due to its ability to 3D print metal parts with complex geometries that are very difficult and sometimes impossible to achieve with machining. The Gas Metal Arc Welding (GMAW) process stands out in the AM field because it combines high productivity with low operating costs. However, the heat input applied by the GMAW process is one of the biggest challenges to the AM process, affecting the mechanical properties of the manufactured part, causing cracks and distortion. Therefore, different short circuit process variations from different power sources are being tested to analyze their impact on the heat input on the AM process. These processes are used to produce a weld bead with defined geometry. Comparison is made with macrographs to observe penetration and the theoretical heat input is calculated. Three processes between those tested are used to develop an additive manufacturing of a wall assisted by a thermal camera. The temperature distribution during the AM process is presented and the mechanical characteristics of the walls are compared with geometry, hardness test, macro and micrographs. The results showed that the improvement of the standard short circuit by power control and retractable wire feed technique could lead to a reduction of 20% of the heat input and up to 50% of the penetration reduction. The comparison of the processes applied to an AM process showed differences in the geometry produced, with the retractable wire feed processes producing a thinner and continuous wall. The hot process could not maintain the controlled wall thickness and produced a deformed body. Hardness tests and micrographs showed no significant differences between the processes tested.

Key words: Additive manufacturing, 3D printing, GMAW, heat input, short circuit process variations, power sources, thermal camera, hardness test, macro and micrographs.

Index

List of Figures

List of Tables

Symbols and abbreviations

AM	Additive Manufacture
GMAW	Gas Metal Arc Welding
WAAM	Wire Arc Additive Manufacturing
GTAW	Gas Tungsten Arc Welding
PAW	Plasma Arc Welding
MIG/MAG	Metal Inert Gas / Metal Active Gas
STT	Surface Tention Transfer
CMT	Cold Metal Transfer
LAM	Laser Additive Manufacture
EBM	Eletron Beam Manufacture
WFS	Wire feed speed
TS	Travel speed
BW	Bead width
BH	Bead height
P_{av}	Average power
I_{av}	Average current
V_{av}	Average voltage
H_{net}	Liquid heat input
A1	Area 1
A2	Area 2
TAZ	Thermal Affected Zone

1 Introduction

Additive manufacturing (AM) has grown in the manufacturing industry in recent years due to its ability to produce complex metal parts that cannot be machined. Defined as "the process of combining bulk raw materials to create parts from 3D model data, usually layer by layer, as opposed to subtractive manufacturing and forming methods" [1], AM parts can be produced by several different processes. Laser powder bed fusion and electron beam bed fusion are options for developing AM parts that are highly accurate, but have low productivity and high cost. Gas Metal Arc Welding (GMAW) stands out in terms of AM production using short-circuit processes, characterized by high productivity due to its high deposition capability and also low cost. However, these processes, which belong to the category of wire arc additive manufature (WAAM), are known to apply a high heat input in the part during the AM process, which can induce residual stresses and part distortion [2]. Therefore, the research of methods to improve the GMAW short-circuit process regarding its high heat input was developed by the welding companies and led to the creation of different mechanism welding machine controls. These different welding methods have different approaches in handling the heat input, which generates different impacts in the body manufactured.

The short circuit is a good option to use GMAW with low heat input application. [3, 4] The short-circuit process operates in the lower power ranges of GMAW, giving this process the advantage of low heat input compared to other GMAW processes. The high power used for droplet detachment and metal transfer occurs only during short circuit times, keeping the average current low [5].

[6] Tested four different power sources and showed how they exhibited different behaviors to develop the same task. Using the same base parameters, there were large variations in weld bead width and height, as well as current peak measurements. It was observed that for the same result, there was a 17% variation in heat input between all the power sources.

[7] presented the influence of wire length on the heat input in a welding process. They showed that the longer the wire length, the less heat is transferred to the workpiece and the more is lost in the Joule effect, heating the wire itself. This affected droplet formation, showing that the shorter the wire length, the smaller the droplet volume and the wetter the weld bead. In fact, the longer the wire length, the larger the droplets, which leads to weld bead deformation and arc unstability.

Since the heat input through the layers is affected by the cooling time, [8] tested four different cooling pauses in the AM procedure: 2, 4, 8 minutes and alternating the time between 2 and 5 minutes in each layer. They showed that the temperature of the wall stabilizes after the first minute, with 32.8% of difference between the temperature after 2 and 8 minutes. However, the mean temperature of the processes shows a big difference as well as the wall quality, with less rudosity the more is the colling pause. Therefore, the cooling time is defined as the balance between quality and efficiency.

Searching for the most influential parameter in the weld bead geometry, [9] developed several tests in which they varied wire feed speed, welding travel speed and voltage. In their results, they showed that wire feed speed is the parameter that has the greatest influence on the width, followed by voltage and welding speed. For the height of the weld bead, wire feed speed was also the most influential parameter, followed by welding speed and voltage.

[10] showed that the parameter used in the AM process does not affect the microstructure of the material, although the thermal curve does. It was indicated the presence of three different microstructures divided in the bottom, middle and top of the wall built. This was also observated by [11], which indicated that the shielding gas flow rate was not relevant to the weld bead geometry, but was relevant to the heat input. [11] classified CO_2 as one of the causes of structural defects in the wall and indicated the use of mixed gases as the best options for developing the AM process.

Apart from the presence of different power source suppliers in the market, each one also has different short circuit methods with its peculiarity. Therefore, the present study focuses on analyzing the differences in the short circuit processes and their impact in the additive manufacturing process. The weld bead geometry is pre-defined to observe the performance of the processes when developing the same task. The theoretical heat input is calculated and the variation of penetration is also observed. The processes with the best performance are compared in an AM image of a wall, as well as a process that did not perform well in the metrics. The temperature distribution in the wall is observed and the results are compared with the thermal behavior, hardness and micrographs of each wall.

2 State of art

2.1 Arc welding

Welding is a manufacturing process of joining parts by heat, pressure or both, where the final result is a one-piece part whose structure is similar to the materials used. Therefore, welding is not only related with metals, but related to any material that fill the characteristics of the process described. [12].

Arc welding is one of the most common processes to develop an welding procedure melting materials, mainly metals, focused on melting parts in a way that the molten material of both join and form a one molten pool that, after stop the input of heat, solidify them together in one body, being the fusion made by an electric arc [13].

This arc is formed between two electrodes, being one of them the workpiece to be melted by the passage of current from one to the other. Since both have different polarities, one cathodic and the other anodic, the air between the electrodes is ionized and charged ions pass from one electrode to the other by the potential divergence, forming the electric arc. This transfer of ions occurs from anode to cathode and generates high heat, which in welding processes goes up to 3590°C, causing the melting of the material [13].

Different arc welding processes use different polarities. Since the electrode that has positive polarity is highly melted in the electric arc action, the polarity of the electrode and workpiece can be switched according to the process used. Processes that use negative polarity (anodic) on the main electrode are called non-consumable electrode process, this due to the electrode with negative polarity is not the target of the ions and not melted in the welding process. However, due to the high heat generated by the arc, the electrode is usually also affected and needs to be cleaned and sharpened from time to time. Depending on the power of the process, the heat input will increase and the frequency of electrode maintenance procedure will also increase [13].

On the other hand, processes that use positive polarity (cathodic) on the main electrode are called consumable electrode processes. They use the electrode as an additional material that can melt itself and increase the melt pool volume, in this case by constantly renewing the electrode. In the same way as the non-consumable electrode processes, the electrode with negative polarity, now inserted in the workpiece, suffers melting by the power imposed, having its melt pool added for the molten metal from the main electrode [13].

Within the field of arc welding, there are four main processes: Gas Metal Arc Welding (GMAW) and Stick Welding, both of which use cathodic electrodes, and Gas Tungsten Arc Welding (GTAW) and Plasma Arc Welding (PAW), which use anodic electrodes. Each of these processes has its own qualities and, from these differences, applied to its respective fields of work [13].

The characteristic of being a consumable electrode process with feed allows GMAW to be used in many applications. It can be used in manual and automated form, with a low amount of preparation and maintenance compared to the others. It is a robust process due to the metal addition coming directly from the wire. Therefore, GMAW is the most common in industrial applications. On the other hand, non-consumable electrode processes such as GTAW and Plasma are more sensible and commonly used in delicate applications due to their smaller weld pool size, which reduces the heat input into the workpiece. However, this also reduces their ability to cover defects. In addition, these more sensitive processes are not able to reach the same speed range, as the normal travel speed for GTAW is around 100 mm/min, while the average travel speed for GMAW is up to 200 mm/min [12, 13].

2.2 Gas Metal Arc Welding

Gas Metal Arc Welding (GMAW), also and popularly called Metal Inert Gas/Metal Active Gas (MIG/MAG), is widely used in industry due to its ability to achieve high speed, flawless welds and to be easily automated, thus increasing productivity [14].

A scheme of the GMAW process can be seen in Figure 1. The working principle of GMAW is based on its electrode, which is metal wire. The wire is pulled from a reel constantly by motorized rollers, passing for the contact tip and the nozzle. The wire and the workpiece are melted by the electric arc, forming with materials together the melt pool.

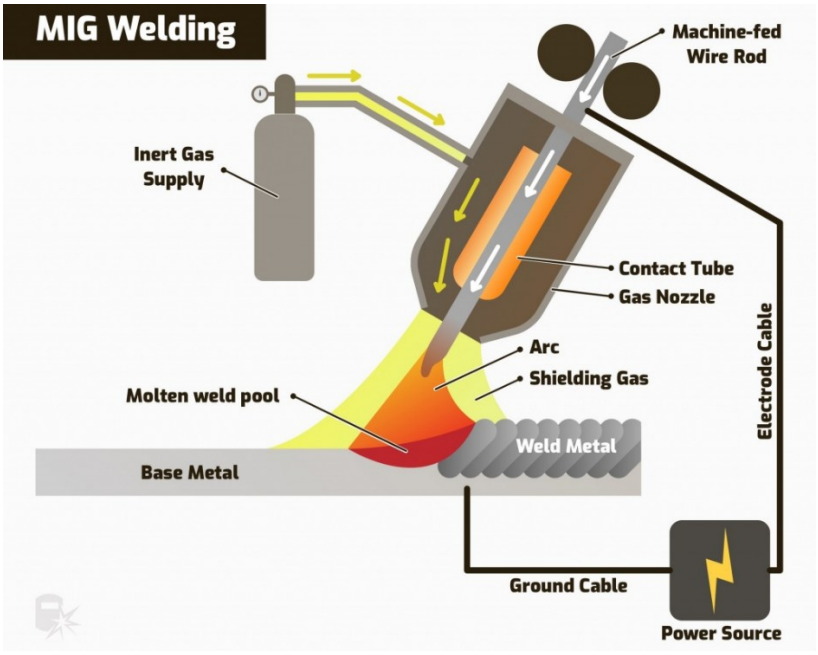

Figure 1. GMAW process diagram. [15]

GMAW uses a continuous electrode. The amount of metal volume in the molten pool is directly related to the wire feed speed, since the greater the wire feed speed, the greater the deposition rate. The GMAW process voltage is controlled, the magnitude of which is generated by the potential divergence, i.e. the distance between the wire and the workpiece. The current of the process increases with the increase of the wire feeding speed, this way keeping the same voltage and increasing the power of the process.

Since contact between molten metal and oxygen causes oxidation due to the quaternary bonds between oxygen and metal atoms, this contact is avoided by injecting shielding gas into the process. The shielding gas acts as a curtain around the arc, preventing oxygen from contacting any part of the process, be it the electrode or the melt pool. The elements of shielding gas composition and flow rate have a significant effect on arc characteristics and stability, metal transfer mode, weld penetration, weld bead profile and welding speed. Different gases elements have its ionization potential and thermal conductivity. For this protection, the GMAW process has a shielding gas cylinder which is connected to the shielding gas diffuser inside the torch. It is responsible for distributing the gas around the nozzle [3].

The GMAW process has the advantage of controlling the relationship between deposition rate and welding speed, so it can be used for high-speed welding or for more deposition at the same point, called heavy duty MAG welding, focused in the high-performance range [16]. The arc types and the ranges of work that is reachable can be seem in Figure 2.

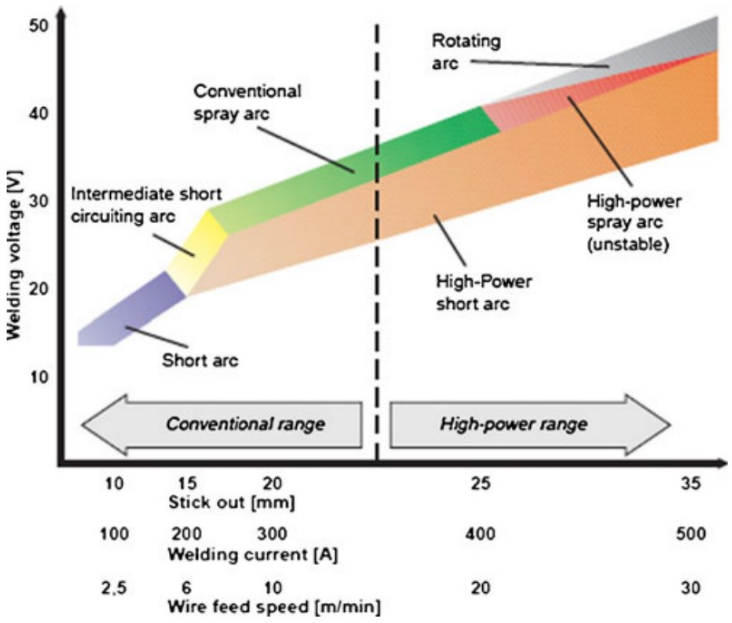

Figure 2. Arc types and their working ranges, solid wire (d = 1.2 mm) shielding gas: argon-rich mixtures. [16]

2.2.1 Short circuit

The working mechanism of short circuit process is showed in Figure 3.

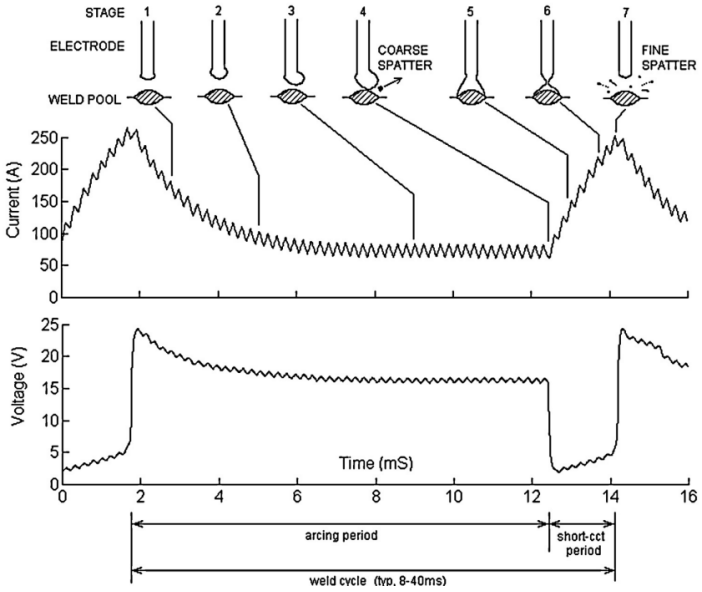

Figure 3. Short circuit process. [3]

It operates in the low power ranges of GMAW, where the wire is constantly fed at a higher speed than the heat input into the wire can melt it [3, 17]. As a result, the distance between the wire and the molten pool decreases (1-4), which causes the wire to dip into the molten metal (5), creating a short circuit. At this moment, the power supply increases, which also increases

the magnetic force in the electrode tip. This causes a squeezing force around the tip, called the pinch effect, which induces the scouring of the molten tip of the electrode (6). The pinch effect is illustrated in Figure 4.

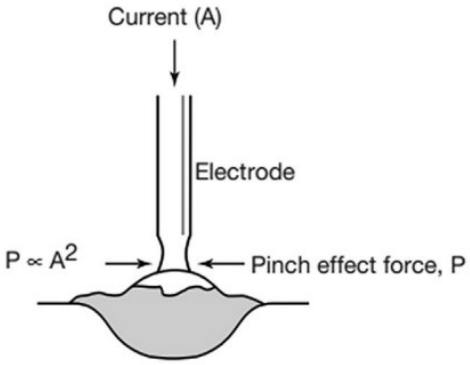

Figure 4. Pinch effect. [17]

By surface tension, this scouring separates the drop formed by pinch from the wire (7), interrupting the short circuit and reopening the arc, restarting the process. The pinch effect is proportional to the square of the current used in the scouring. The short-circuit process is able to reach between 20 to 200 times per second transfer metal into the puddle [3], typically working in frequencies around 100 to 150 Hz, [17].

The use of short circuit method has the benefit of have a low heat input compare to other GMAW processes [3, 17]. High currents are required to generate the pinch effect, typically between 200 to 400 A [5]. However, the arc phase has a low current and is usually longer than the short circuit process. This results in a low average current, which means less heat input and a rapidly solidifying weld pool. Therefore, the short circuit process is suitable for welding thin sheet steels due to the low tension application by dilation and in all positions. However, short-circuit is limited in quality due to its process instability and high spatter levels [5]. This can be controlled by the choice of shielding gas, usually CO_2 or a mixture of gases with less than 25% argon, and electronic techniques [3].

Usually, the power sources on the market have the same number of parameters that can be varied, which changes the behavior of the arc and therefore the molten pool. As a result, the characteristics of the weld bead are also changed. The parameters that can be varied are: wire feed speed, voltage, arc dynamics and shielding gas flow. Some power sources offer more options to vary their processes, usually presented in processes with different procedures, such as pulse and alternating currents, where frequency and amplitude also become parameters. Also, there are a number of short-circuit process variants available on the market from various

manufacturers. These are divided into standard and digitally controlled variations. The digitally controlled versions can be further subdivided into retractable wire feed and electrically controlled versions. The process variants relevant to this work are described in more detail below.

- **EMW ColdArc**

Published by EWM Hightec Welding GmbH [18], it showed in his article the differences between the conventional short circuit method and the patented from EWM, CordArc process, that can be seen in Figure 5.

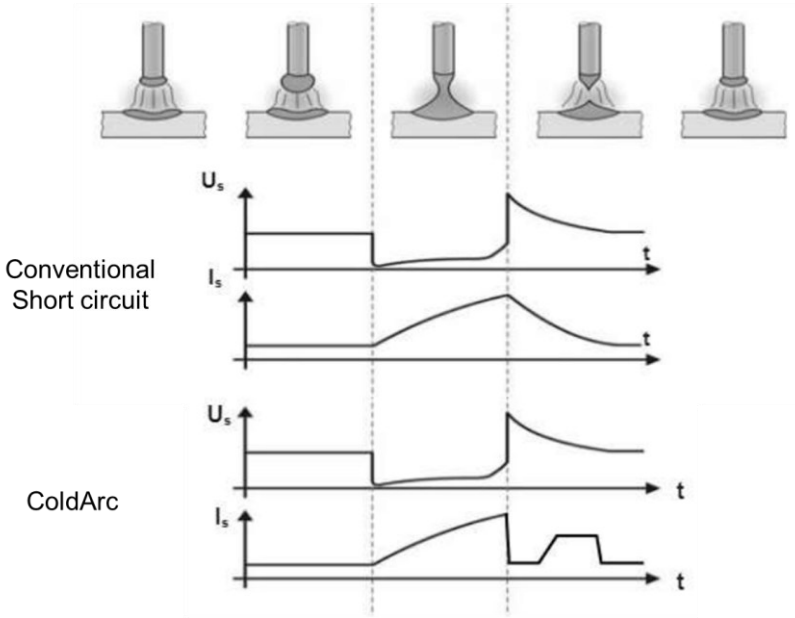

Figure 5. Comparation between conventional short circuit and ColdArc process. [18]

The aim of the process variations is to achieve a low energy process by controlling the current, thus achieving better control of the process phases. The electrical power during the re-ignition process, immediately after the drop has been scoured, is critical to manage the heat input of the process and the spattering. Spattering is caused by the position of the wire at the moment of re-ignition, where the drop is released and the instability of the arc in the opening disturbs the molten metal [19]. By these short circuit characteristics, the difference between the standard short circuit behavior and the ColdArc processes is the current control. The ColdArc process works by controlling the power in the re-ignition of the arc, giving just the power necessary to open it. After the drop, the current is immediately drawn and the re-ignition power is reduced. This allows the arc to stabilize and re-anchor in the melt pool. The power is increased again,

known as the melting pulse, to separate the molten pool from the wire and form a new molten tip [20].

- **Lincoln Eletric Surface tension Transfer (STT)**

Surface Tension Transfer, or STT, was developed by Lincoln Electric for pipe welding with a focus on developing a low heat input process to replace the standard short circuit. The waveform of the process is shown in the Figure 6.

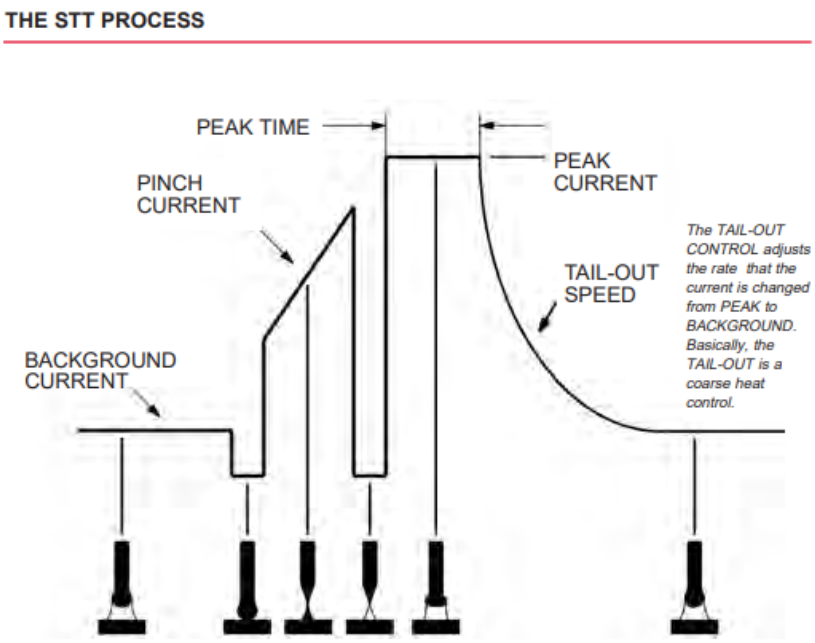

Figure 6. Surface Tension Transfer diagram [21].

The main difference in this process is the waveform control for drop separation, where the drop is formed by the arc and approaches the melt pool. When the drop and the melt pool touch, the power source releases a fast power peak to create the scouring of the drop and consequently its detachment. The power is released just before the drop-wire separation. The reopening of the arc occurs immediately after the separation and generates another drop.

- **Lorch SpeedCold**

SpeedCold, short circuit with the aim of low heat input created by Lorch, focus on developing a short circuit with a synergetic waveform, controlling the power of the power source to make the detachment process of the drop and re-opening of the arc less aggressive to the substrate, with an optimized spatter control. This process has the characteristic of limit the wire diameter in 1 mm. Its waveform is shown in Figure 7.

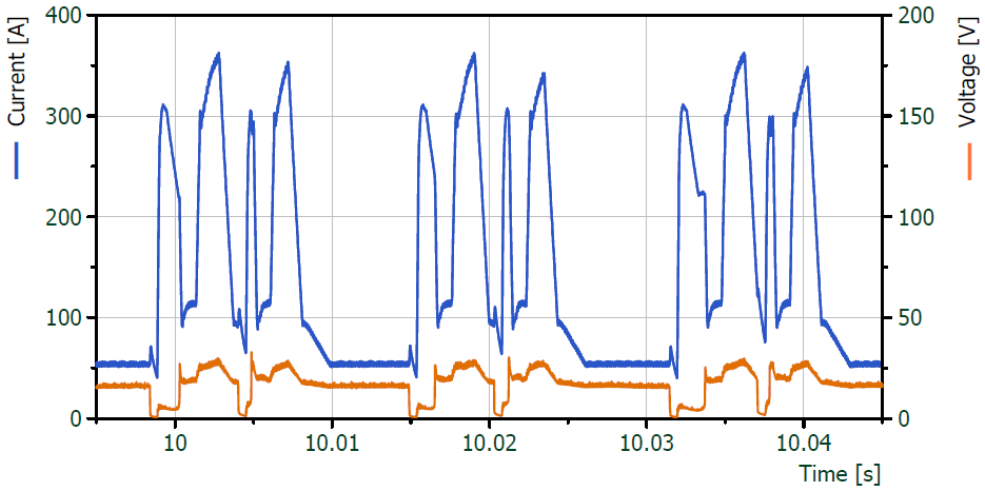

Figure 7. SpeedCold process diagram.

The figure shows four different power peaks per sequence. This behavior is due to the wire speed used, since the 1 mm wire limitation requires higher speeds to develop certain tasks.

- **Fronius Cold Metal Transfer (CMT)**

One of the most famous variants of low heat input welding is the Cold Metal Transfer (CMT), created by Fronius and patented in 2004. Fronius process, Figure 8, is based on short-circuiting and works with dynamic wire feeding, using inverters that mechanically support the method and move the wire when it is needed. Therefore, a retractable wire feed process.

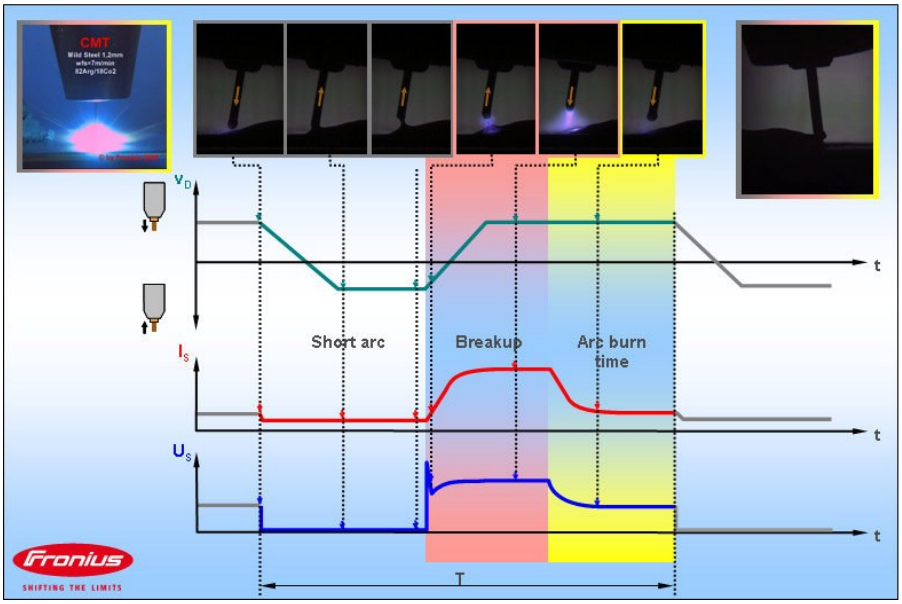

Figure 8. Cold Metal Transfer (CMT) principle of process. [22]

The CMT process has an arc phase to melt the wire tip and workpiece, feed the wire into the molten pool, and complete the short. However, instead of using a power peak to create the

drop separation, the dynamic wire feeder pulls the wire out of the molten pool. The movement causes the drop to separate from the wire tip by surface tension and inertia of the molten metal. This minimizes the power of the arc and reduces the heat input to the workpiece [20]. It can be observed that the peak current is used only for the re-opening of the arc, while the release of the drop is made in minimum current using the wire retraction.

- **OTC Synchrofeed**

OTC has a method called Synchrofeed. It uses a retractable wire feeder that pulls the wire out of the melt pool during the short-circuit phase without the need for a current peak [23], reaching until 100 Hz of retracting frequency. In the Figure 9 is showed the electrical wave characteristics from this process.

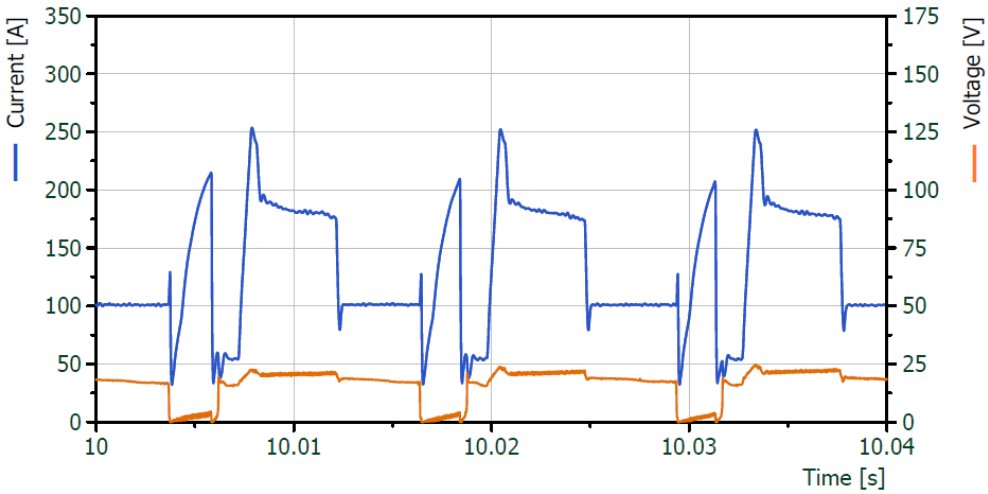

Figure 9. Synchrofeed process diagram.

This process uses a power peak to complete the drop separation associated with the wire retraction. The power supply decreases after the drop detachment and creates a new power peak to re-open the arc in the sequence. This process has three different power phases in the arc phase, that is the power peak to re-open the arc and melt the wire, a high-power phase to continue the drop wire melting and a low power phase to approach the wire to the melt pool with the wire push.

2.3 Additive manufacturing

AM is officially defined by as „additive manufacturing is a process of joining bulk raw materials to make parts from 3D model data, usually layer upon layer, as opposed to subtractive manufacturing and formative methodologies.“ [1]. Divided in seven groups, AM parts can be produced by binder jetting (BJT), directed energy deposition (DED), material extrusion (MEX), material jetting (MJT), powder bed fusion (PBF), sheet lamination (SHL) and vat

photopolymerization (VPP) [24]. The one of interest in this thesis is DED, focused on thermal energy to fuse metals while they are being deposited. Can be used to make this fusion process Laser Additive Manufacturing (LAM), Electron Beam Manufacturing (EBM) and electric arc, divided into Gas Metal Arc Welding (GMAW), Gas Tungsten Arc Welding (GTAW) and Plasma Arc Welding (PAW).

LAM and EBM are known for their precision and low heat input. While LAM can weld non-metallic materials in the additive manufacturing process, such as polymers and ceramics, EBM is preferred for welding more reactive materials, such as titanium [25]. GTAW, on the other hand, have medium to high productivity, low cost and friendly operation, being the best in terms of mechanical properties generated. GMAW can achieve higher productivity also having low cost and easy operation. However, the problem of excessive heat is one of the major limitations of GMAW processes, which affects the mechanical properties, process stability and component accuracy of the part produced by WAAM [25]. This problem presented in GMAW is investigated.

GMAW follows the same operating principle when used in additive manufacturing. The wire and workpiece are melted and form a melt pool. The GMAW process as applied to AM is illustrated in Figure 10.

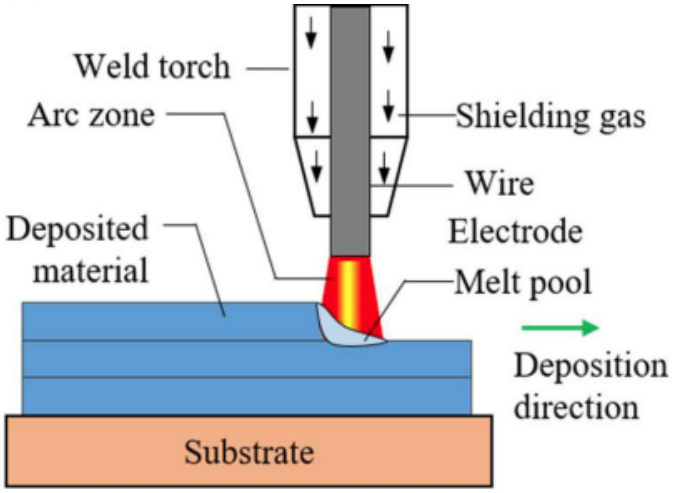

Figure 10. GMAW applicated to additive manufacturing [26].

When GMAW is used for additive manufacturing, this process has its goals defined as: high deposition rate for layer formation and low power arc range to avoid over-melting the layers already produced. Minimizing the heat input is the last critical for this process, since it generates stress in the welded part produced and deforms its body.

Since there are several options of power supplies on the market, each one with different parameters processing and control, the AM process can be affected by these variations. To

study and show the results variations between different power sources, [6] compare four power sources and apply them to pulse spray welding. This is a welding method that follows the pinch effect principle of short circuit, releasing the drop by a high peak current, however, the wire does not touch the melt pool during the process, although the drops are detached from the wire in the air and falls in free fly to reach the melt pool. This process of free-flying drops in the melt pool is called spray. In their work, welding between 12.5 and 64 cm/min of speed, with ER70S-6 steel wire and mixed shielding gas of 90% Argon and 10% CO_2, [6] showed that for the same base parameters, other parameters suffer big variations between power supplies. In [6] can be seen the current variation of these four processes, for the same wire feed speed, travel speed and arc length, the current of the peak presented have a considerable range of different values, observed in the frequency of drops as well. These variations had a great impact in the weld beads, making varied bead width and height relation sizes and different penetrations. As pointed out by the authors, it was found heat input variation of 17% between the colder and hotter weld, proving that for different power sources, different results are expected.

The heat input proved to be one of the biggest challenges in AM, being the main responsible for dilatation and shrinkage in welding processes, applying visible changes in the welded shape by generating tensile residual stress [27]. Knowing that, [7] studied the influence of the distance between the contact tip and the feed wire tip, called the free wire length, on the energy input into the process. According to them, the greater the free wire length, the less current is directed to the workpiece because it is dissipated as a Joule effect heating the wire. For the printing of the walls, an EWM Alpha Q 552 Puls power source was used, wire length range between 12 and 44 mm and a cooling time procedure based on the temperature of the top layer, adding a new layer when the top one reaches 100°C, this way with all layers made under the same thermal conditions. [7] found that due to the current dissipation in the larger wire length, the frequency of deposition was smaller. This is due to the lower current in the wire tip, which has less power to generate the pinch effect. This resulted in a longer short-circuit time and larger drops as the wire melting range remained the same. In the same figure, the difference between the arc power in the wire tip can be seen, which shows that the energy in the arc increases as the wire length decreases. Due to this difference in arc and drop behavior, the walls presented different shapes, since the wetting, the relationship between bead width and drop adhesion height, of the low wire length process is greater, generating lower and wider weld beads, consequently lower walls. This behavior can benefit the AM process by requiring fewer passes to achieve the same wall height. However, as noted by [7], welding with high wire length can only be performed at low speeds, and even in these cases, the edges and the body of the weld

bead are affected, with deformation and more spatter formation, combined with an unstable arc, resulting in an inhomogeneous layer. On the other hand, welding with short wire length proved to be a very stable and robust process, with low spatter and homogeneous layers.

The lower heat input with the larger wire length was shown by the microstructural analysis, where the grains presented by the larger wire length process were considerably finer, this being caused by a shorter cooling time, caused by a colder weld bead, which results in less grain growth. Since the cooling time was not defined but the temperature, this process reached the desired temperature in less time, restarting the process and giving less time for the grains to coalesce. This behavior is very beneficial to the AM process, since it reduces the deformation and stress of the structure, avoiding defects such as cracks. However, as shown in [7] work, the change in arc and drop separation behavior imply that these defects by themselves, not caused by heat input, although caused by new instabilities.

[8] studied the heat input behavior in GMAW additive manufacturing throughout the bead layers. Welding with H08Mn2Si steel wire, they tested four different cooling times applied between the welding of 20 layers to analyze the cooling behavior and resultant welded walls, being tested cooling times of: 2, 5 and 8 minutes, with the fourth one alternating between 2 and 5 minutes per layer. According to the thermal measurement, [8], they showed that the temperature in the cooling stage acts like a curve and starts to stabilize after the first minute, being the difference between temperatures presented from 2 to 5 min of cooling of 27,6% and, from 2 to 8 min of 32,8%. However, in their work is shown the mean temperature measured throughout the rolling process, where can be seen a relevant difference between them, being the temperature in colder process, with 8 min of cooling, and the hotter one, with 2 min of cooling, different by more them 200°C. The difference observed in the wall quality for each one is shown, where can be seen that as much time is given by the cooling phase, better is the wall quality, presenting less rugosity in the wall surface. Therefore, as indicated by [8], the cooling time of the process is a balance between speed and quality, since more cooling time results in better walls, but the amount of time to be made can be four times greater. On the other hand, the difference between the wall produced in Test 2 and Test 3 was not as remarkable as the difference between Test 1 and Test 2, which means that the quality stabilizes after some time and that the increase of the cooling time after that is redundant. The alternative time of cooling taken in test 4 did not make any difference, being in the middle term between the bodies with 2 and 5 minutes of cooling, as already expected.

In the scientific field of GMAW additive manufacturing, [9] studied in their work the behavior of parameter variation and optimization of GMAW applied to AM of thin walls using wire and substrate based on 316L stainless steel with a KEMPPI PRO MIG-530 power source. The range of parameters was selected and divided into three that would be varied: wire feed speed (WFS), travel speed (TS) and voltage. After the welding tests, the relationship between these three parameters and their influence on bead width (BW) and bead height (BH) were equated and plotted, where it can be observed as the biggest contributor to the bead width variation is the WFS, followed by voltage and TS [9]. In the same way, WFS, TS and voltage were defined as the main responsible for the variation of bead height on experimental tests, successively. [9] shows the variation of BW and BH according to a Pareto-based variation of WFS, TS and voltage for 50 different parameter combinations, showing an almost linear behavior in the relationship of bead size increase. This growth occurs as WFS and voltage increase and TS decreases.

As described by [9], the optimal AM process focuses on giving the same weight in the result for BW and BH, since they are equally important for AM, depending on the goal of the process. Therefore, an AM welding process was designed using the developed size equation and focused on achieving the mean term of bead sizes, using a WFS of 5.50 m/min, TS of 14.1 cm/min and 19 V voltage, aiming to produce a 5.01 mm BW and 7.81 mm BH weld bead per pass. A 15 second cooling time was used between passes with room temperature air. The result was 5.17 mm BW (3.47% error) and 7.53 BH (3.72% error) per pass in a 130 mm long and 60 mm high wall layer, where they observed a uniform bead-on-bead deposition with very few lumps of metal at the beginning and end of the wall.

[10] discussed the difference in microstructure throughout the height of the additive manufactured wall made of ER70S-6 steel, where they found three different grain formation zones: The lower one, just above the substrate, characterized by a ferritic structure with bands of pearlite and finer grains, this leads to high value of thermal shock in the process, being the first layer the most thermally affected; the middle zone, in the middle height of the wall, characterized by equiaxed grains of ferrite; and the upper zone, in the top of the wall, characterized by a lamellar structure, typically bainitic. According to [10], the microstructure of the walls is not strongly influenced by the parameter difference, but by the cooling curve of the material. The walls were made by superimposing 15 layers of metal with the welding direction interspersed, with a cooling pause of 60 seconds between layers, using air at room temperature. The distance between the torch and the workpiece was 10 mm and the welding

speed varied between 30 and 45 cm/min in the tests. Each welded wall showed porosity in the body.

[11] had a similar result in microstructure analyses as [10]. The shape of the bodies made by AM consists of a square and a cylinder, both empty, with 15 wall layers made of ER70S-6 steel, nozzle distance of 10 mm and cooling time between layers of 15 s. They observed three grain zones throughout the walls, being the lower one composed of ferrite and pearlite fine grains, coarse grains in the middle and fine grains at the top, with ferrite and bainite. The flow rate variation was considered irrelevant for the melt pool and weld bead geometry, but it influences the amount of heat, appearance and spattering of the weld. Also, according to the authors, the use of pure CO_2 as shielding gas could be one responsible for cracking and porosity generation in the top layers, due to the increased possibility of oxidation combined with the rapid solidification that the top layers suffer. The use of mixtures with inert gases such as argon has been shown to give better results. The hardness of the walls presents a U curve, being harder in the fine grains in the lower and upper regions and softer in the middle region of the coated grains.

3 Material and experimental setup

Power sources and auxiliar items to welding development used:

- Cloos QINEO Next 452 Premium with feeder QN WD M4;
- EWM Alpha 552 with feeder drive 4X HP;
- Fronius TPS 400i, with a WF 25i Reel R wire feeder, SB 60i R splitbox;
- Lincoln S 500 CE with feeder 84 Dual power feed;
- Lorch S8 RoboMIG XT with feeder RF-06;
- OTC Welbee P502L;
- OTC FD-V8L robot OTC FD19 controller;
- ABB IRB 2600 robot IRC5 controller;
- Cloos robot xyz;
- High speed camera Prothon Fastcam SA4;
- Thermal camera Optrix Xi 400;
- ATM/QATM machine model Carot 930 microscope.

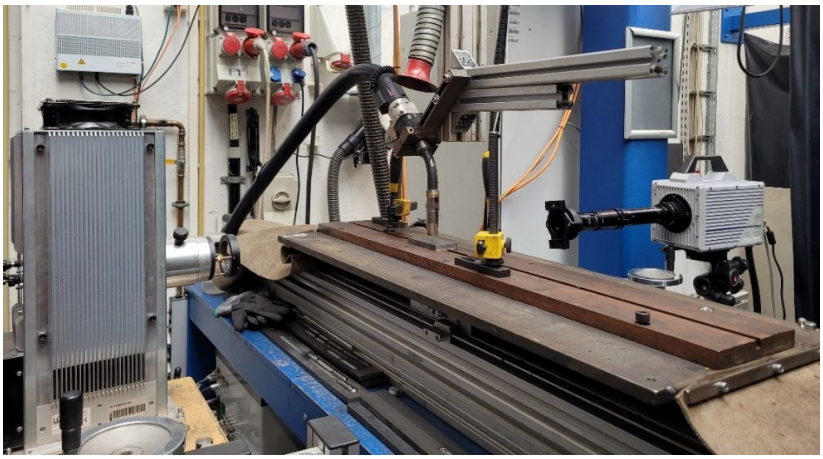

Figure 11. Welding parametrization workspace.

4 Methodology

This work was divided into two phases, as shown in the diagram in Figure 12. In the 1st phase, the focus is on comparing different short circuit variations and defining their characteristics. In the 2nd phase, three of these short circuit processes will be selected to develop an additive manufacturing process of a wall and then compare their results.

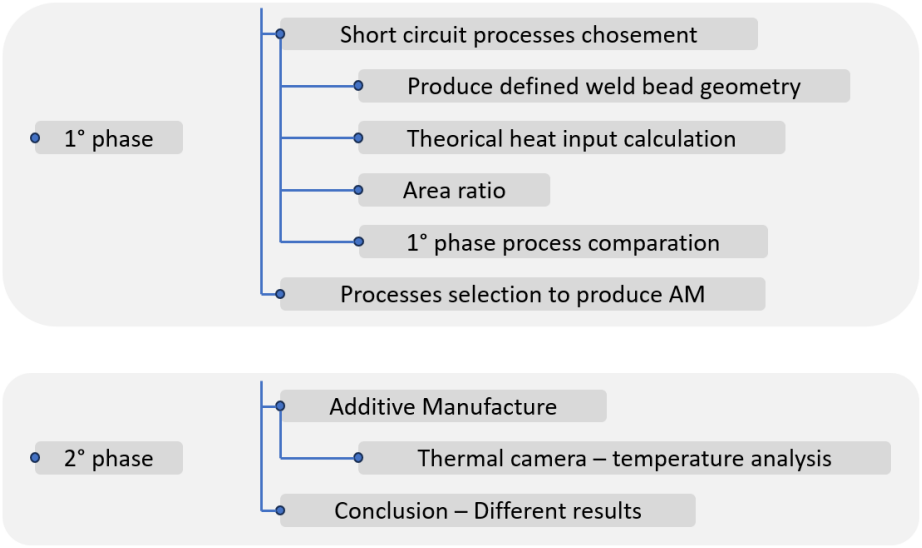

Figure 12. Representation of the two work phases.

4.1 1st phase – Welding parametrization and comparison

In the 1st phase, all available power sources will be tested for their short-circuit process variations. The goal is to produce a weld bead that represents the first layer of an AM process. The weld bead geometry sought shown in Figure 13 is achieved with all the different short circuit methods. The goal is to analyze the different behaviors of each power source in developing the same task and compare their results.

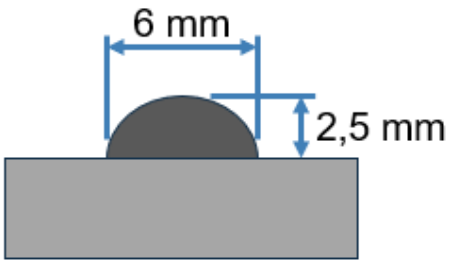

Figure 13. 1° phase weld bead geometry.

The welding is made using the parameters and materials showed in the Table 1 for all the processes tested.

Table 1. Standard parameters for all the welds made.

Welding standard parameters	
Welding speed	0,4 m/min
Stickout	10 mm
Materials	
Gas / gas flow	ISO 14175 – M12 ArC-8 15 l/min
Wire	EN ISO 14341-A G 3Si1 1,2 mm
Substrate	mild steel S235JR

Using the substrate plate of 100x20x8 mm (length x width x height), the arc is started and the table moves forward, keeping the torch still while the weld bead is created. The parameterization ends when the weld bead reaches the expected size. The parameters obtained are used to produce a high speed video to analyze the metal transfer behavior and the electrical parameters are measured. This process is repeated for the different short circuit variations of the power sources, producing a single layer weld bead for each short circuit process of each power source.

Throughout the electrical measurement, the theoretical heat input is calculated using the average power, with is the most accurate way to calculate when related to a current variation process [28]. The equation (1) is used to calculate the average power of the process, represented by P_{av}, using average current and voltage, I_{av} and V_{av} respectively. The liquid heat input is calculated by the equation (2) and represented by H_{net}, based on power, welding travel speed of TS = 6,667 mm/s, and a correction of process efficiency, approximate in the literature

by η = 0,8 for short circuit processes [29], considering arc power losses by radiation, convection and conduction to the environment.

$$P_{av} = I_{av} * V_{av} \quad (1)$$

$$H_{net} = \frac{P_{av} * \eta}{TS} \quad (2)$$

The area ratio comparison is made with the weld beads previously produced. Since the mechanism of each process is different, different results are expected [6]. As shown in the Figure 14, The weld bead has been divided into two areas. The first, A1, refers to the area of filler metal measured above the line of the substrate. The second, A2, is the penetration area or the area where the substrate has been melted, measured below the line of the substrate.

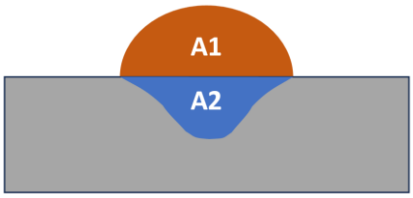

Figure 14. Definition of additive material area (A1) and penetration area (A2).

The area ratio is defined by the division between the penetration area and the added material area, according to the equation (3). This ratio compares the processes in which one is able to produce the same weld bead using the smaller penetration, given the imposed metric.

$$Area\ ratio = {}^{A_2}/_{A_1} \quad (3)$$

With the theoretical heat input and area ratio numbers, both are multiplied with each other and the result is multiplied by 100. The smaller the two numbers, the smaller the result of the multiplication. This is done to split the results and make it easier to observe which process is performing better in the metrics.

All the processes are compared in terms of their characteristics and performance in developing the weld bead. The final step of the 1st phase is to select three processes among all those tested to continue with the 2nd phase.

4.2 2nd phase – Additive manufacture

The 2nd phase consists of creating a wall by AM. The same parameters found in the 1st phase parameterization are recreated, but now used to create a wall as shown in Figure 15.

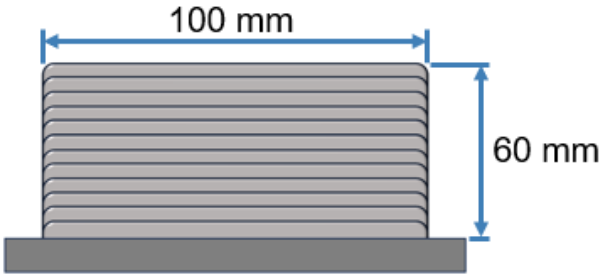

Figure 15. Additive manufactured wall scheme.

The AM process use the materials and parameters showed in Table 1. Each layer is 100 mm long and has a 60 second pause between layers to cool. The layers are made in opposite directions, overlapping in each layer. The process continues until the wall reaches a height of 60 mm.

All AM processes were accompanied by a thermal camera to analyze the heat distribution, the peak of each process and the temperature decreasement over time in the walls made. The camera was positioned perpendicular to the torch path to observe the wall building from the side. The emissivity of the metal used was 0.997 and the frame rate of the measurement was 1 Hz. With the video generated, four areas were set to analyze the temperature for each wall, Figure 16.

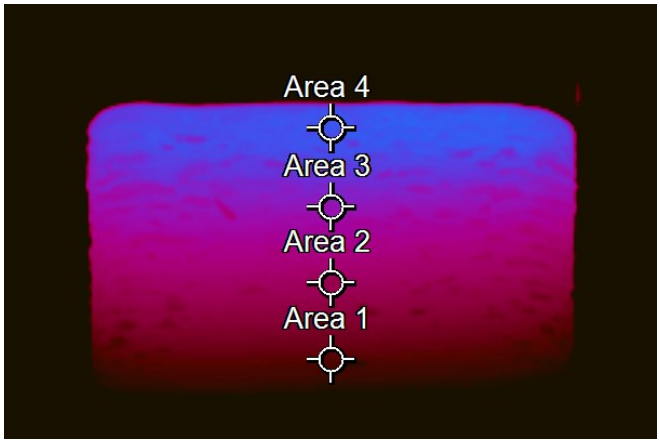

Figure 16. Distribution of thermal measurement points on the additive manufactured wall.

The first area is positioned at the bottom of the wall, the fourth at the top, and the second and third areas are positioned in the center of the body, with all areas equally spaced and ordered

in the direction of wall growth. The temperature measured in the areas are compared to indicate the difference between the three processes developing the same procedure.

To investigate the influence of process variations on the micrograph properties, cross sections and hardness measurements are made. The position of the micrographs and the course of the hardness measurements are shown in Figure 17.

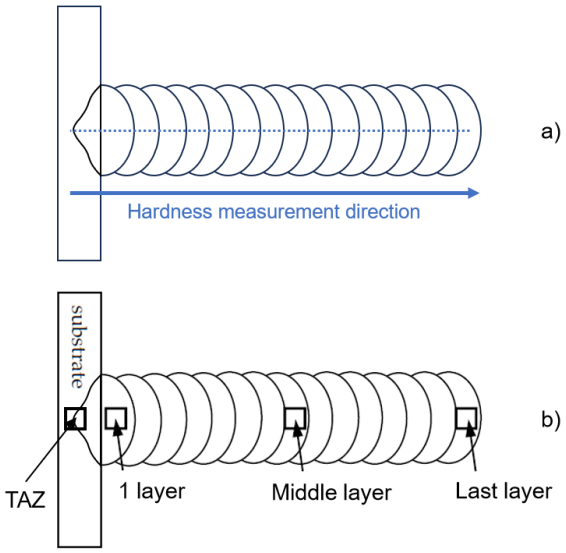

Figure 17. Scheme of: a) Hardness measurement; b) Micrographs areas.

The hardness was measured longitudinally in the wall body, Figure 17 a), from the bottom to the top of the sample. There were 125 measurement points, each 0.5 mm apart, with the last point calibrated to be 1 mm from the edge of the last layer.

Each layer of the wall experiences a different thermal behavior and also time under the influence of heat. Therefore, the microstructure of the material is analyzed to observe the effect of this in the material characteristics. The micrographs were made with x500 of approximation from four different areas, being them: the division between thermal affected zone and melted area, the first layer, the middle layer and the last layer, Figure 17 b). This process was done for the three walls and they are compared.

5 Results

5.1 Preliminary tests - Metal transfer characterization based on parameters variation

To identify the differences that the parameters variation cause in the electric wave, drop detachment and weld bead, a section of tests was made. It was varied four different parameters around a model weld using the standard GMAW short circuit as welding method. The Table 2 shows the parameters and its variation throughout the nine welds made.

Table 2. Parameters variation on standard GMAW short circuit

Variation	Weld n°	Travel speed (m/min)	Wire feeding speed (m/min)	Voltage correction factor	Arc dynamic factor
	1 (model)	0,4	4	0	0
Wire feeding speed	2	0,4	2	0	0
	3	0,4	10	0	0
Voltage	4	0,4	4	-3	0
	5	0,4	4	+3	0
Arc dynamic	6	0,4	4	0	-20
	7	0,4	4	0	+20

The flow rate of the shielding gas does not affect the geometry of the weld bead [11], which is one of the reasons for this observation. Therefore, the shielding gas flow rate was not considered in this analysis and a flow rate of 15 l/min was used in all tests.

The model weld made using the power source EWM WPQR EN 1090 is showed in the Figure 18. The weld was recorded with high speed camera and its electrical wave was also measured.

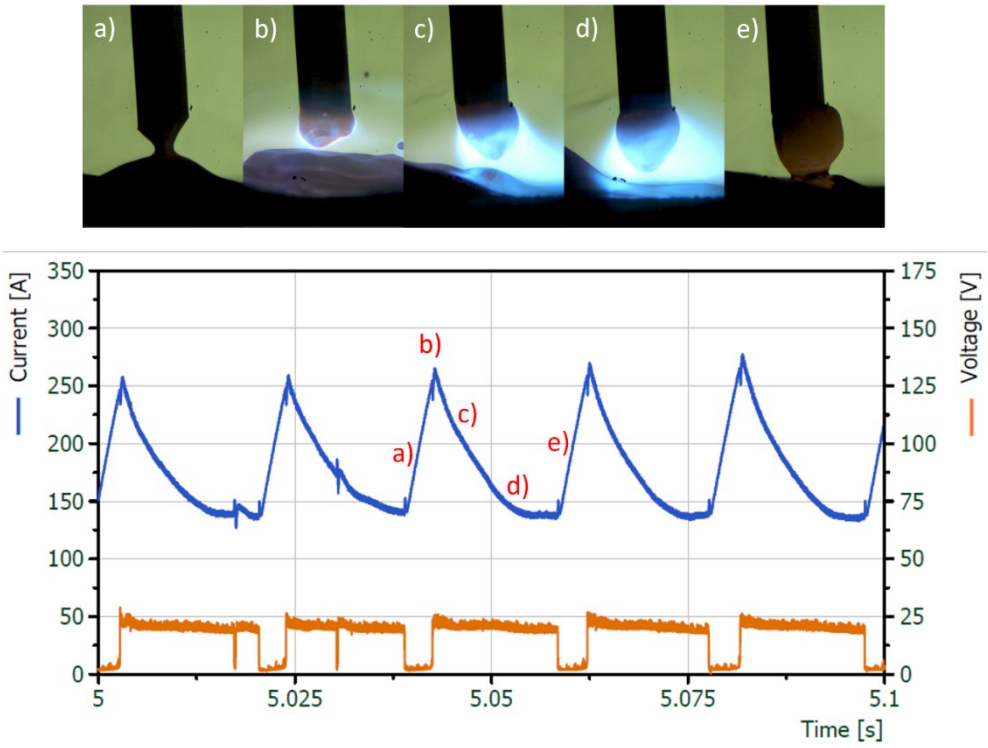

Figure 18. Preliminary welding test n° 1: standard parameter.

The second test consisted in reduce the wire feed speed only, the result is showed in the Figure 19.

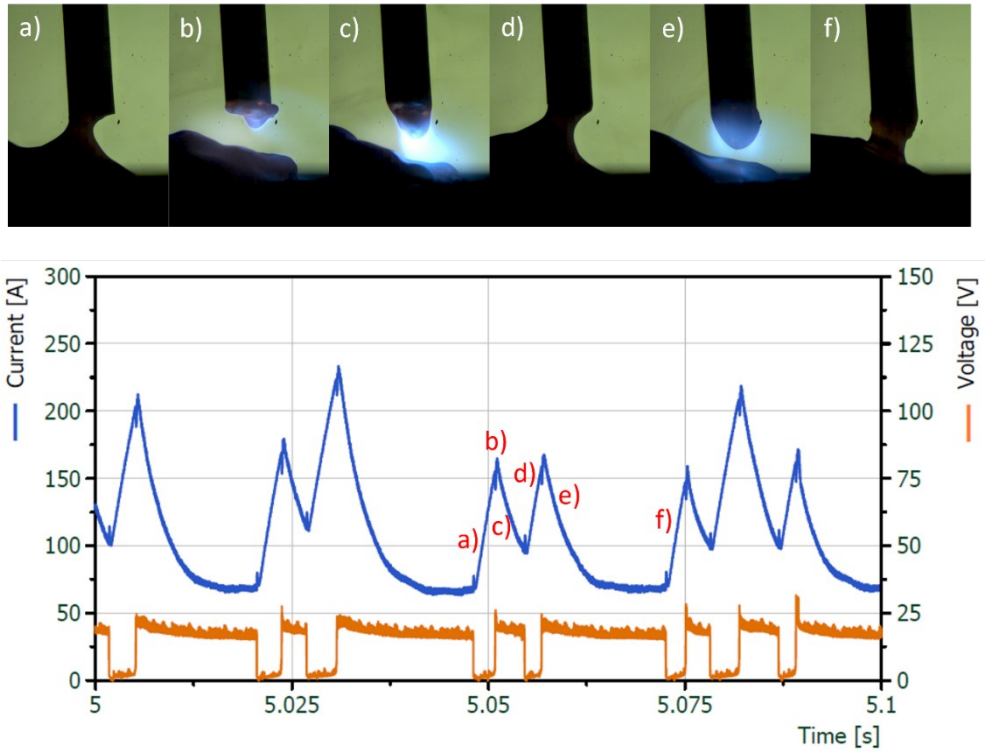

Figure 19. Preliminary welding test n° 2: wire feed speed decreasement.

It can be seen that the drop volume decreased significantly from weld 1 to weld 2, Figure 18 d) and Figure 19 e). The frequency of detachment also acquired a characteristic behavior, where two drops were constantly detached one after the other, Figure 19 b) and d), followed for a longer drop grown phase, Figure 19 e). The proximity between wire and molten pool in this process is very small due to the arc power, which generates an easy contact between them and leads to sequential drop separation. The result of this process is a narrow and poorly penetrated weld bead. The low power melts a small volume of the substrate and concentrates the molten wire into a round weld bead.

The third test focus on the opposite, increasing the wire feed speed to a very high level. The result can be seen in the Figure 20. The effect of a high wire feed rate is a high power consumption to melt the wire. In this power range, the wire is melted at such a rate that there is no drop formation and no short-circuiting, only a continuous flow of molten metal that behaves like a waterfall. The penetration of the process at this power level is extremely high and has a very wet weld bead.

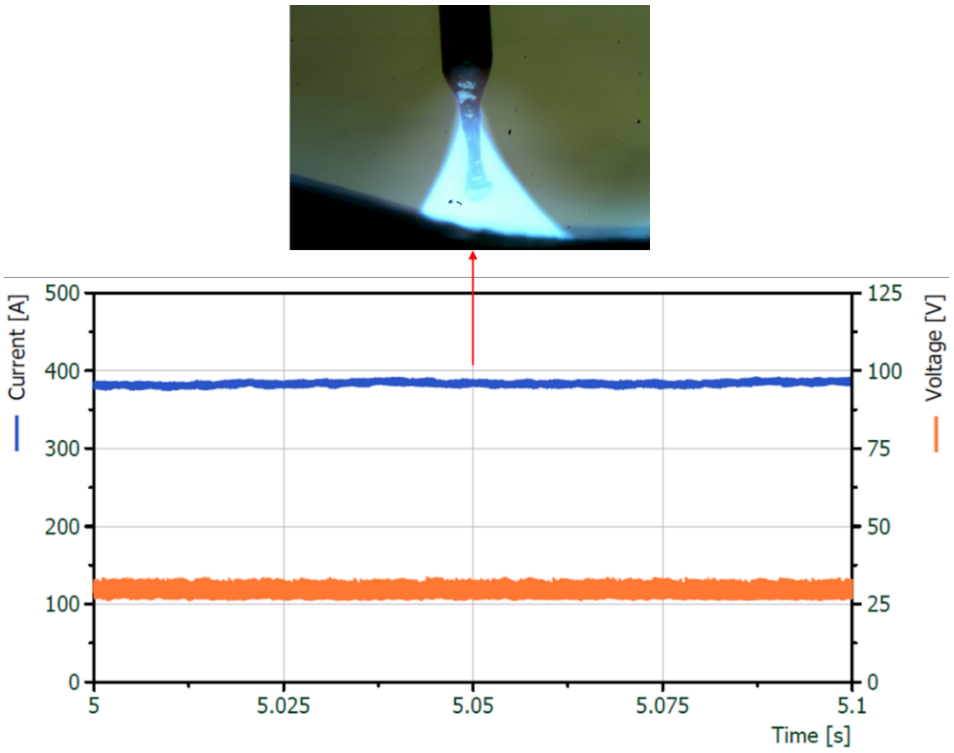

Figure 20. Preliminary welding test n° 3: wire feed speed increasement.

The fourth test consists in reduce only the voltage of the process in 3 volts. The result of this reduction is showed in the Figure 21.

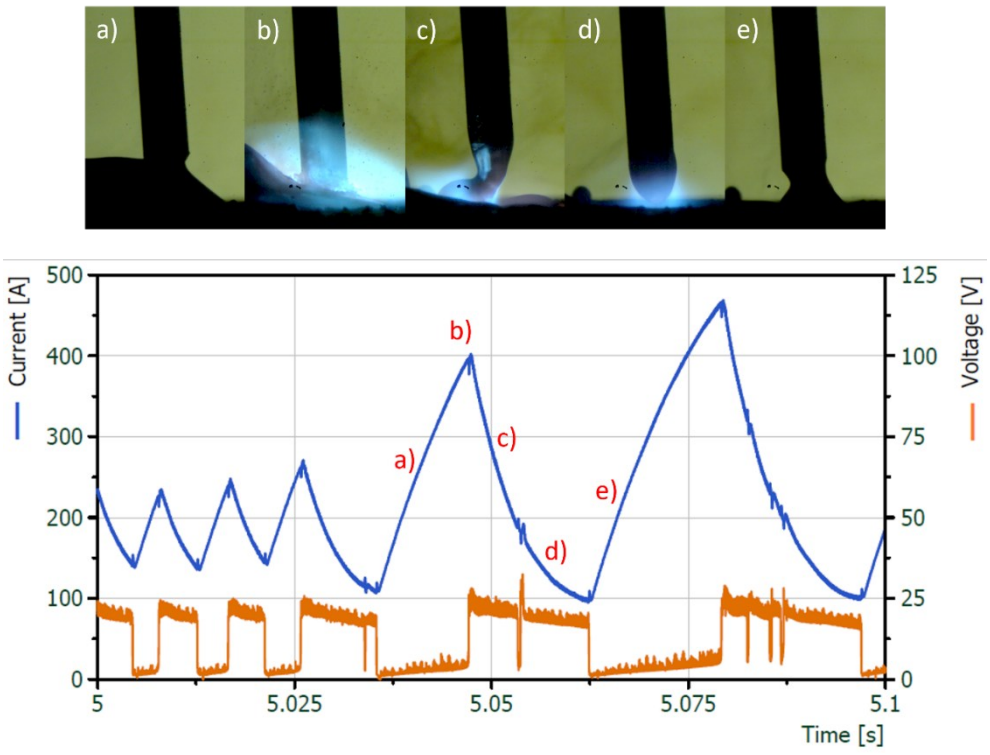

Figure 21. Preliminary welding test n° 4: voltage decreasement.

The amount of voltage set in the process directly affects the power applied to the weld by the power source. Reducing it implies in a shorter arc due to the melting rate of the wire, which one turns smaller. The solid wire approaches more for the melt pool and start to detach with more frequency, as can be seen in Figure 21 in the interval of 5 to 5,03 s. In this phase, the wire is very close to the melt pool, causing a sequence of drop and melt pool touches as it continues to approach. In the subsequent phase, shown by the high-speed camera images, the wire dives into the melt pool while still solid, Figure 21 a). The power is increased to separate wire and melt pool and it happens only with the melting of the wire tip, Figure 21 b). This sequences of high power peaks is not terminated until the wire has melted enough to gain distance from the pool and begin the process of droplet growth and detachment again. This variation in voltage makes the weld bead narrower, although the deposition of material is more random and the surface quality is very low.

The fifth process focus on the increasement of the voltage in 3 volts. The result is showed in the Figure 22.

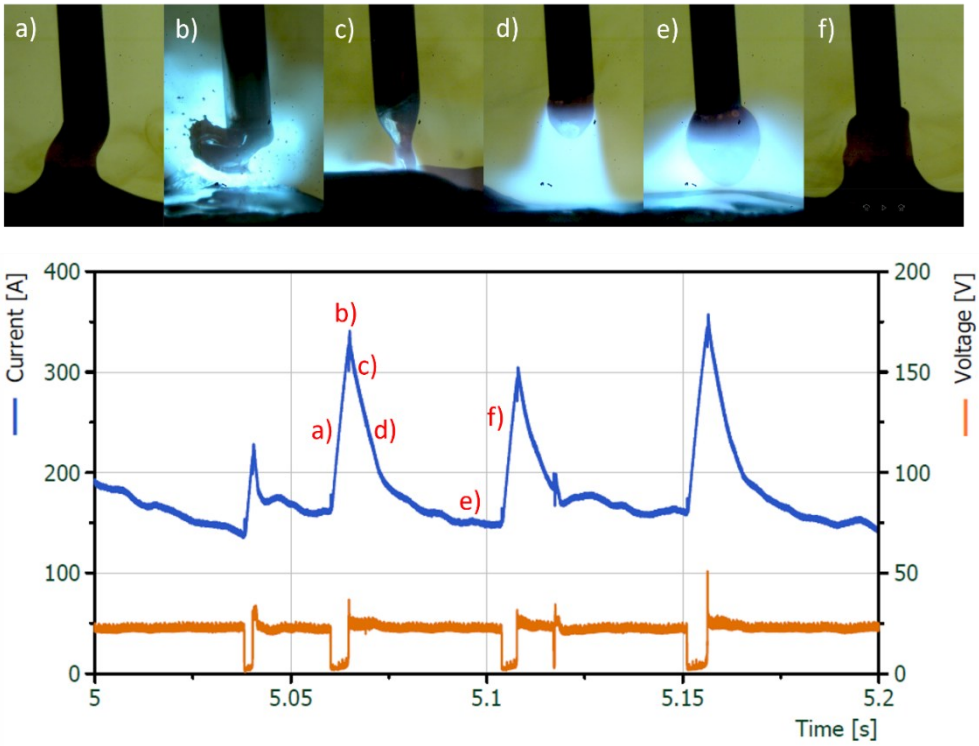

Figure 22. Preliminary welding test n° 5: voltage increasement.

The increase in voltage generates a less frequent drop detachment, the opposite effect as de decrescent. Comparing Figure 21 and Figure 22 It can be seen that the drop growth phase of the higher voltage process is more time consuming. This is due to the higher amount of power used, where the wire melting rate is greater and generate a slower approach between the solid

wire tip and the melt pool. In the Figure 22 d) It can be seen that the wire reaches a greater height from the substrate than the process with lower voltage, it caused for more powerful phases. It is noteworthy that the process with higher voltage rarely goes below 150 A, unlike the previous one, which often reaches 100 A of current. Therefore, the increase of the voltage generates a hotter process what implies in a more wet weld bead. The consistency of the drop separation frequency turns the surface quality better.

After varying the voltage, the sixth test is based on decreasing the arc dynamics. This is defined in the literature as the arc concentration range where the arc can be set to be more open and produce low penetration, or more concentrated and produce higher penetration. The result of the arc dynamic reduction is shown in Figure 23.

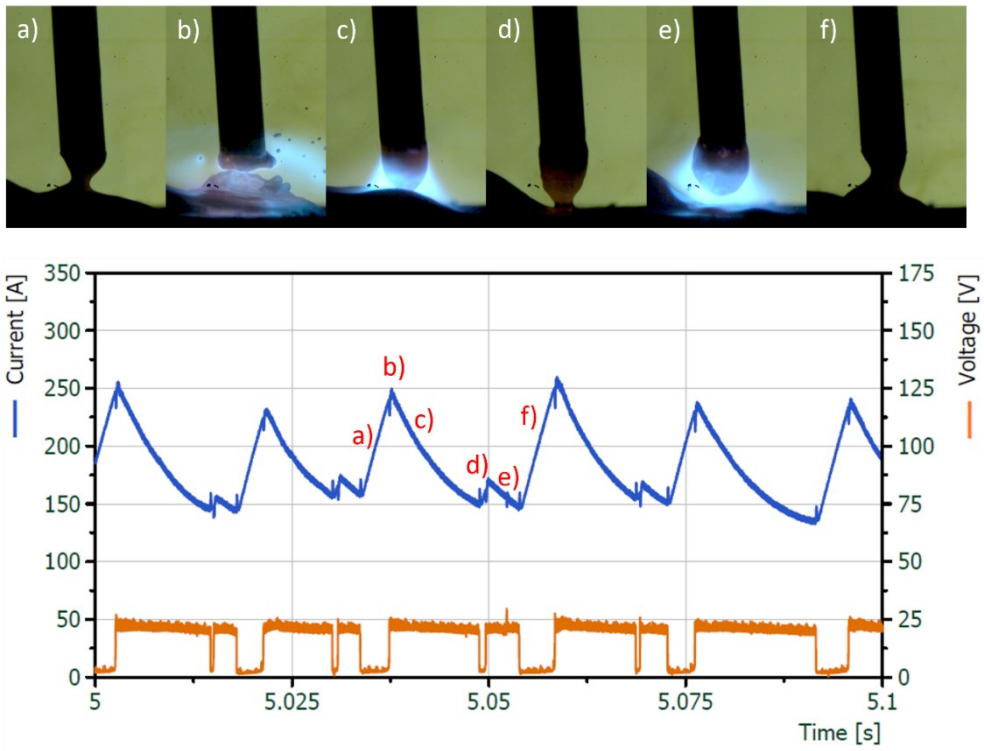

Figure 23. Preliminary welding test n° 6: arc dynamic decreasement.

The decrease in arc dynamics was found to be very close to the standard weld. The drop separation frequency was quite the same. However, the main difference shown by this variation was the concentration of the current around the average, near to 200 A. In the graph of Figure 23 It can be observed that this process with less arc dynamics rarely exceeds 250 A in the peak power and also less than 150 A in the short-circuit phase. The current range of the short circuit with no variations goes normally up to 270 A and back 135 A. In the Figure 23 d) and e) shows a characteristic that is repeated throughout the process, which is a little contact between drop and melt pool. This generates a rapid power peak that just separates the two without drop

detachment. However, this power peak generates a turbulence in the drop that immediately after the separation goes towards the melt pool and complete the metal transfer.

The last test consisted in increase the arc dynamic range by 20. The result is showed in the Figure 24.

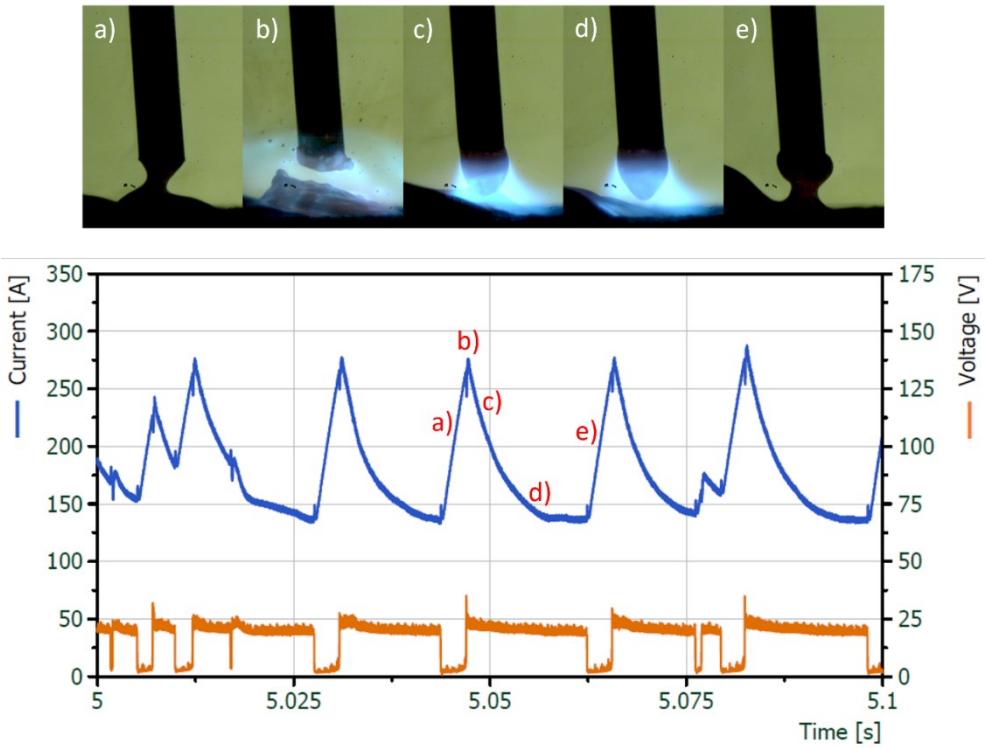

Figure 24. Preliminary welding test n° 7: arc dynamic increasement.

As expected, this behaves as the opposite of the arc dynamic reduction, with the standard process in the middle of the range. While the arc dynamic reduction concentrated the power closer to the average current, the arc dynamic addition increased the range of the current. The power peaks normally reached around 280 A, easily going to 300 A, and the lower current normally placed near 130 A. The waveform of the increased arc dynamics has power peaks much more aggressive than the previous reduced one, with the power increase happening in a shorter time, Figure 24 a). In fact, the power reduction used for the drop growth phase is also shorter, Figure 24 c), followed for a current stabilization, Figure 24 d). The pinch effect was found to be more abrupt in this process due to the arc concentration being more centered in the wire tip. This resulted in a more unstable process as the drop detachment was more violent, such as the reopening of the arc. This effect can be seen in the time interval between 5 and 5,025 s on Figure 24, where the drop detachment happened in the middle of the drop, quickly scoured, generating a new turbulent drop that went towards the melt pool. This kind of occasion end up by generating wire material expel.

The result is that decreasing the arc dynamics produces a more wet weld bead, while increasing it produces a more rounded one. The surface quality is quite the same, with the arc dynamic decrease being more continuous.

5.2 Welding tests

With the weld bead geometries reached, the Table 3 shows the parameters set on the machines to generate this weld beads.

Table 3. Parameters of welding set on power sources.

Welding Power source	Process variation	Wire feed speed (m/min)	Voltage correction factor	Arc dynamic factor
Cloos	ControlWeld	4	-0,5	0
EWM	ColdArc	3,9	+0,4	0
	RootArc	3,9	0	0
	Standard	3,7	-0,3	0
Fronius	CMT	4	0	0
	CMT Synchropulse	6[1]	-6	10
Lincoln	STT	3,81	1,1	0
Lorch	SpeedArc	3,7	-8	0
	SpeedCold	6	5	0
	SpeedRoot	4,2	0	0
OTC	Synchrofeed	4	0	0

Cloos ControlWeld, EWM Standard and Lorch SpeedArc are the standard short circuit processes of three different brands. As standard short circuits they follow the behavior commented and shown in Figure 3 [3, 17], where the contact of the droplet with the molten pool generates a voltage drop and a current peak, which in turn cause the droplet to scour and the arc to reopen, forming a new droplet and working in this loop.

[1] Lorch SpeedCold used a 1 mm diameter wire.

The electrical measurements of the standard processes are showed that, even though they represent the same process and use nearly the same wire feed speed, their behavior is not equal.

Cloos ControlWeld presents a longer phase of low power than the others with quick power peaks for drop separation, maintaining a very constant process as shown in the Figure 25.

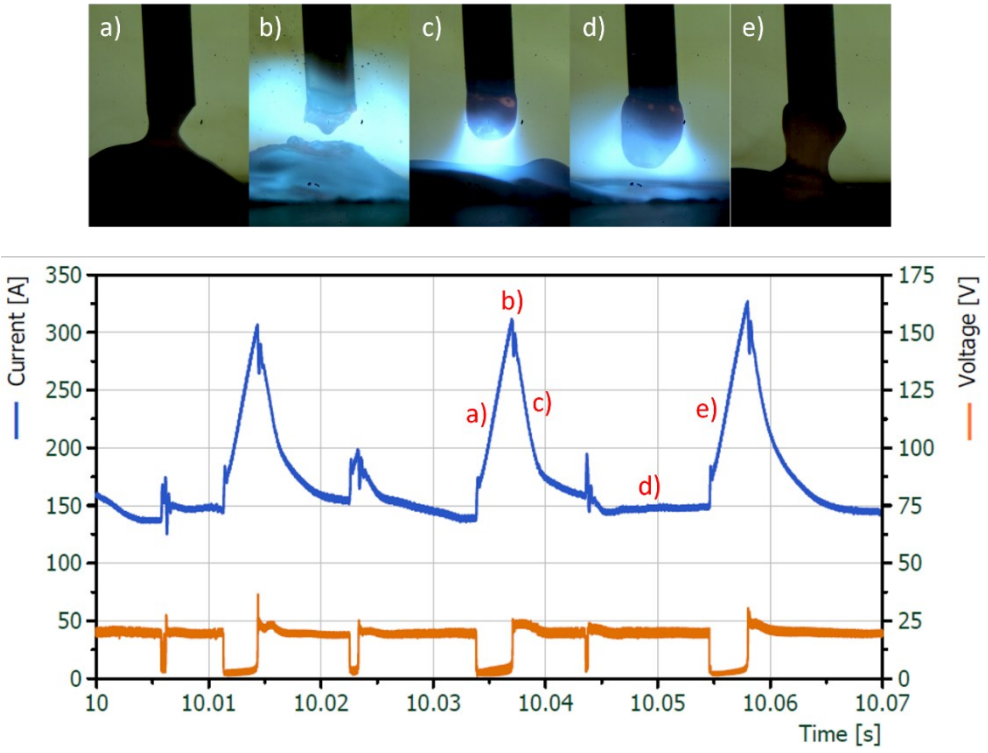

Figure 25. Cloos ControlWeld step by step process.

The big power peak that this process has, causes a big disturbance in the melt pool, as showed in Figure 25 b), where the explosion of the re-opening arc is very aggressive. This acts to blow the metal from the pool and also from the drop. This generates a turbulent melt pool and occasionally material expulsion. However, this drop grown phase shown in Figure 25 d) is more continuous and time consuming, which gives time for the melt pool to stabilize and avoid early contact with the drop.

EWM Standard present this early touch constantly in the process, however forming less volume drops, as showed in the Figure 26.

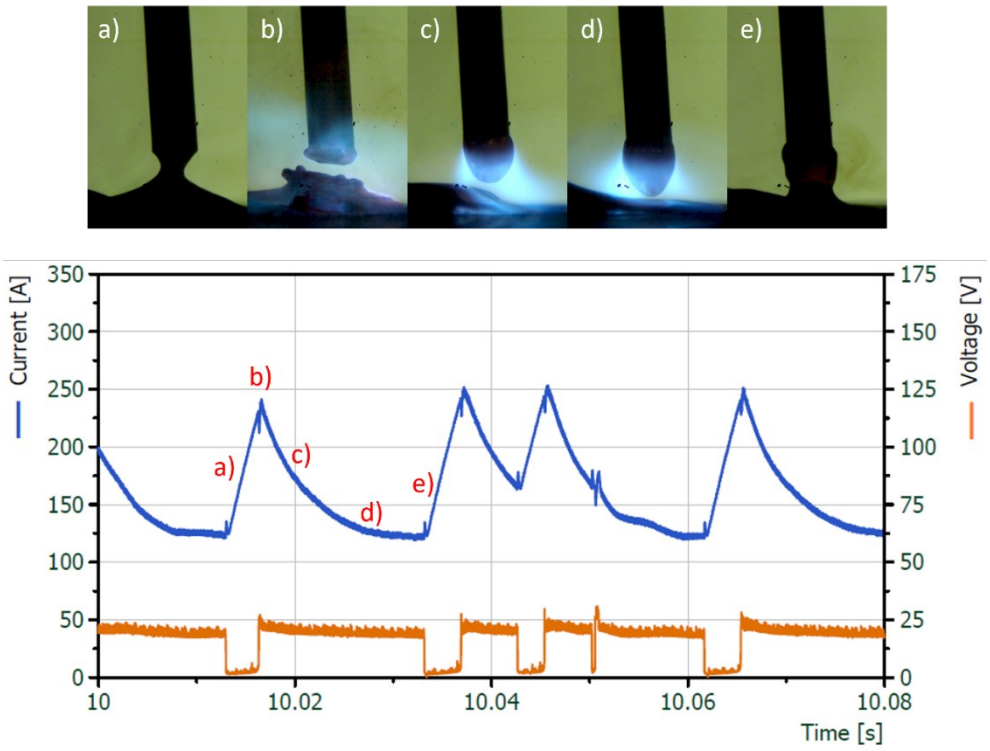

Figure 26. EWM Standard step by step process.

When the drop is in phase d), it sometimes touches the molten metal very quickly, being this contact generated by the molten metal and the drop turbulence. This causes a power peak when the drop is not yet well formed or the melt pool is too turbulent and scouring does not occur. The result is usually a waste of power in a useless peak, with a separation between the drop and the melt pool without the drop scouring. The process is restarted until the drop has grown enough to complete the metal transfer. Although the early touch commented normally does not cause metal transfer, the drop detachment from EWM standard showed itself very stable, with the arc power peak happening with the drop almost separated from the wire, where the arc explosion stays focused in the scour between drop and wire, not in the bottom of the drop where it touches the melt pool. This feature avoids the expulsion of molten material as it is all transferred to the melt pool.

Lorch SpeedArc presented the early touch pattern also. Indeed, In the Figure 27 where Lorch SpeedArc process is shown, it is noticeable the difference between the waveform of SpeedArc and the standard short circuit.

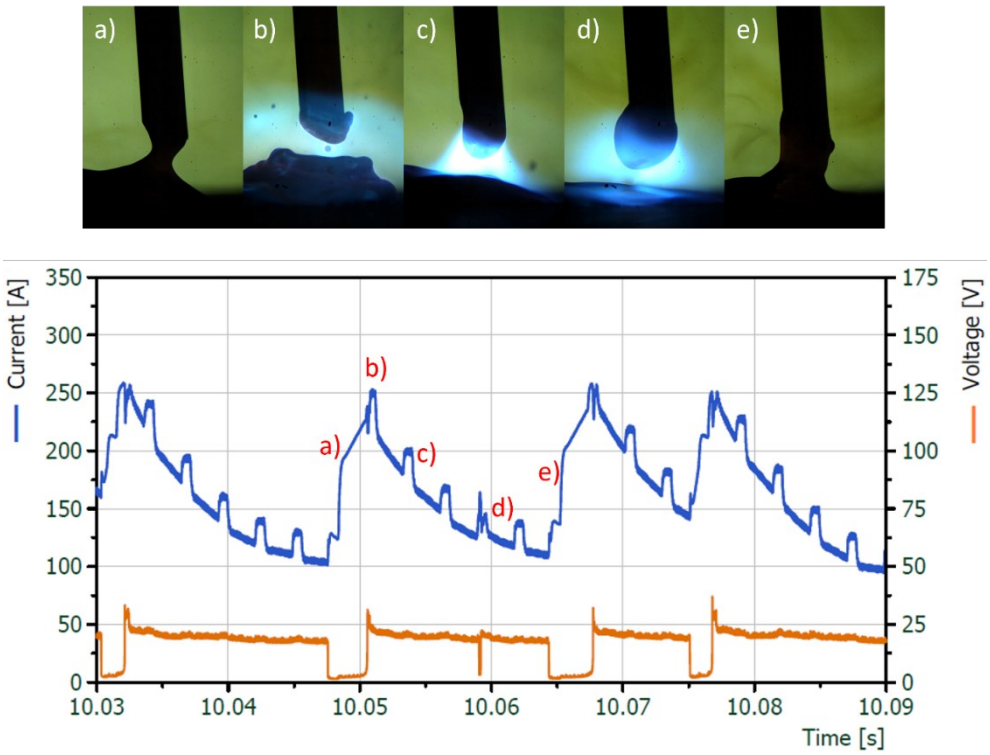

Figure 27. Lorch SpeedArc step by step process.

In this process, the characteristic wave of standard GMAW has a sequence of small current pulses in addition. This behavior ends up by causing a more frequent drop detachment, forcing the pinch effect on the drop and changing its shape, acquiring an elongated shape instead of a spherical one. This aggressive drop grows against the melt pool, united with the turbulent melt metal caused by the high frequency detachments, generates a sequence of metal transfers, not always transferring all the drop, although generating metal expel. Due to the highest frequency of detachment, either melt pool and melted metal remaining in the wire adopt an unstable behavior, with drop and melt pool going toward each other and distancing as well.

Lincoln STT, EWM ColdArc and Lorch SpeedCold shared the same characteristic in metal transfer as they focused on low heat input. Below it can be observed the Figure 28, Figure 29 and Figure 30, which represents the STT, ColdArc and SpeedCold processes respectively, where the electrical measurement and high-speed images show the operating behavior of each process. It can be noticed that some characteristics are similar between them and also separate them from a standard short circuit. The main difference is the quick power peak used to generate the drop separation, present in all the figures commented, where the power is reduced immediately after the separation happens, followed by a new power peak to reopen the arc and start the process of wire melting and drop formation. Knowing this key characteristic of the

electrical controlled processes, it is possible to analyze the differences between the working methods of each brand.

The waveform presented by Lincoln gives the drop a very smooth transfer with a small volume and a higher detachment frequency, as shown in Figure 28.

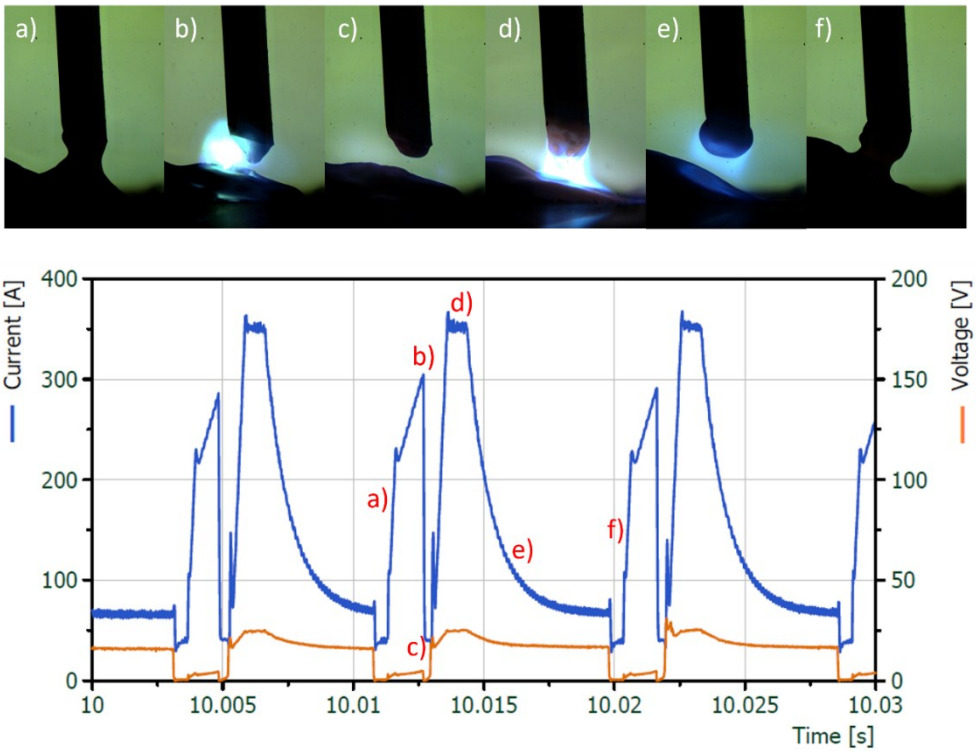

Figure 28. Lincoln STT step by step process.

In the short circuit phase, Figure 28 a), the power increases at the moment the drop touches the melt pool, allowing the drop to start the transfer by surface tension and followed by a power peak, Figure 28 b), which finishes the scouring of the drop. This characteristic gives to Lincoln STT a very clean transfer, since the arc explosion for the detachment takes place only between wire and drop, far from the melt pool and not blowing the molten metal, what can be seen in the Figure 28 b) and c), where the melt pool keeps controlled all the time.

The reopening of the arc also occurs smoothly due to the previous separation between drop and wire. The wire stays far away from the molten pool and a power peak occurs, Figure 28 d). The power peak holds still for a short period of time, which with the amount of power used, forms a new small size drop instantly. The power is smoothly decrease to generate the drop

grown, Figure 28 e), and then it touches the melt pool completing the metal transfer, Figure 28 f).

EWM ColdArc is showed in the Figure 29 and follows the same principle of work and steps with different charcateristics. However, the droplet formation was large while maintaining the smooth separation.

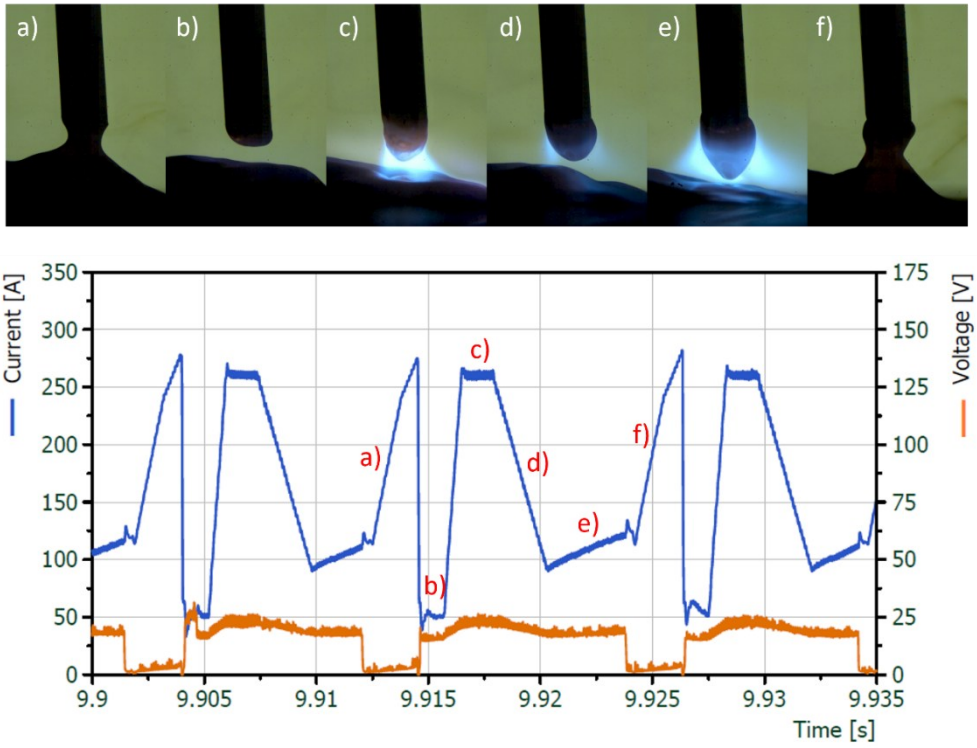

Figure 29. EWM ColdArc step by step process.

As showed in the Figure 29 b), the separation is clean and the normal explosion generated by the power peak is rarely seen, what means that the power is reduced just before the separation between drop and wire, with the complete separation being made by surface tension. This characteristic avoids disturbances in the melting process and spattering, since the strong blow caused by the arc explosion is inexistent.

The peak to arc reopening showed to smooth in be most of the detachments. However, the drop formed in the wire tip by ColdArc is considerably big and its size changes from time to time, growing more or having a fast detachment while small. This characteristic gives to this process, which is stable most of the time, some sequences of drop instabilities, with mistouches what causes a power peak when the drop has not started to make the transfer. The arc explosion happens so in the scour between drop and melt pool instead of drop and wire, blowing the drop against the wire. This generates some occasional material expulsion and spatter.

Lorch SpeedCold metal transfer has the characteristic of having two drop detachments per interval, showed in the graphic of Figure 30, where can be seen four power peaks in sequence.

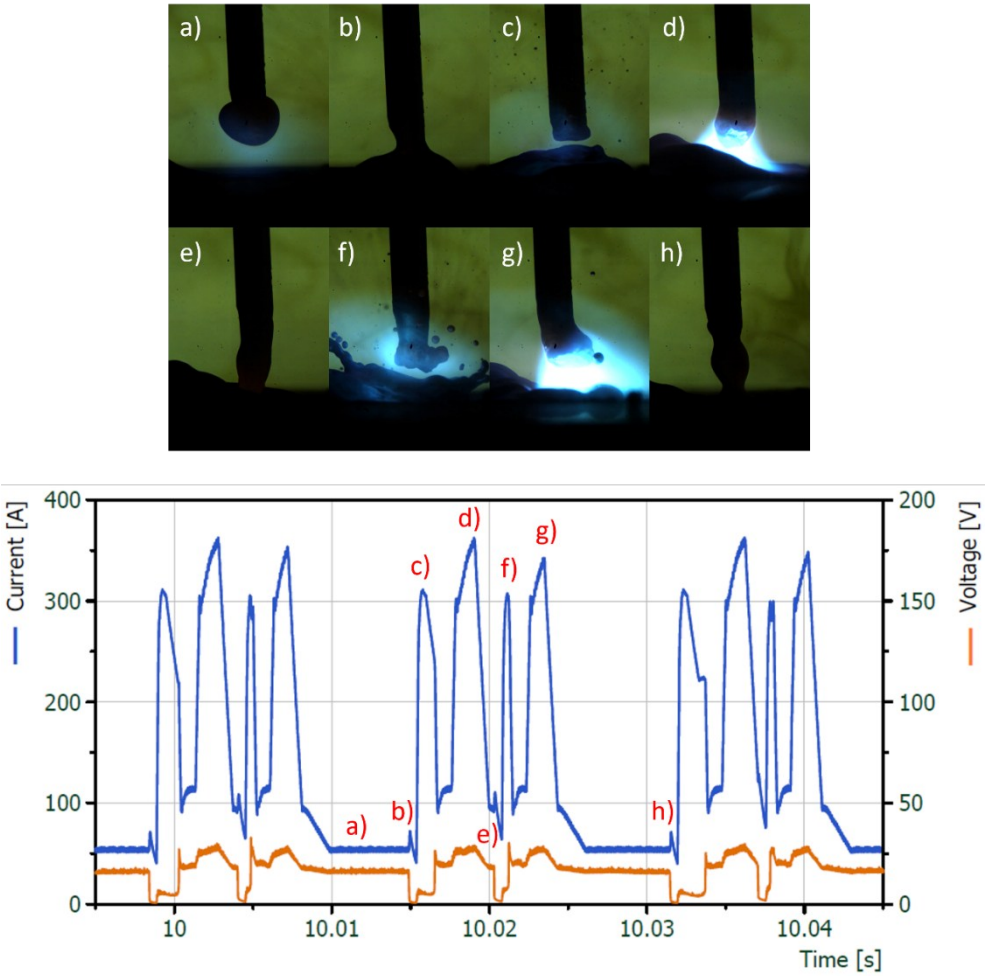

Figure 30. Lorch SpeedCold step by step process.

The power peaks c) and f) are those used for drop detachment. The other two peaks, d) and g), are the ones for the arc reopen and drop formation. This sequence happens due to the first power peak to drop detachment and arc reopening, represented by c) and d), respectively. In this process, the arc explosion due to the power peak does not happen in the connection between wire and drop, although it happens in the middle of the drop. The effect is that some of the material is added to the molten pool and some remains in the wire tip. In the next step, Figure 30 d), when another peak reopens the arc, the remaining material in the wire tip is stretched by the arc pressure. This one together with the material melted in the power peak, goes against the melt pool, Figure 30 e). The result is a new touch generated by the arc reopening peak, which is followed by a new detachment peak, Figure 30 f), and a new arc reopen. The sequence is broken when the second power peak to open the arc, or the last one in the case of more than two consecutive metal transfers, does not elongate the drop enough

to cause a new touch. Normally it happens after the second drop detachment. Since the wire is melted in each peak, after the second peak the wire tip finds itself too high, so the drop does not reach the melt pool and can be formed slowly. This process has a lot of spatter and very frequent material expulsion, much due to the drop instabilities and not very well regulated detachment pulse.

Another process from Lorch, called SpeedRoot, is to be observed here. The detachment peak, followed by a power drop and a new peak to open the arc, Figure 31 b), c) and d), are the steps normally seen in the low heat input processes and also showed here.

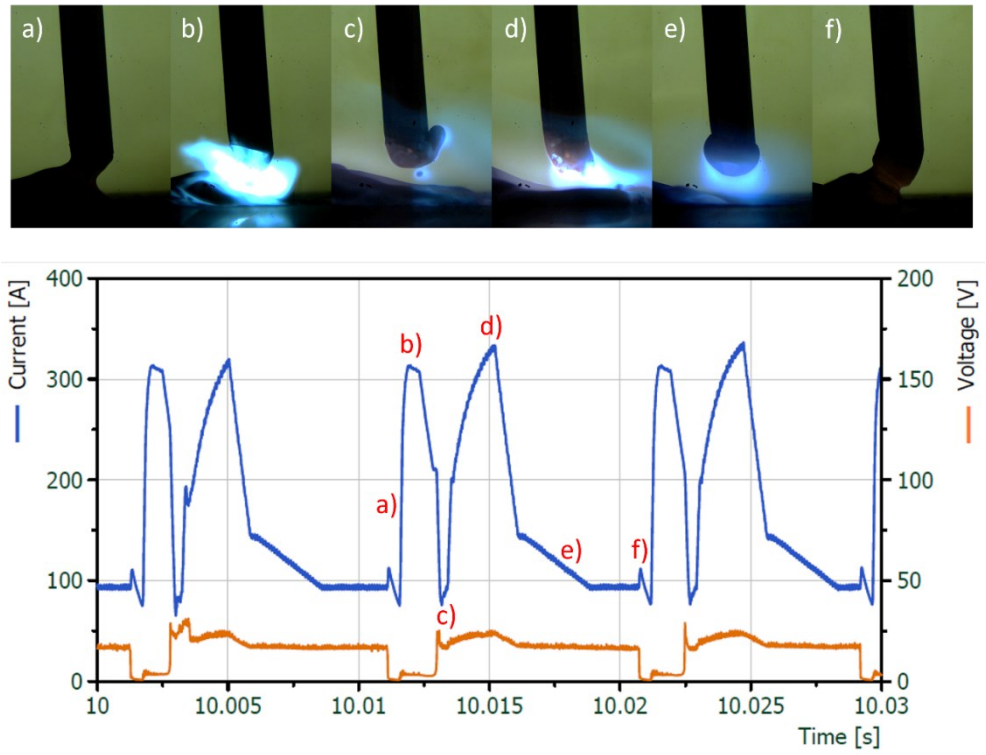

Figure 31. Lorch SpeedRoot step by step process.

However, SpeedRoot has the drop scouring most commonly in the connection between drop and melt pool, Figure 31 b). Due to the process, there is no time between the drop touch and the first power peak, so the drop does not have time to start the transfer by surface tension. This results in an arc explosion in the smaller transverse area, which is localized in the bottom of the drop, separating drop and melt pool without the complete metal transfer, Figure 31 c). This behavior ends by generating spatter, blowing the molten metal in the wire and resulting in a turbulent melt pool and drop, Figure 31 d).

OTC Synchrofeed process showed in the Figure 32 worked very mechanically. This is because there are no variations in voltage and arc dynamic factors to achieve the desired weld bead geometry.

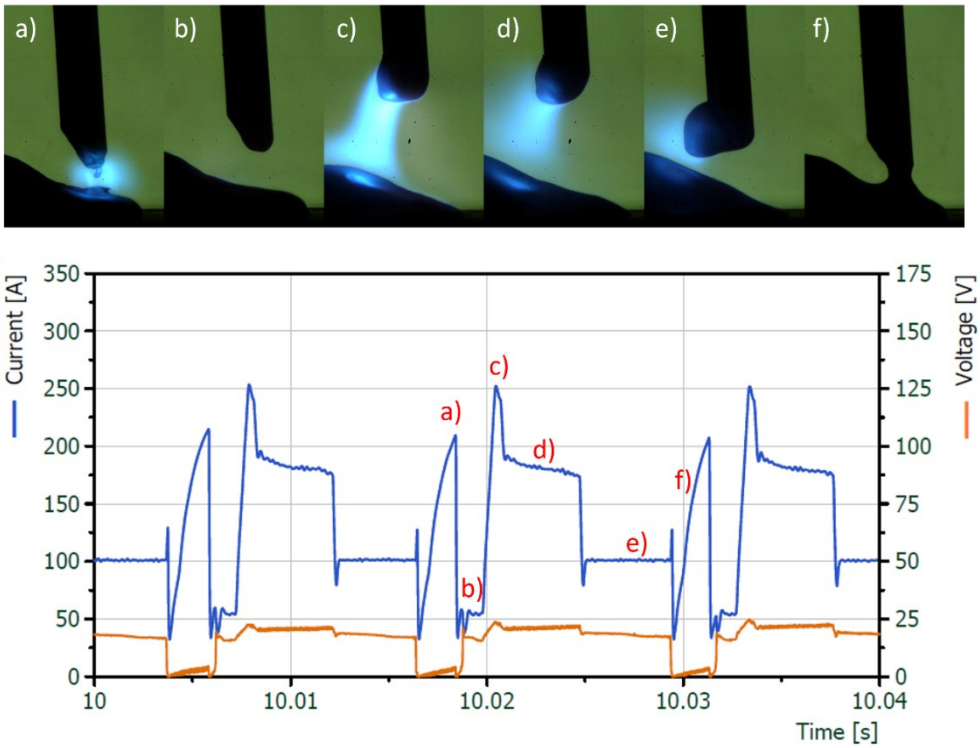

Figure 32. OTC Synchrofeed step by step process.

In the OTC Snychrofeed process, the height of the wire is maintained at approximately 3.5 mm from the substrate during the wire melting and drop forming phases, Figure 32 c) and d), presenting this behavior continuously. The arc remains open longer than the pause time to metal transfer. Although, it adopts three phases of power, with a quick peak of power to finish the drop detachment, Figure 32 a), a second peak to reopen the arc, Figure 32 c), and then reduce its power to approximate and dive the drop in the melt pool, Figure 32 d). After the drop formation is complete, the process of pushing gives the drop inertia in the melt pool direction, Figure 32 e). That makes the detachment easy when it is pulled out, since the drop already start a process of detachment with the inertia that can be seen in Figure 32 f). As the arc phase, the metal transfer phase shows a mechanical characteristic, with a very repetitive behavior and precise arc peak time, making the Synchrofeed the only process in this work with really no spatter.

In the first and standard weld, Fronius CMT had a very stable operation, where there were no exceptional adjustments in any parameter. However, some instabilities appeared in the waveform as some variations had to be applied in the process, as shown in Figure 33.

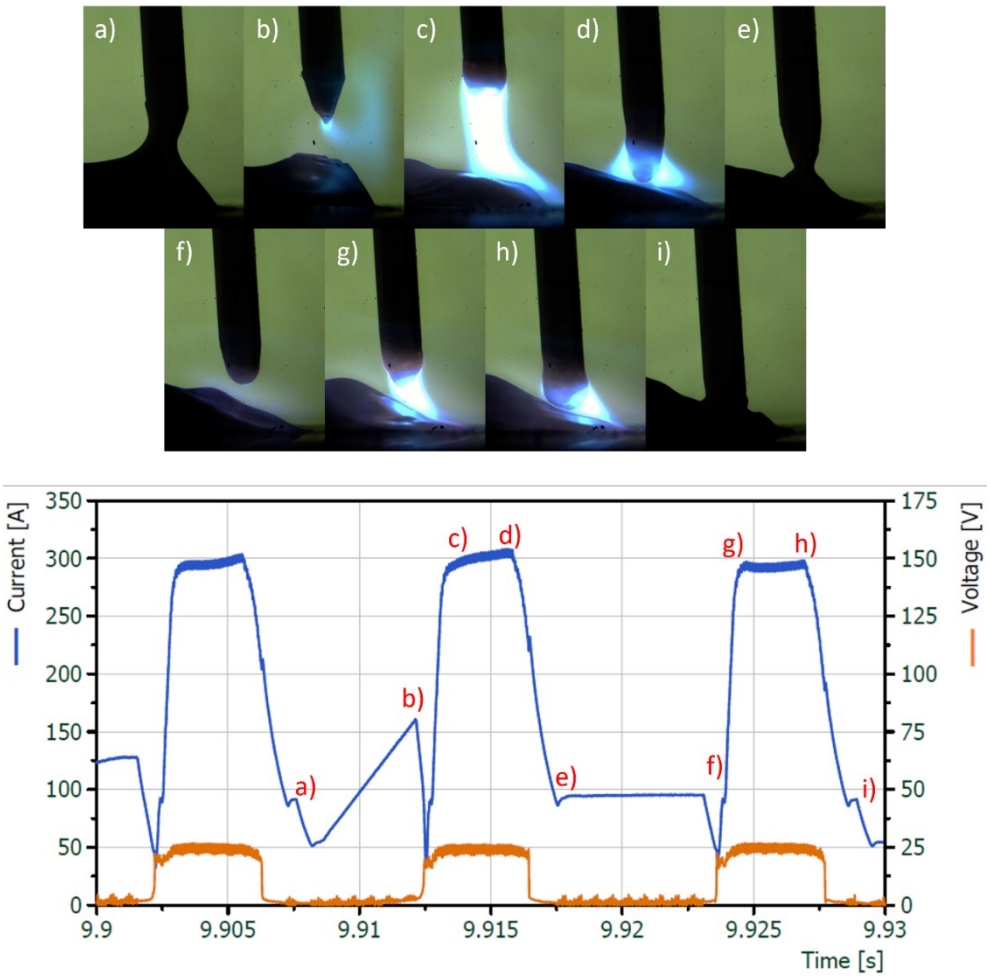

Figure 33. Fronius CMT step by step process.

These processes try to adapt every moment of the electrical feedback, constantly changing its behavior. The wire push time does not behave equally throughout the process, changing high and time of contact with the melt pool constantly, Figure 33 c) and g), what gives to the molten metal of the pool a turbulent behavior. The drop separations end by happening by different reasons in each separation, sometimes by surface tension, Figure 33 f), and sometimes by power peak, when the molten pool and the wire do not separate, Figure 33 a) and b). This behavior generates the random characteristic of the process, since with them the reopening of the arc occurs immediately after the separation between the wire and the molten pool. This generates sequences of arc openings, one after another, until the molten pool normalizes. This can be seen in Figure 33 c) and g). With this random characteristic, the control of the spatters of Fronius is not so precise, however still remarkable, presenting spatters from time to time. This commonly when the early disconnection happens, the arc reopening occurs too close to the melt pool, blowing the molten metal and.

The behavior of CMT Synchropulse was similar, with no variations in the drop separation method and occasional spattering. In the Figure 34 can be seen the electrical measurement and analyze the waveform of the process where present a high current phase followed by a low current phase, set in 50% balance of frequency. This characteristic produces the effect shown and described in the Table 4 g), where the weld bead acquires wave marks. That is generated by the different amount of metal fusion and solidification hate throughout the weld, since the amount of power and consequently the heat given to the melt pool vary in time.

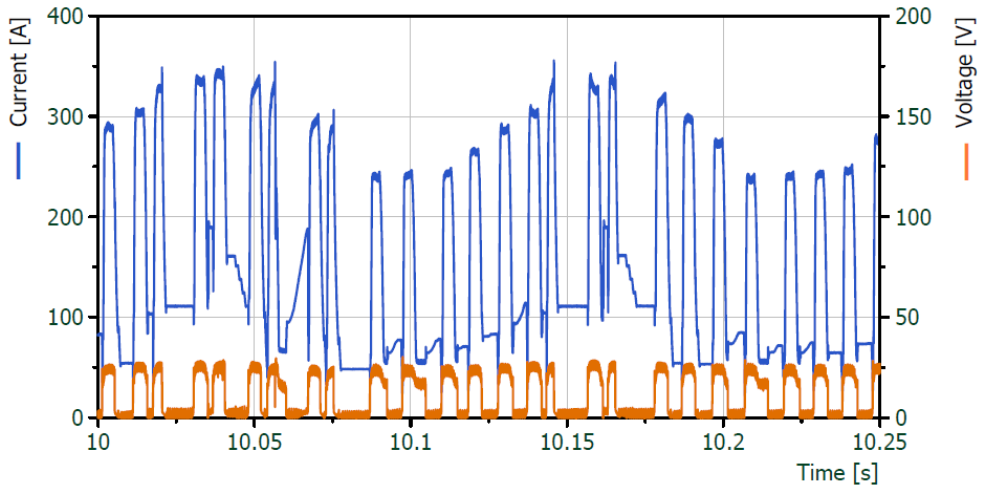

Figure 34. Fronius CMT Synchropulse process electrical measurement in 1 second interval.

EWM RootArc showed in Figure 35 is the last to be commented because it is similar to no other process tested. The wire feed rate and the wire melting rate were not the same, which causes a unique behavior in the process.

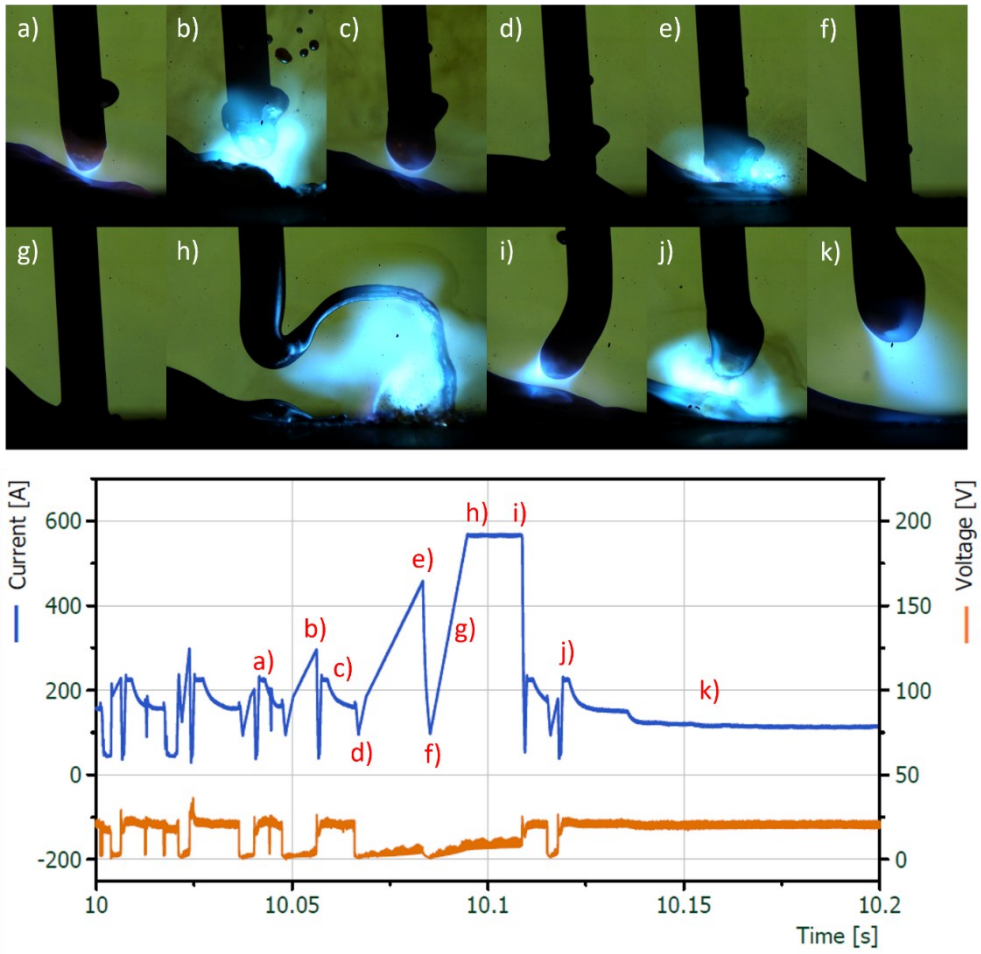

Figure 35. EWM RootArc step by step process.

Its behavior will try to follow the standard short circuit, with the drop transfer by surface tension and power peak, followed by the arc reopen peak and drop grown until it touches the melt pool again. However, the RootArc process gives to the arc less power than it needs to melt the wire at the same rate that it is fed, which can be observed in the Figure 35. The wire slowly approaches the molten pool, the arc becomes shorter and shorter, Figure 35 b) and e), until the moment the wire is fed completely in the melt pool. In Figure 35 e) the wire is already immersed in the molten metal, however due to molten metal turbulence, the molten metal retracts enough to generate a separation between the wire and the molten metal. Figure 35 f) and g) show when the power peak is no longer sufficient to cause the scouring, since there is no more drop and the solid wire is touching the molten metal from the pool. What happens next is an uninterrupted increase in power until the wire is completely melted and separated from the molten pool, generating a large energy and material expulsion, Figure 35 h) and i). With the amount of power liberated for a long time, around 580 A, big part of the wire is melted, letting the tip in a very high distance, as can be seen in Figure 35 i). The melt metal from the drop stays in the wire tip by surface tension and the wire melting continues. However, due to the

high that the tip is after the over melting, the drop keeps growing until the drop touches the melt pool again, transferring all the melt metal, Figure 35 k). This amount of melt metal transferred all at once generates this wave effect seen in Table 4 d), caused by the different volume of melted metal in the melt pool throughout the weld.

The samples can be seen on the Table 4, where is showed the weld bead and the surface details.

Table 4. Weld beads generated by each process.

Weld bead	Weld surface detail
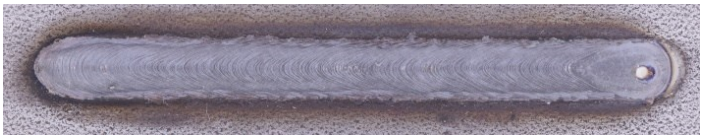 a) Cloos ControlWeld	
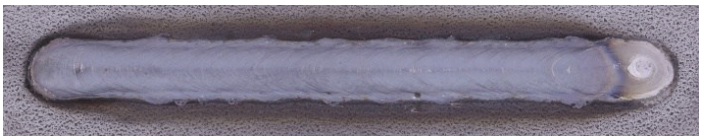 b) EWM ColdArc	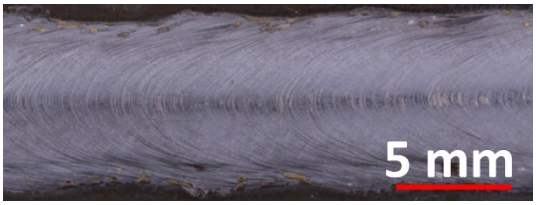
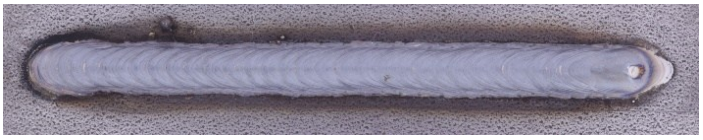 c) EWM RootArc	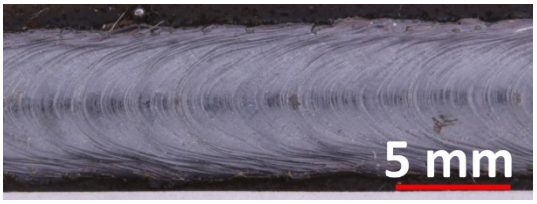
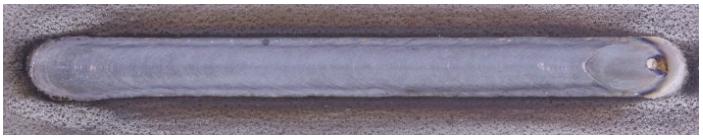 d) EWM Standard	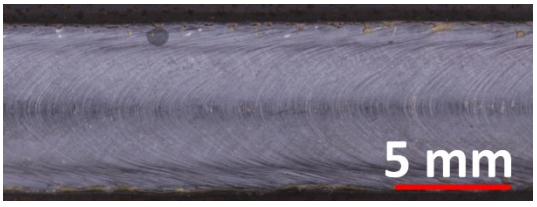
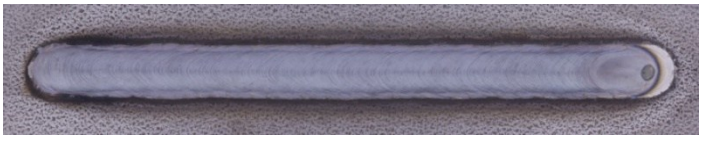 e) Fronius CMT	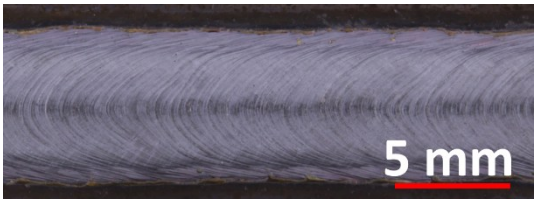

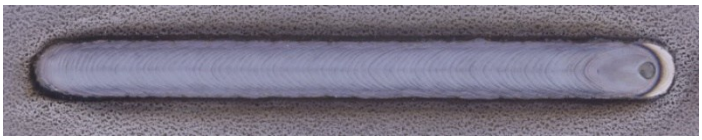

f) Fronius CMT Synchropulse

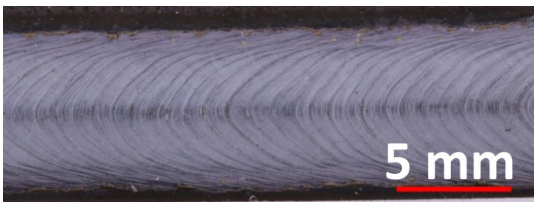

g) Lincoln STT

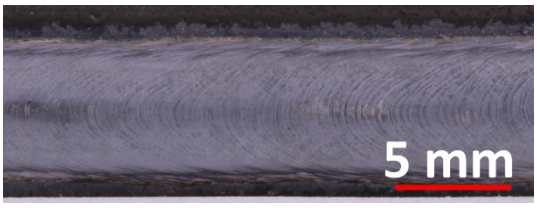

h) Lorch SpeedArc

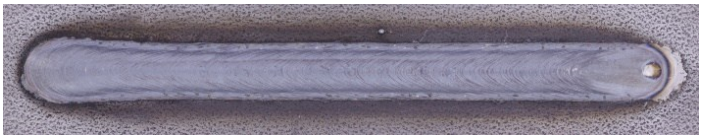

i) Lorch SpeedCold

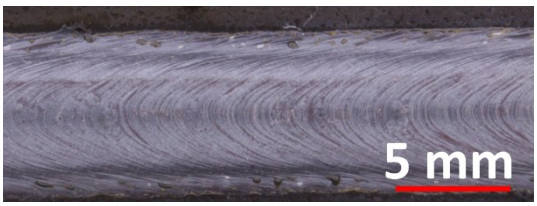

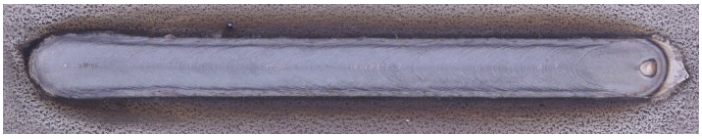

j) Lorch SpeedRoot

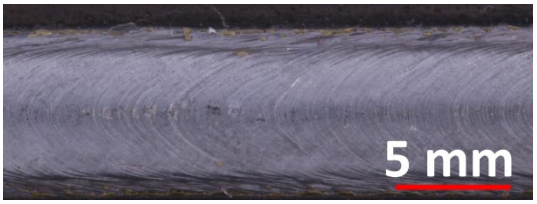

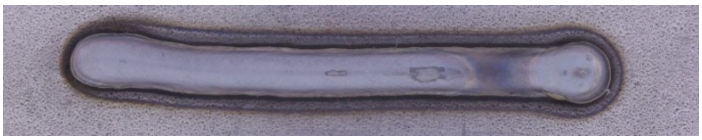

k) OTC Synchrofeed

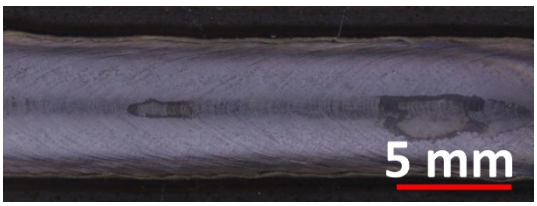

The theoretical heat input of each process is shown in Table 5, with Fronius CMT, Fronius CMT Synchropulse and OTC Synchrofeed having the lowest heat input between all the eleven processes, consecutively.

Processes such as EWM's ColdArc and Lorch's SpeedCold, two low heat input options, showed a high theoretical heat input number. On the other hand, EWM Standard and Lorch SpeedArc, which should not have dynamic control of power, have lower theoretical heat input than the previous ones.

Table 5. Theoretical heat input of each welding process.

Welding power source	Process variation	I_{av} (A)	V_{av} (V)	Power (W)	Heat input (J/mm)
Cloos	ControlWeld	183,93	17,92	3296,03	395,50
EWM	Standard	171,89	17,59	3023,55	362,81
	ColdArc	177,89	17,93	3189,57	382,73
	RootArc	203,85	18,36	3742,69	449,10
Fronius	CMT	183,16	14,54	2663,15	319,56
	CMT synchropulse	180,26	14,98	2700,29	324,02
Lincoln	STT	169,2	16,84	2849,33	341,90
Lorch	SpeedArc	168,58	17,63	2972,07	356,63
	SpeedCold	178,2	18,31	3262,84	391,52
	SpeedRoot	191,05	17,19	3284,15	394,08
OTC	Synchrofeed	144,7	18,87	2730,49	327,64

Using macrographs of each process, showed in Table 6, it was possible to analyze the amount of material deposition, characteristic format and the penetration area, being the penetration one of the best metrics to observe the heat input in the samples. In the Figure 36 the ratio is compared from the smallest to the largest.

Table 6. Macrography of welding made by each process.

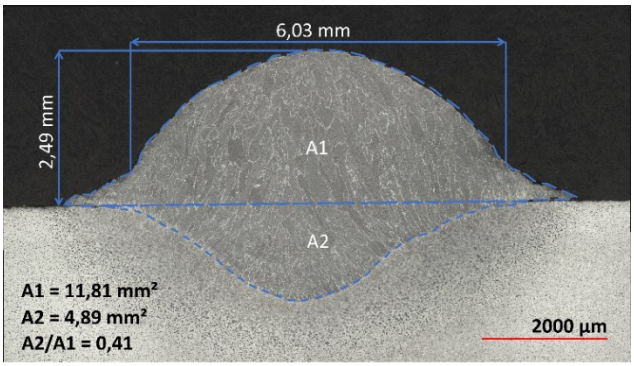

a) Cloos ControlWeld

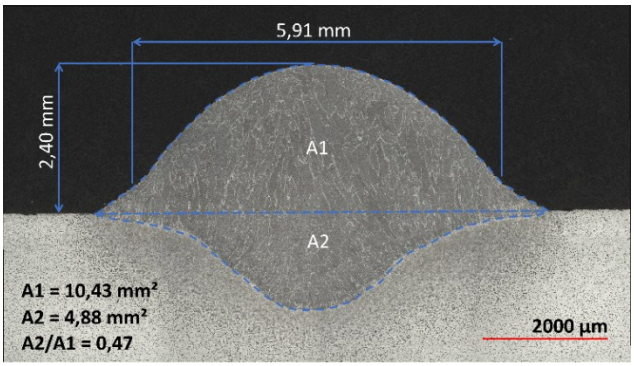

b) EWM Standard

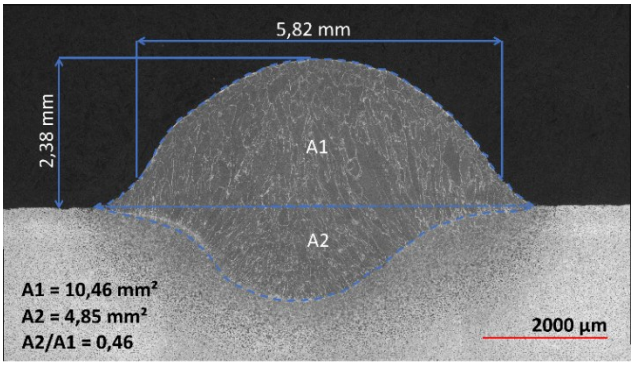

c) Lorch SpeedArc

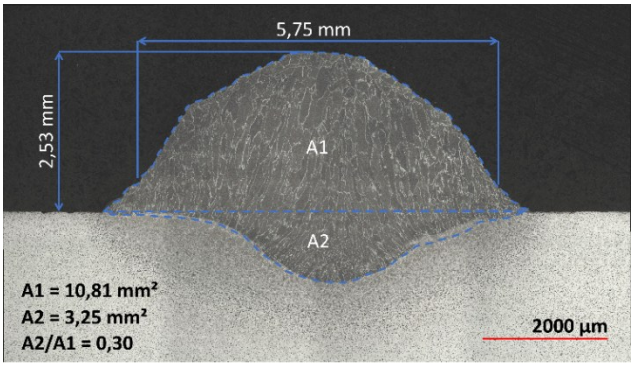

d) EWM RootArc

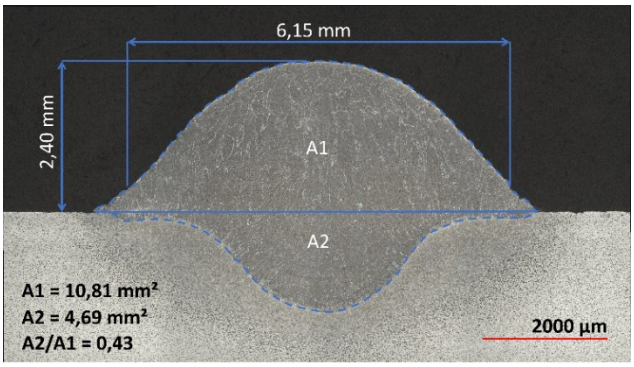

e) EWM ColdArc

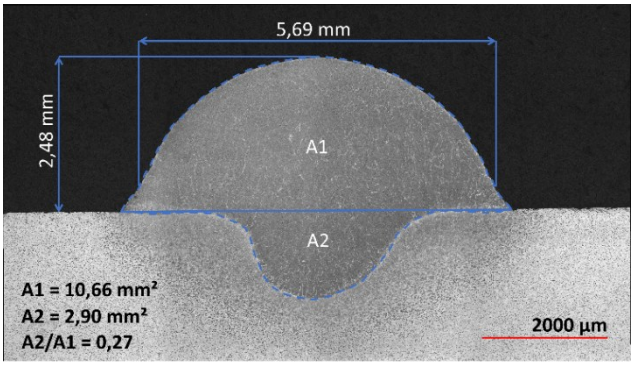

f) Lincoln STT

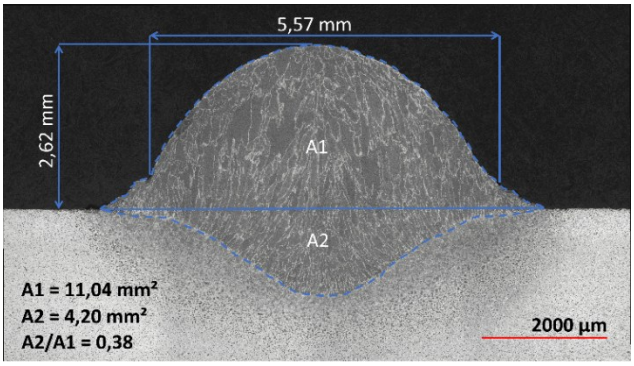

g) Lorch SpeedCold

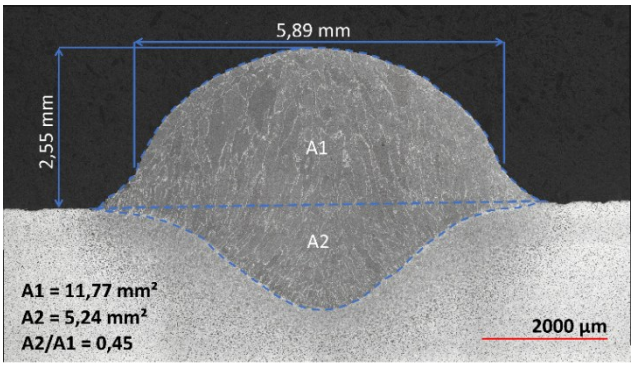

h) Lorch SpeedRoot

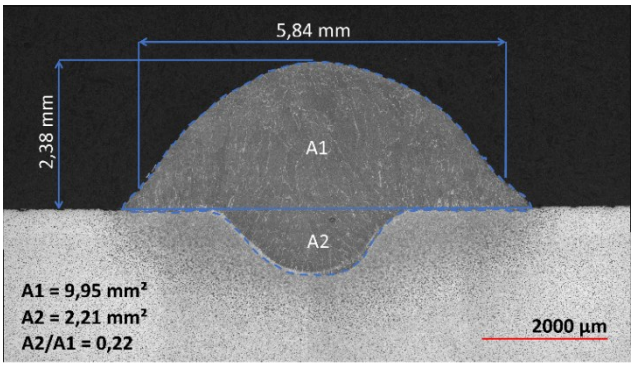

i) Fronius CMT

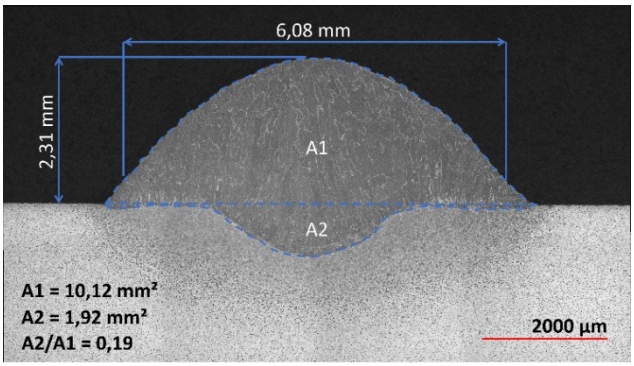

j) Fronius CMT Synchropulse

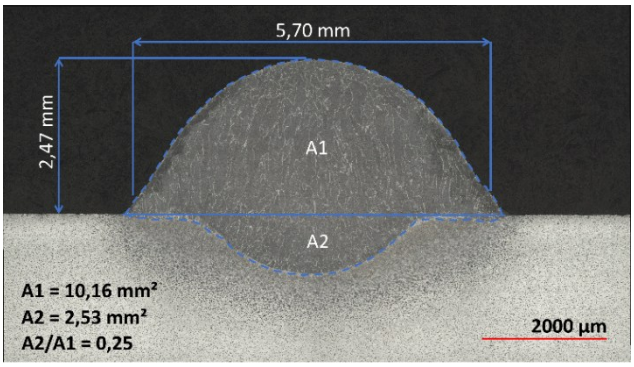

k) OTC Synchrofeed

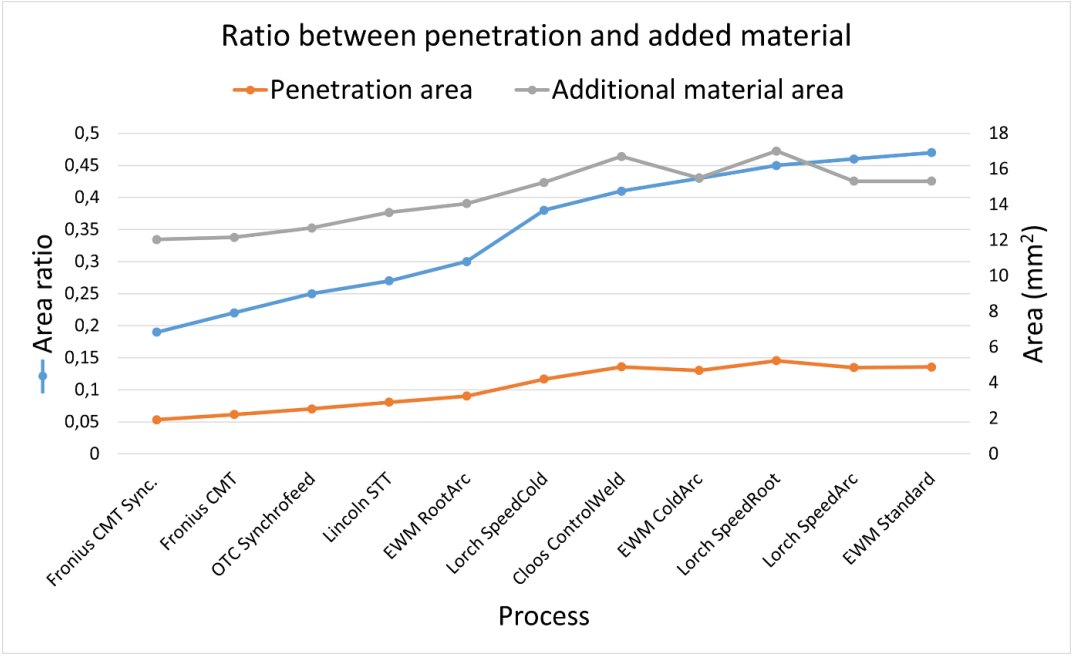

Figure 36. Area ratio relation with the respective penetration and additional material areas from each process.

The biggest penetration area was showed by Lorch SpeedRoot with 5,24 mm^2. The standard processes Table 6 a) and b) came next, reaching 4.89 mm^2 and 4.88 mm^2 respectively. However, c) presented a smaller penetration area with 4.20 mm^2, presenting better results than other processes as e), EWM ColdArc, which reached 4.69 mm^2 of penetration area. Although this process is the low heat input option of EWM, it is placing behind EWM RootArc, d), with a penetration area of 3.25 mm^2.

As expected, the largest ratios came from the standard processes, with EWM Standard having the largest ratio of 0.47, followed by Lorch SpeedArc with a ratio of 0.46. However, the next largest were Lorch SpeedRoot with 0.45 and EWM ColdArc with 0.43. This is followed by Cloos ControlWeld with 0.41.

In turn, as expected, the processes using retractable wire feed developed the weld with the lowest ratios, with Fronius CMT Synchropulse with a ratio of 0.19, Fronius CMT with 0.22 and OTC Synchrofeed with 0.25. Synchropulse proved to be the more wet of the three and OTC the more rounded. Lincoln STT achieved one of the lowest ratios with 0.27, even without retractable wire feed.

5.2.1 Choose of process to develop additive manufacture

Macrographs and electrical measurements showed in the Table 7 were used to compare processes for use in additive manufacturing, where topics regarding to penetration and energy used were considered.

Table 7. Welding process score based on its characteristics.

Process	Area ratio	Heat input (kJ/mm)	Total
Fronius CMT Synchropulse	0,19	0,324	6,2
Fronius CMT	0,22	0,320	7,0
OTC Synchrofeed	0,25	0,328	8,2
Lincoln STT	0,27	0,342	9,2
EWM RootArc	0,30	0,449	13,5
Lorch SpeedCold	0,38	0,392	14,9
Cloos ControlWeld	0,41	0,396	16,2
Lorch SpeedArc	0,46	0,357	16,4
EWM ColdArc	0,43	0,383	16,5
EWM Standard	0,47	0,363	17,1
Lorch SpeedRoot	0,45	0,394	17,7

The lowest total number showed in Table 7 represents the colder process, which is a combination of low area ratio and also low heat input. The three lowest processes were those using retractable wire technology, Fronius CMT Synchropulse, the colder one, Fronius CMT second and OTC Synchrofeed third. Lincoln STT was the only process without retractable wire feeding which can be placed between the coldest results.

In this metric, electrical controlled processes such as EWM ColdArc and Lorch SpeedCold showed a small difference compared to the standard processes, with ColdArc developing a weld similar to the standard Cloos and Lorch. Lorch SpeedCold remained almost 5% less heat input than Cloos ControlWeld and 7% less than EWM Standard. EWM RootArc ranked fifth on the scale, developing better weld in the metric than EWM ColdArc itself.

5.3 1st phase processes comparison and characteristics

5.3.1 Power sources operation

Different power sources presented with the same initial parameters produced very different weld bead geometries, which can be related to the manufacturer's goal for the process. Processes such as EWM ColdArc and Lincoln STT almost achieved the expected weld bead geometry on the first try, presenting a less wet weld by default and requiring few more welds to complete their parameterization. They also showed a reliable relationship between parameter control and resulting weld bead variation, with predictable geometry changes. OTC Synchrofeed is characterized by achieving the target geometry in the first weld with standard parameters, without the need for variations in voltage or arc dynamics. Therefore, its toughness in dealing with parameters and bead changes was not tested.

On the other hand, some processes were very far from the target and were very difficult to parameterize, usually focused on different types of welding, such as SpeedArc from Lorch, where the main objective of this process, even with the use of short circuit, is a more wet weld and high penetration. EWM RootArc achieves in the standard parameters a geometry very close to that aimed at, since the characteristics of processes made for root welds are the high deposition of material and low arc power, prepared to work with thin geometries and gaps. However, the relationship between the variation of the parameters and the result of the weld bead proved to be very unstable, often going in the opposite direction to that expected.

Moreover, the control of the parameters turns into an interesting characteristic between the different power sources. Some of them allow the user to directly modify the parameter, like EWM and Cloos, that allows to set the desired voltage, and also Lorch, that make it possible to modify the current. However, power sources such as Fronius, Lincoln and OTC have a parameter control that only allows the user to change a parameter range, without clearly showing what and how much is being changed. In this way, it is necessary a measurement system to have an idea of the variation of parameters made by these power sources. On the other hand, these three lasts mentioned are the ones that have a synergic functioning, where

the system adapts itself to perform a specific behavior, using the request of the user as a guide of operation.

5.3.2 Welding processes and their performances

- Standard processes

Contrary to what was expected, the waveforms of the standard processes were not always similar to each other. Since Cloos ControlWeld and Lorch SpeedArc required large variations in their voltage to achieve the weld bead geometry, the waveform normally suffered some kind of variation with respect to each of the allowed ranges. The pattern shown by Cloos was as expected after the changes. It had a 0.5 decrease on voltage factor to achieve the geometry target, with the waveform showing a strong characteristic of long low power phases. This characteristic is similar to the process of Figure 22, where the standard short circuit had a voltage increasement of 3 V. Therefore, the voltage adjustment of Cloos works in opposite direction.

Lorch SpeedArc showed a waveform that can be seen in Figure 27 which appears to be electrically controlled. The power peak presented by this process differs from the other two standard short circuits and also from the literature. It smooths the power just before the drop detachment and after, in the drop formation phase, several small power peaks. This characteristic can be related to an attempt to improve the metal transfer. Decreasing the power before the complete detachment can avoid a more aggressive power explosion in the melt pool, which generates spatter and molten metal turbulence. This kind of behavior is already used in the electrical controlled processes studied in this work, where a controlled power peak is used to generate a gentle detachment. Also, the small power peaks in the drop formation phase help the drop to flow close to the melt pool. The drop from Lorch SpeedArc is narrower and long in most part of the process, generating a more frequent detachment, as can be compared between all the standard processes in the Figure 49.

These differences and similarities between the three processes result in three different heat input results that are not within the same group. The voltage decrease used in Cloos produced a process with low drop separation frequency compared to the others. However, the waveform with few power peaks does not necessarily make this process the colder one, but probably the most unstable, due to the larger drop sizes produced by this long drop formation phase. Lorch SpeedArc, on the other hand, had the faster drop detachment frequency. However, these faster detachments also occur with small drops because the fusion rate must be the same. Therefore, the instability associated with these smaller drops did not have the same effect on the spatter

and melt pool turbulence. This is why Cloos ControlWeld proved to be more continuous, but the formation of large droplets makes its less frequent instabilities catastrophic. This can be better observed in the weld beads of the three processes, Table 4 a), d) and h), where EWM Standard and Lorch SpeedArc have the smoothest surfaces and Cloos had it more unstable and behavior changing.

Since the theoretical heat input is shown in the Table 5, The standard process that had more heat input was Cloos ControlWeld, followed by EWM Standard and then Lorch SpeedCold. The same order can be seen from the largest drop formation to the smallest. This effect is caused by the amount of power used to form larger drops. As can be seen in the Figure 25, Figure 26 and Figure 27, compared with these three processes, Cloos ControlWeld has a significantly larger drop. This relationship is related to the wire melting rate, because the higher the power, the higher the melting rate and the more voluminous the drop.

However, as can be seen in the macrographs of the Table 6, the opposite is true for the area ratio, where Cloos ControlWeld had the smallest ratio between the standard processes, followed by Lorch SpeedArc and EWM Standard. Even when using considerably more power, 8% more than EWM and 10% more than Lorch, Cloos had a ratio 10% lower than Lorch and 13% lower than EWM. EWM Standard and Lorch SpeedArc compared to each other had very similar behavior in these metrics, with 0.47 and 0.46 of area ratio, respectively.

Therefore, the relationship between area ratio and power used is directly related to the proximity of the wire to the molten pool and also to the arc density. A more powerful process has a higher wire melting rate and keeps the wire away from the molten pool until the drop is large enough to make contact on its own. The unpredictable behavior of a large volumetric drop and the lack of a tip causes the arc to scatter and reduce the substrate melt. This happens differently when the wire melting is not faster than the feed, where the wire keeps aways proximity with the melt pool. The drop formed is smaller and easily conducts the current in a more constricted area, allowing the arc to be more concentrated and also closer to the substrate.

In this line of thinking, Lorch SpeedArc should have the most penetrating process, since the smaller drops and the wire in short distance with the melt pool would allow more substrate melting. However, as shown in the Figure 26 and Figure 27, the wire in the Lorch process is much higher. This is due to the small peaks that it has in the drop formation phase, where the drop is smaller, although elongated, which allows the wire tip to remain high and also have high frequency detachments.

- Power controlled processes

The electrical controlled process variations of the brands tested are Lincoln STT, EWM ColdArc and Lorch SpeedCold. All of them use the standard short-circuit process as a base, however with some electrical improvements. These processes only use power control to develop a weld with less heat input.

Lincoln STT proved to be the most stable of the three. The drop size of Lincoln STT is one of the main characteristics that allows it to be the most stable among them. The detachment becomes predictable and constant as shown by the attachments Figure 46, where this repeatable behavior is clearly seen. This process is followed by EWM ColdArc and Lorch SpeedCold in terms of process stability. EWM ColdArc has a considerably larger drop than Lincoln, which can be compared between Figure 28 e) and Figure 29 e). However, the power peak generated by EWM ColdArc proved to be very precise and almost invisible in the high-speed videos, as shown in Figure 29 b). This power control does not allow the arc to explode after the detachment, so the large drop size is not a problem. Nevertheless, the melting rate used in EWM ColdArc was not as precise and did not synchronize perfectly with the wire feed speed. This resulted in the drop and melt making contact earlier than they should in the arc reopening. This lead to power peaks at moments when the drop cannot be smoothly scoured, which generates metal expulsion. Finally, Lorch SpeedCold was the most unstable process and the only one limited to a 1 mm diameter wire. The geometry required more power than usual for a 1 mm wire weld, therefore the melting rate of the wire is higher than the process can maintain itself stable. The melting rate has to be the same as the process with 1.2 mm wire, so the behavior seen in Figure 30 of sequences of droplet detachment that make the process unstable is inevitable for Lorch SpeedCold.

Some similarities can be observed between these three processes cited. The two considered here as the most stable ones, Lincoln STT and EWM ColdArc, have the peak time for arc reopen longer, Figure 28 d) and Figure 29 c). It gives more time for drop formation, smoothly decreasing the power after, Figure 28 e) and Figure 29 e). Also, the first power peak for drop detachment has its increasing slower, presenting an inclined line in the detachment point and an instantaneous decrease after de detach, Figure 28 b) and Figure 29 b). Lorch, in other hand, presented the opposite in the same points, having an instantaneous peak to maximum power for drop detachment and a slower decrease after, Figure 30 c) and f) and Figure 31 b). In the drop formation phase, the power is increased slower in a parabolic curve and decreased immediately after, Figure 30 d) and e) and Figure 31 d) and e). These differences can be better observed in Figure 49 where the processes are directly compared.

The power and heat input of each process followed the same order of performance, with Lincoln STT as the lowest heat input process, followed by EWM ColdArc and Lorch SpeedCold. In the electrical measurements of Figure 28, Figure 29 and Figure 30 from Lincoln STT, EWM ColdArc and Lorch SpeedCold, respectively, shows that the key characteristics of each wave are very different. Lincoln STT and Lorch SpeedCold have the larger currents in the drop detachment power peak of around 300 A, with EWM ColdArc placing close to 260 A. The arc reopening power peak is stronger for Lorch with 360 A in the first peak and 340 A in the second, followed by Lincoln STT with 350 A and EWM ColdArc with the weaker peak of 260 A. The lowest current is shown by Lorch SpeedCold with 50 A before the short circuit, with a long low power phase. It is followed by the Lincoln STT process, where the lowest current occurs near the short circuit phase with 75 A, also with a long low power time. In the interval between the first and second power peaks, the Lincoln STT current drops to 40 A. EWM ColdArc has the higher low current among these three, with 100 A in a short time after the second power peak, and it rises immediately afterwards.

Even though EWM ColdArc uses less power in the power peaks, this does not make the process colder. In fact, the use of 1 mm wire and the lowest power phase did not prevent Lorch from being the hottest process. In the Figure 49 on attachments, The waves are compared directly. In this comparison it can be seen that EWM ColdArc takes more time with the power peaks open than the other two processes, decreasing this power more slowly and never going below 100 A. Lorch SpeedCold in other hand ends up by using more power in the power peaks sequences. The amount of power peaks used turn the heat input of Lorch SpeedCold process into the biggest, although it uses only nearly 2% more power than EWM ColdArc. Lincoln STT uses high power peaks, but it maintains them for a very short time, the shorter between these three. Therefore, the amount of fluid power used by Lincoln is significantly less.

The macrographs reflect these process characteristics. The penetration of Lincoln STT is significantly less than the others, 30% less than Lorch SpeedCold and 38% less than EWM ColdArc. In fact, the penetration was concentrated in the center of the weld bead, with a more rounded bead. This can be related to the size of the drop and the behavior of the arc. The Lincoln arc remains at high power for a short time and this arc is concentrated just below the drop, Figure 28 d). After this the arc has a low power that can not increase the substrate melting area, Figure 28 e). EWM ColdArc and Lorch SpeedCold showed similar penetration and different arc behavior than Lincoln STT. EWM arc in reopening phase was concentrated enough to be close to Lincoln behavior, Figure 29 c). However, the drop grown phase of EWM either

generate a big drop and use higher power. The result is a very open arc as showed in Figure 30 d), which, unlike Lincoln, uses high power of around 140 A. Lorch SpeedCold, on the other hand, had a very open arc in all moments, as shown in the reopening phase in Figure 30 d), which promotes a large area melted.

- Retractable wire feed processes

Fronius CMT and OTC Synchrofeed both use the retractable wire feed to develop the short circuit process. In this type of process, the metal transfer is not mainly made by increasing the power, but by pulling the wire from the melt pool, transferring the drop by surface tension. However, there are some characteristics that distinguish one process from another, such as the frequency of drop detachment and the way to use the arc power.

OTC in these points showed a better control of the parameters, with a process more mechanical than dynamic, with very low variations of behavior between each detachment, what could be seen in the high-speed video and electrical measurement, Figure 32. In the Figure 47 on attachments can be observed that the behavior of the arc and the retractable wire process have the same characteristics throughout the process. Fronius CMT and CMT Synchropulse showed the opposite behavior to OTC, less mechanical and more dynamic. The relationship between arc time and metal transfer time is more random, as shown in Figure 33 and on the attachments the Figure 48. This is due to the parameters variation imposed, what influence the pull phase when the separation between the drop and the wire occurs. The drop separation acquires an unpredictable behavior generated by the melt pool turbulence and the wire adaptative push.

As the processes power controlled, these three also have the same working behavior with their own characteristics. In this point, CMT Synchropulse will not be considered due to its process actually be a normal CMT with current oscillation. The remaining characteristics are still the same. OTC had the most continuous points as the first and second power peaks, low current phase and short circuit current. All of them had the same behavior throughout the process. In the first power peak to drop detachment, it was used 210 A as maximum of an increasing parabolic line, Figure 32 a). Fronius did not show this breakaway peak, with most of the drops being scored only by surface tension. The second power peak to reopen the arc used by OTC was 250A, Figure 32 c). This peak is characterized for not maintaining the power still, the maximum is basically a point, decreasing it right after the peak to 200 A. This one decreases again slowly and parabolically until 175 A, Figure 32 d). Fronius uses only one power state in the second power peak, with the peak constantly reaching 300 A and maintaining this power until the wire is pushed, Figure 33 c). In the short circuit phase, these two processes have the

wire push time, where the arc power is reduced to immerse the wire in the molten pool. In this phase, OTC controlled the current to stay in 100 A continuously, Figure 32 f), while Fronius presented two different currents, sometimes giving 50 A and others a 100 A, Figure 33 c) and i).

As with EWM ColdArc, the process with shorter peaks is not necessarily the colder process. Fronius CMT and CMT Synchropulse both used less power than OTC Synchrofeed by 2.5% and 1% respectively, which is not a significant difference. OTC had the shorter peaks and also the lowest average current of all eleven processes. However, the use of a long low current phase and the power given in the push process resulted in a higher power requirement than the Fronius process. Nevertheless, Fronius had a significantly higher average current, 20% higher for both CMT and CMT Synchropulse. However, the average voltage developed by Fronius was 4 volts lower. This is caused by the difference of interval that the arc is maintained open. In the graphics of both processes is visible that the voltage of Fronius CMT spend more time near to zero, this due to the CMT process spend more time dived in the melt pool than with the arc open. OTC Synchrofeed has the opposite behavior, spending most part of the time with the arc open and with the voltage high. Therefore, in the calculation of power, these three processes are the best in opposite parameters and end up by developing a lowest power welds.

The weld bead formed by these three processes were the best ones in the metrics, proving the efficacy of the retractable wire method also practically. The penetration area was concentrated in the center of the weld bead for all of them. The retractable wire acted to use the power to melt mainly the wire, not the substrate. With the help of the pull phase, the power peak to drop scouring does not need to be as aggressive and may even not be used, as Fronius demonstrated. OTC used the fast peak time to reduce the arc power over the substrate and Fronius removed the detachment power peak of the process, which resulted in the same. The more rounded weld bead was shown by OTC, followed by Fronius CMT and CMT Synchropulse as the most wet.

- Root welding processes

The root welding category is a process that focuses on low heat input, high deposition rate, and great ability to feel gaps, normally used to make the first weld in a multi-pass process. Although it is not considered a low heat input category, its behavior is quite similar to one. They showed the same characteristics as Lincoln STT, EWM ColdArc and Lorch SpeedCold previously cited, as can be seen in Figure 31. SpeedRoot's waveform can be easily compared to that of the

electrical controlled processes. However, the electrical control of SpeedRoot proved to be not as precise as Lincoln STT and EWM ColdArc.

The same does not happen with EWM RootArc. Its behavior showed in the Figure 35 is very unique. It figured between the processes with better area ratio relationship, although it was also the process with higher heat input by far, 10% higher than the second, Cloos ControlWeld. Therefore, the EWM RootArc results show that the analysis must be approached carefully. The peculiarities of these processes can generate a big change and influence on the metrics taken. In this case, as shown in the Figure 35, the workflow of EWM RootArc has some high power points that can reach almost 600 A, what increases the average current and then the power. These pointless moments can generate bad characteristics for the weld bead, as different penetration throughout the weld, material expulsion and heterogeneous surface.

The main difference between these two processes is the time interval in the low power phase. Lorch SpeedCold showed a first power peak of 310 A, followed by a second power peak of 340 A and a low power phase of 100 A, Figure 31 b), d) and f), consecutively. EWM RootArc, on the other hand, showed colder phases with 200 A in the first peak, 225 A in the second and in the low current phase it used 150 A as a minimum, Figure 35 b) and c). However, the transition of the arc re-open power peak to the low current from EWM is a slowly and parabolic change, maintaining the current high.

5.4 Partial discussion

Between the eleven processes tested, the three that performed better on the set of metrics were Fronius CMT Synchropulse, Fronius CMT, and OTC Synchrofeed, in this order. The three that used retractable wire technology. The electrical controlled processes did not produce the expected results, with the exception of Lincoln STT, which was able to achieve the same level of performance as Fronius and OTC. EWM ColdArc and Lorch SpeedCold had a performance not far from the standard GMAW short circuit, presenting even worst results by the metrics chosen. The root welding processes, EWM RootArc and Lorch SpeedRoot, showed opposite results, with EWM having by far the biggest heat input weld but one of the lowest penetration areas, while Lorch showed a controlled heat input weld with higher penetration.

Based on these tests, the three processes selected for the development of additive manufacturing were Fronius CMT, OTC Synchrofeed and EWM ColdArc. The process of selection had the goal of observing the difference in heat input that two of the best performed processes apply to the same process. Also, to compare this difference between a process that uses the retractable wire technique and a process that uses only power control. Fronius had

two of the best processes based on the metric, however analyzing different power sources using the same technique with different characteristics can give a better idea of what differences make one process better than another. Fronius CMT was chosen over CMT Synchropulse to have a direct comparison with OTC Synchrofeed. Also because of CMT's relevance in the market, being one of the most cited processes in relation to additive manufacturing. EWM ColdArc was chosen for its not good results, being able to show the effect of a high heat input process in the same environment as the low ones.

5.5 Additive manufacturing

The walls made from this three processes are showed in Table 8, with front, side and top view. All walls are approximately 60 mm high, measured along the centerline, and 100 mm long.

Table 8. Walls made by additive manufacture using different power sources.

Process variation	Front	Side	Top
EWM ColdArc			
Fronius CMT		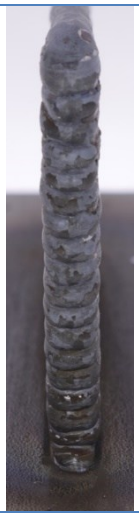	

The parameters used in the AM processes were those defined in Table 3. Between them, EWM ColdArc took more layers to finish the process with 37, which implicate in more material used. This figure also shows that the EWM process was the one that suffered more from surface distortion. It has no divisions visible between layers due to deformation. EWM ColdArc presented also the biggest presence of silicate solidification. There are three main reasons for silicate formation in the GMAW process: the voltage used, the oxidation potential of the shielding gas and the alloying elements in the wire [30]. Fronius CMT took the least number of layers to build the wall, with 34 layers. It has some variations in the path of the layers. In some points it is not possible to distinguish one layer from another. CMT developed a mean voltage of 19.66 V during the AM process, what on practical did not put this process far from the others. However, the average current of Fronius was 155 A building the wall, what generate a different current range between the processes. OTC Synchrofeed needed 36 layers to build the wall. In fact, OTC has the most visible layer division, being possible to indicate a specific layer in the wall that is very defined.

5.6 Thermal camera

A thermal camera was used during the welding process to build the walls. The graph of the temperature for each area in the wall was generated for each wall and is shown in Figure 37 for EWM ColdArc, Figure 38 for Fronius CMT and Figure 39 for OTC Synchrofeed. The camera's precision range is set between 150°C and 900°C, so the values outside this range were not considered.

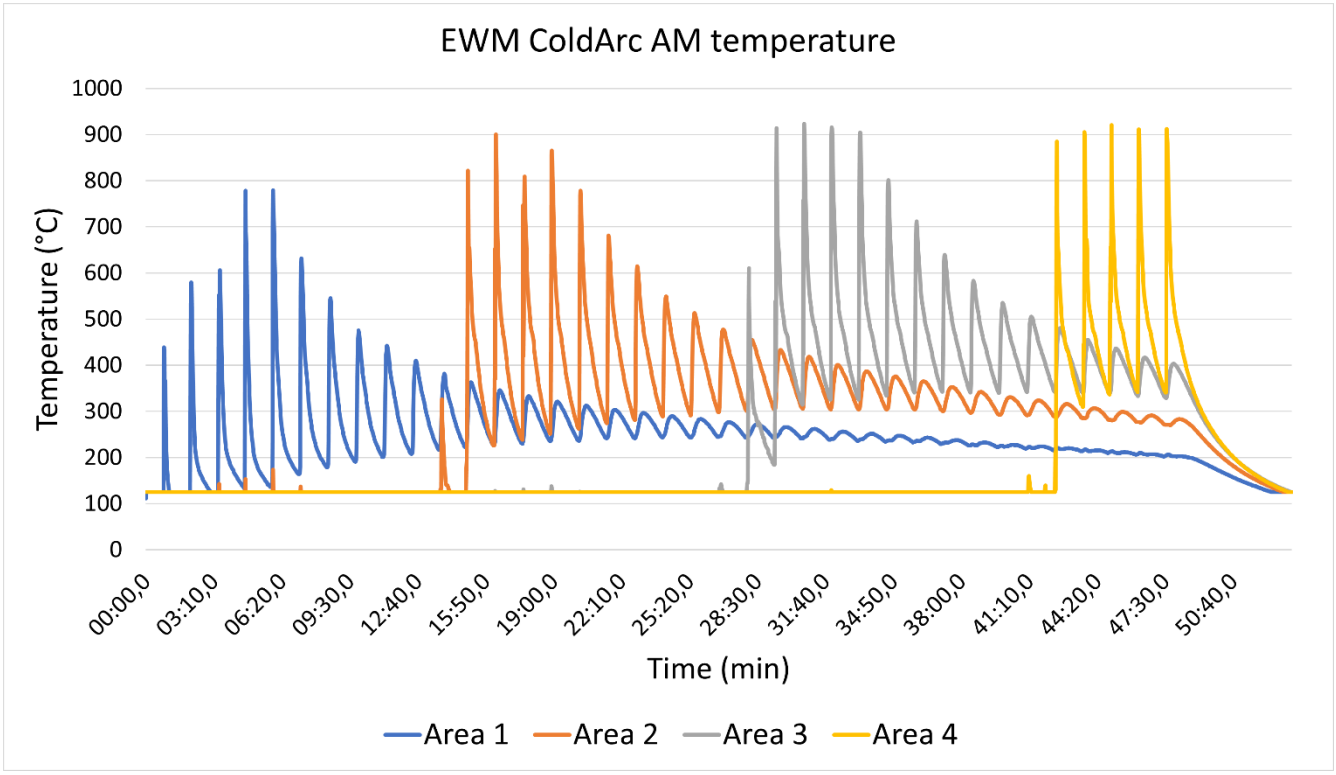

Figure 37. Temperature measured in Area 1, 2, 3 and 4 throughout the construction of the wall made by EWM ColdArc.

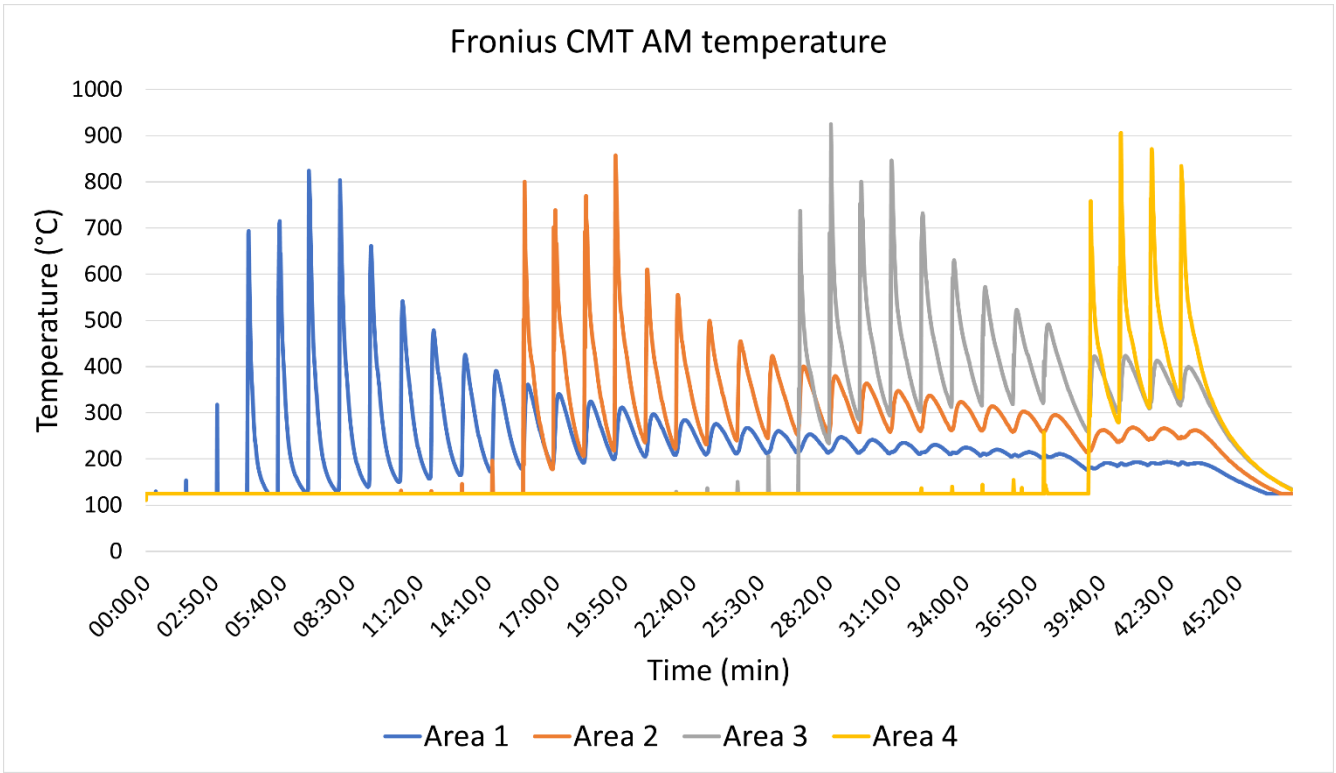

Figure 38. Temperature measured in Area 1, 2, 3 and 4 throughout the construction of the wall made by Fronius CMT.

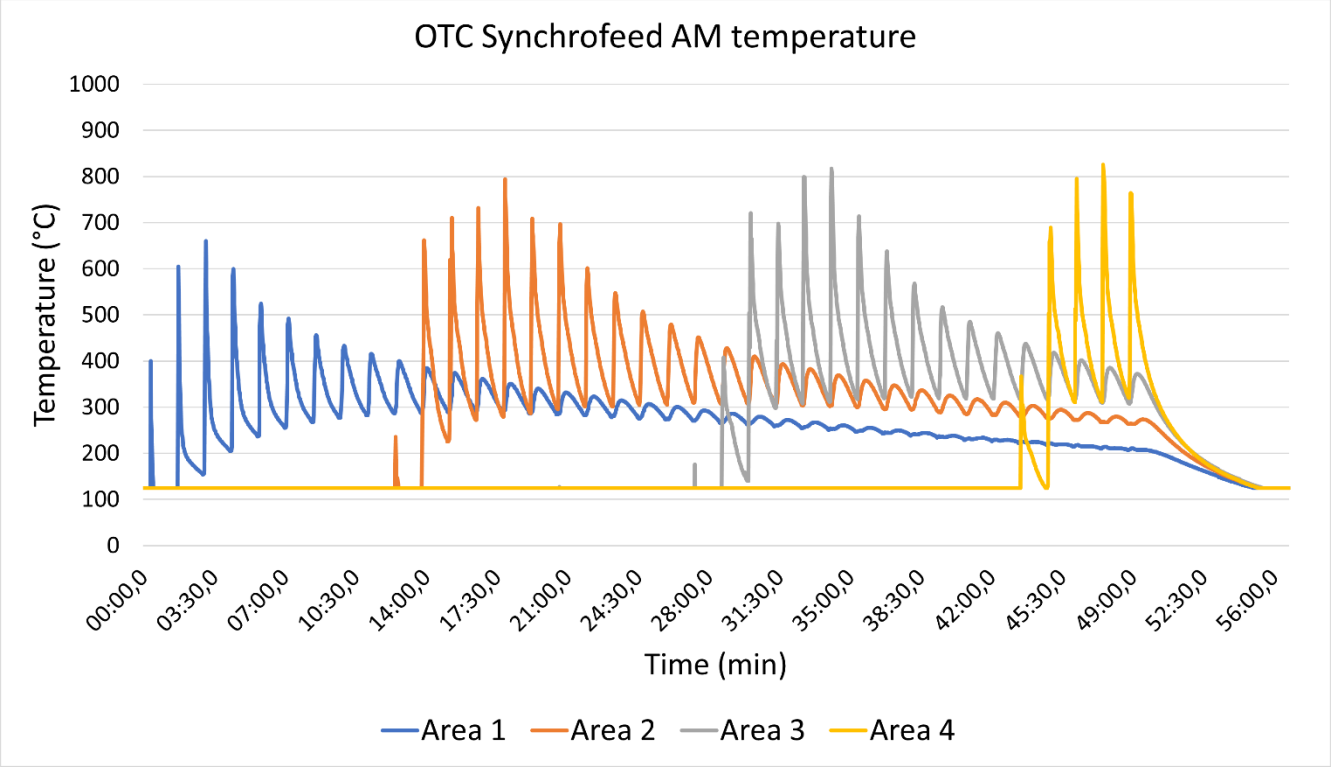

Figure 39. Temperature measured in Area 1, 2, 3 and 4 throughout the construction of the wall made by OTC Synchrofeed.

As shown in the figures and as expected, the three processes had different characteristics. EWM ColdArc proved to be the hotter process in the AM procedure, as it was in the first layer tests. This process was the only one to reach at least 900°C in three different areas, the 2°, 3° and 4°. Fronius went close to 900°C several times, reaching this temperature in the 3° and 4° areas. However, it remained around 800°C for most of the process in the areas analyzed. OTC maintained itself around 700°C throughout the process, reaching a temperature peak of 800°C in the 2°, 3° and 4° areas.

The direct comparison between the temperature in each area was made to analyze the maximum temperature in each process and also the decrease in temperature over time. The graphs comparing the temperature of each measurement area from each process are shown in the Figure 40, Figure 41, Figure 42 and Figure 43, regarding to the measurement areas 1, 2, 3 and 4, respectively.

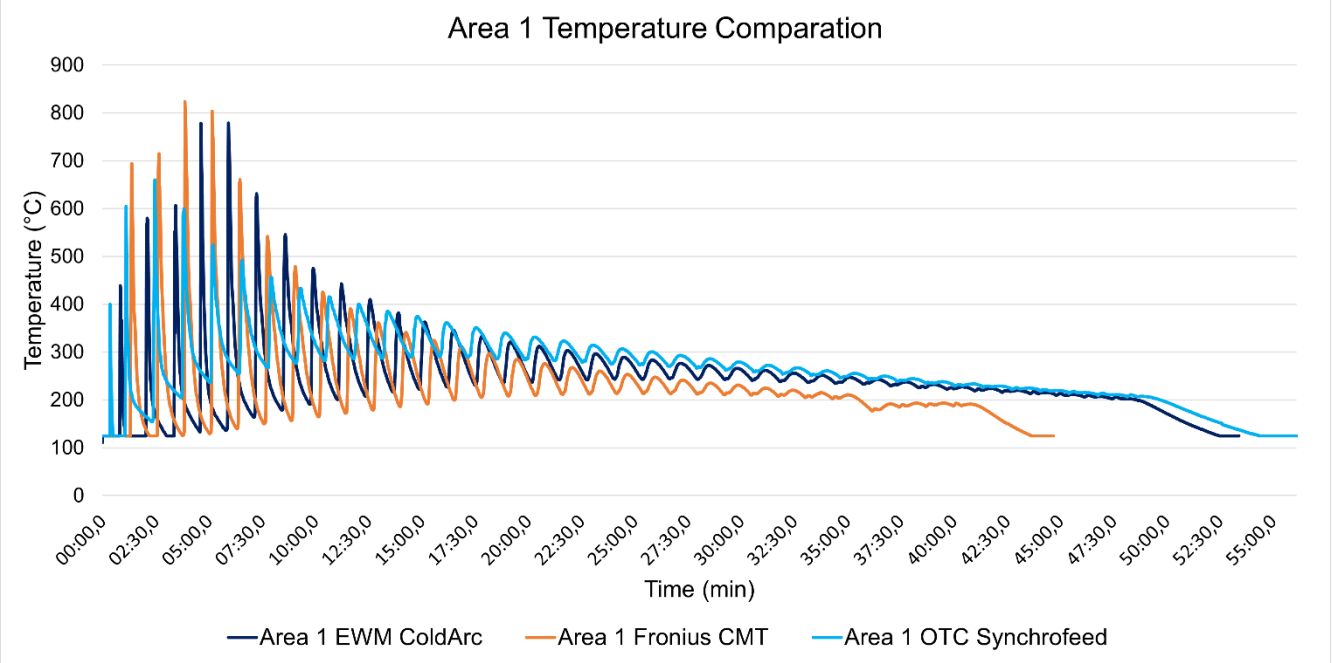

Figure 40. Comparation between the temperature behaviour in the measurement area 1.

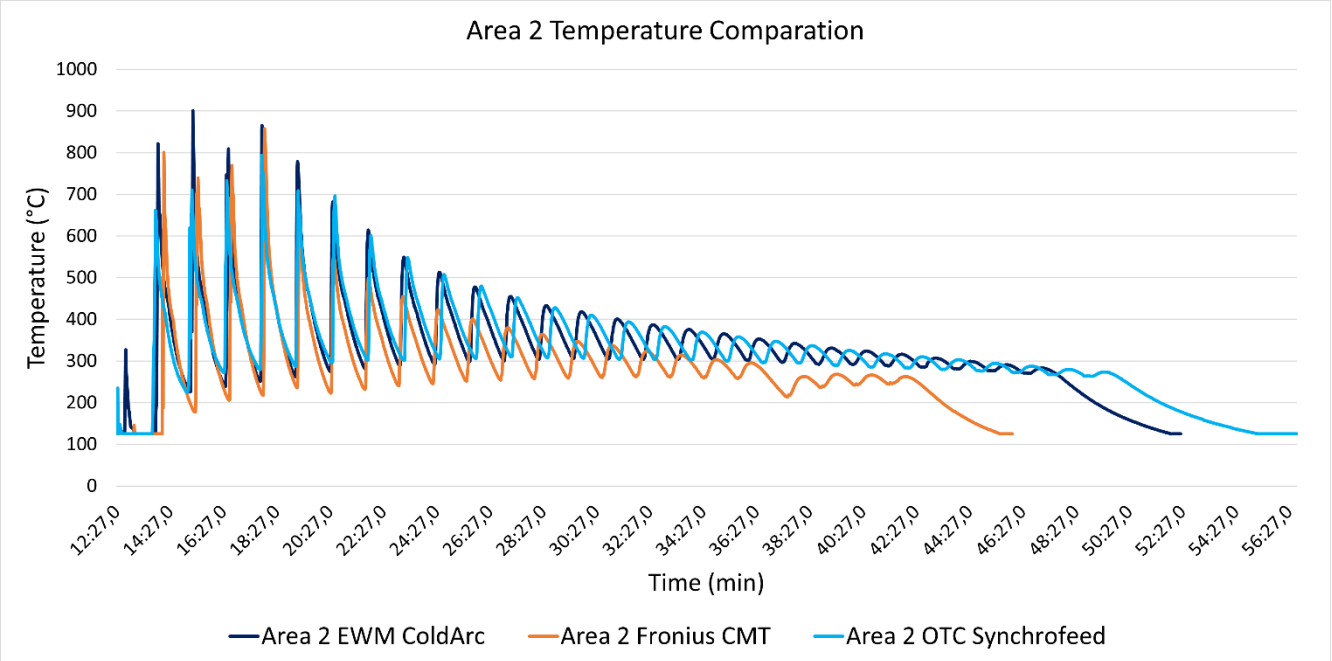

Figure 41. Comparation between the temperature behaviour in the measurement area 2.

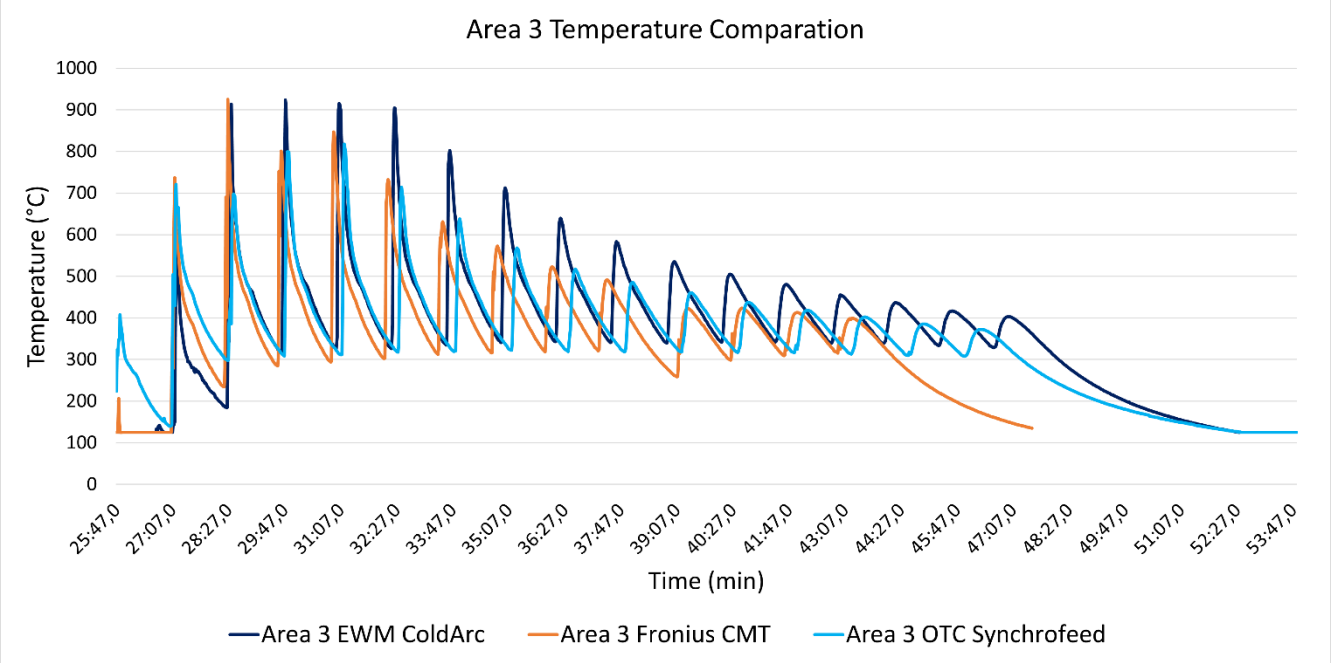

Figure 42. Comparation between the temperature behaviour in the measurement area 3.

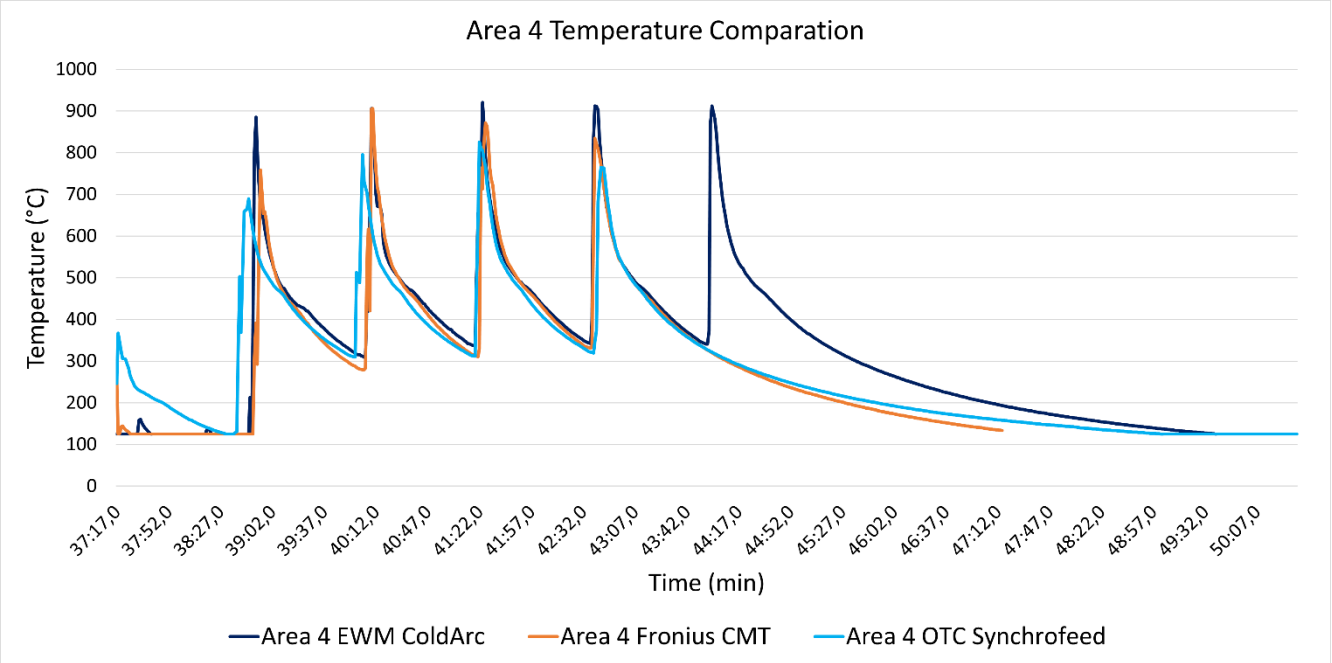

Figure 43. Comparation between the temperature behaviour in the measurement area 4.

It can be seen from these four figures that OTC Synchrofeed was the process that had the coldest temperature peaks throughout the wall building and the temperature difference measured in the areas for each process was quite large. In Table 9 shows the maximum temperatures reached by the process in each zone. In all the measurements, OTC had a

temperature 10% lower than the maximum, except in the 1º area where the difference was almost 20%. In the 4° area OTC stands out by being the colder process with at least 50°C difference from the second coldest. EWM and Fronius alternate in the hottest process, with Fronius being the hottest in the 1° area and EWM in the 2° area. Both showed a 5% difference. In the 3° and 4° area, EWM and Fronius reached the maximum temperature of 900°C measured, with EWM reaching this temperature almost in all depositions, 9 times considering both areas, and Fronius 2 times.

Table 9. Maximum temperature reached in each measurement area for each process in the AM process.

	Process maximum temperature (°C)		
	EWM ColdArc	**Fronius CMT**	**OTC Synchrofeed**
Area 1	779,0	823,8	660,1
Area 2	900,7[2]	857,6	793,8
Area 3	923,4[3]	925[3]	817,5
Area 4	920,4[3]	905,9[3]	825,5

However, as can be seen in the temperature comparison for each area, OTC and EWM had a similar temperature decrease. Nevertheless, the temperature amplitude in the decrease process of OTC was smaller than the others, as shown in the Figure 40. It can be seen that the amplitude between maximum and minimum temperature by deposition is almost half of the amplitude shown by the other two processes. Fronius had the decrease early due to its wall had a smaller number of layers and the process had the finish earlier. Indeed, Fronius had the coldest minimum temperatures in the 1° and 2° ranges. In the 4° range, the minimum temperature per layer was almost the same for all processes and was consistently close to 300°C.

5.7 Macrostructure, microstructure and hardness

In the Figure 44 is presented the macrographs of the three walls bilt, where it is easyer to observate the geometry characteristics of them.

[2] Exceeded the measurement range of 900°C.

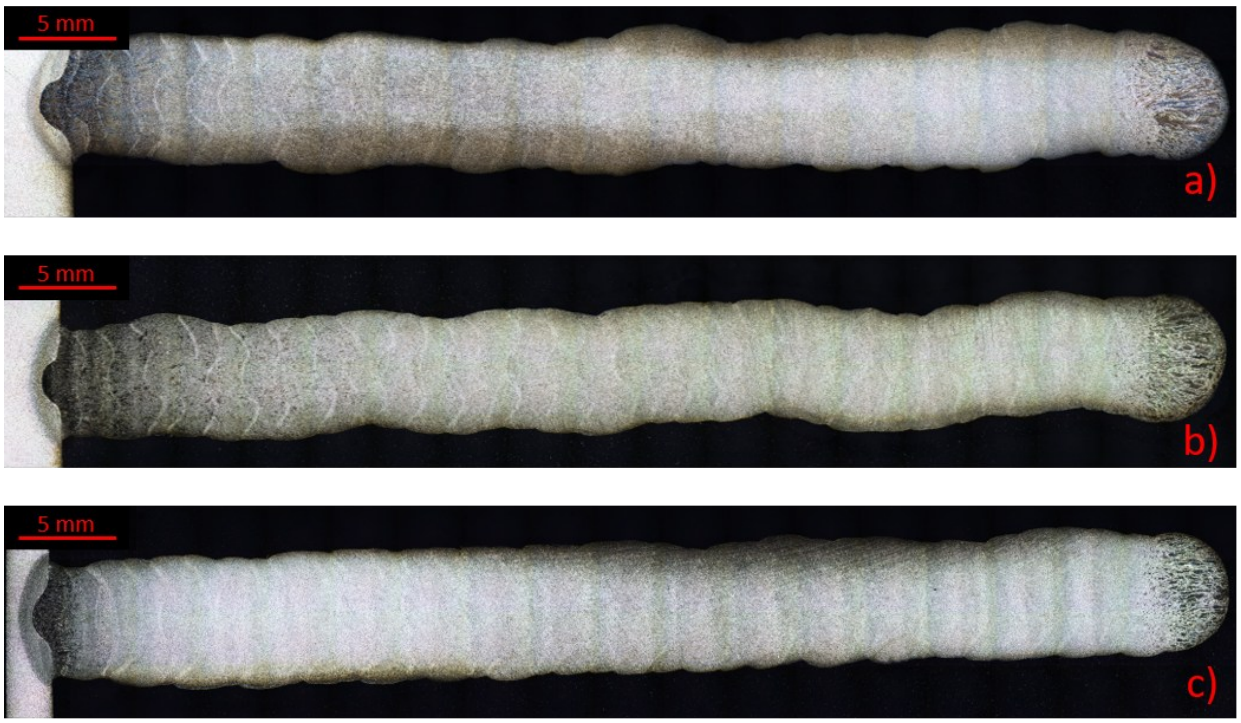

Figure 44. Macrography of the wall built by a) EWM ColdArc; b) Fronius CMT; c) OTC Synchrofeed.

OTC end up by having a bigger height than the others, what is possible to notice in the Figure 44 c). The height of the three walls was 59.2 mm for EWM, 59.7 mm for Fronius, and 60.2 mm for OTC. From this, it is possible to approximate the average layer height based on the number of layers of each wall. Thus, Fronius had the highest average layer height at 1.76 mm per layer, followed by OTC at 1.67 mm and EWM at 1.60 mm. A difference of about 1 mm between the processes.

It is possible to notice that Fronius CMT has the greatest variation in wall growth, changing directions several times. However, the thickness of the whole wall does not have big changes. These changes happen with EWM, Figure 44 a), where the wall has a straight growing, but not straight surface, with material accumulating randomly on the sides. Finally, OTC didn't have either problem. The growth of its wall was straight and consistent in all layers.

The hardness test was carried out on the samples to observe the differences caused by each process in the mechanical behavior for the same material. In the Figure 45 is presented the hardness profile of each wall.

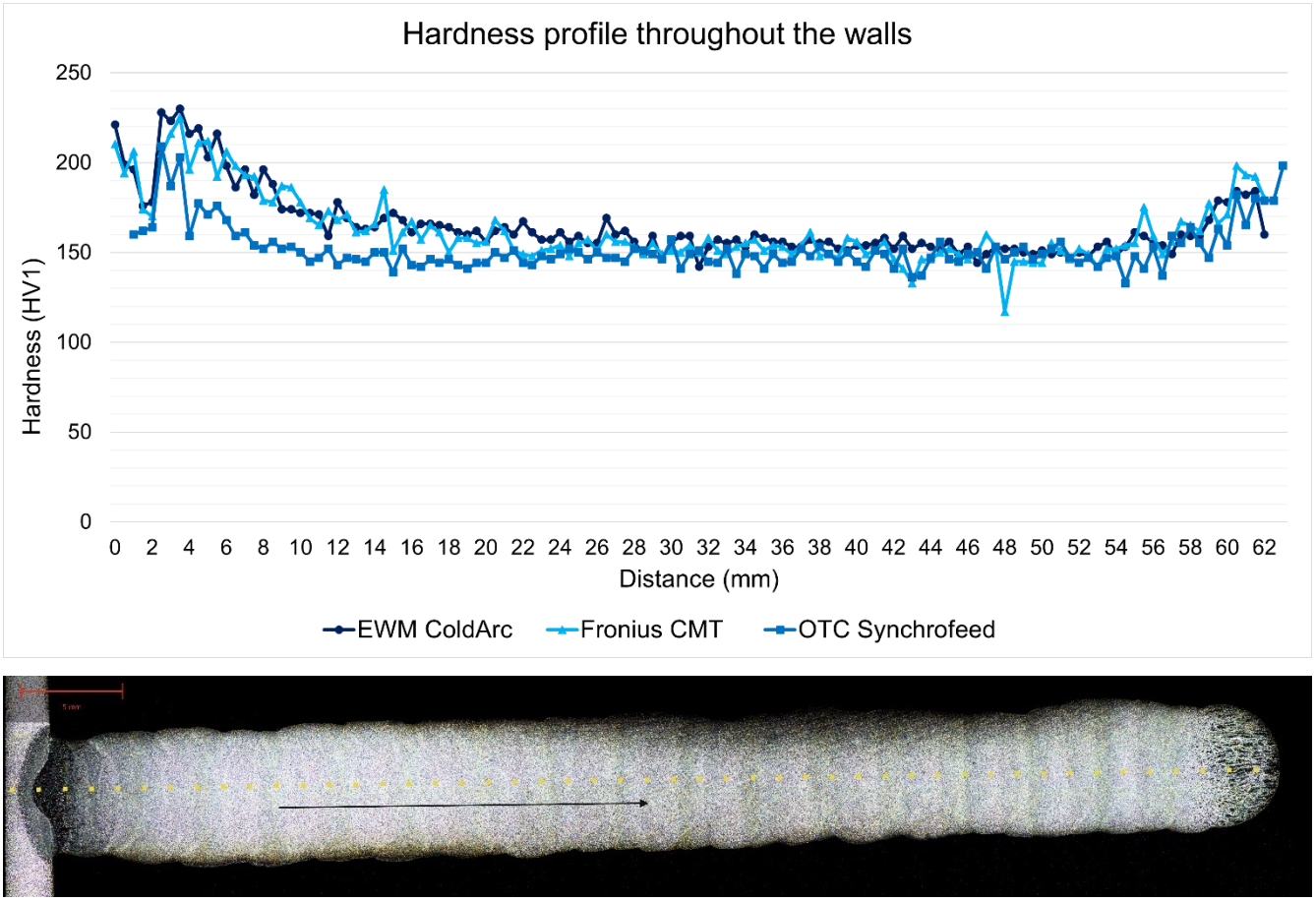

Figure 45. Hardness test of the three walls made by different processes.

The thermally affected zone is located between 2.5 and 3.4 mm, characterized by the hardness peak in the graph. As can be seen in Figure 45, the hardness profile did not show much difference between the processes in the middle and final areas of the walls. However, OTC showed a rapid hardness decrease in the first layers, placing around 30 HV less than the other two between 4 and 12 mm, with its hardness stabilization happening in 6 mm of the wall (10 mm, Figure 45). Fronius had its hardness stabilizing slowly happening in 18 mm of wall (21,5 mm, Figure 45) and EWM in 25,5 mm (29 mm, Figure 45). The average hardness in the wall body is 165 HV, 163 HV and 152 HV for EWM, Fronius and OTC respectively, which represents a difference of 8% between the extremes. As a basis for comparison, the last layers follow the same behavior for each process, except for the last point of each, which shows a hardness of 160 HV, 180 HV and 198 HV for EWM, Fronius and OTC, respectively. The successive increase of almost 20 HV represents a difference of 19% and 9% in the hardness. Both processes using retractable wire feed achieve close to 200 HV in the last four points.

The micrographs of the key points of the walls were made to help analyze these punctual differences for different heat inputs. The micrographs were taken in the thermally affected zone

(TAZ), the first layer, the middle of the wall body and the last layer for each process and they are shown in Table 10.

Table 10. Macrography of first, middle and top layer of each wall made by different processes.

	EWM ColdArc	Fronius CMT	OTC Synchrofeed
TAZ		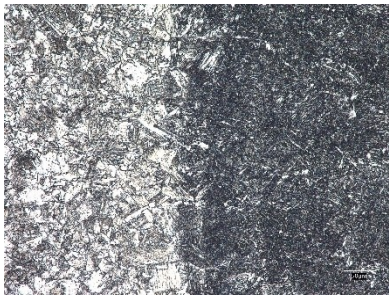	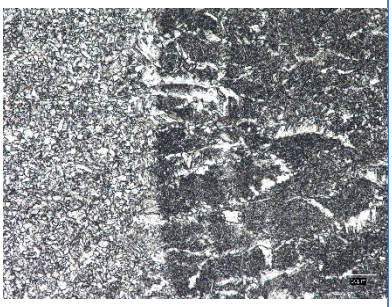
First layer		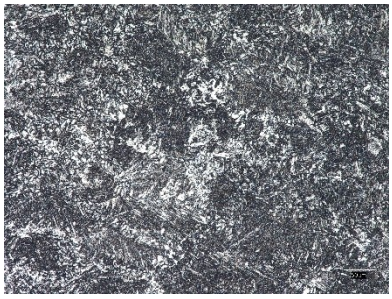	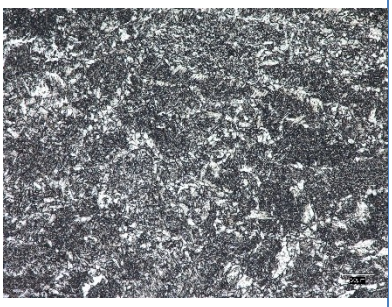
Middle layer			
Last layer	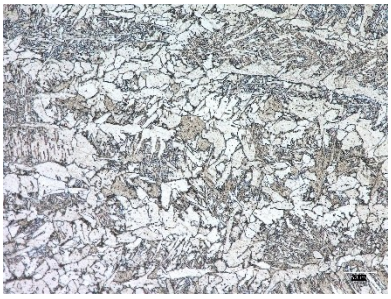	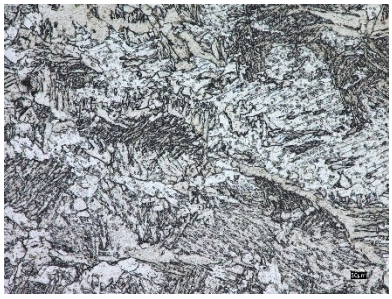	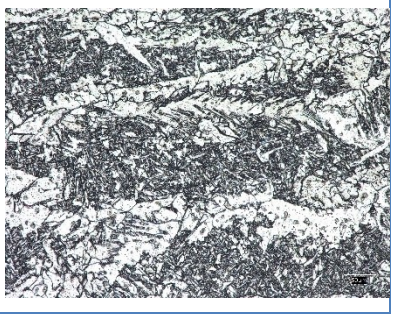

It can be seen that the grains presented by the EWM macrographs are coarser with well defined edges for the middle layer macrograph. In the last layer there are already large areas of lamellar grain formation. The size of the grains produced by the Fronius CMT and OTC Synchrofeed processes were similar in all macrographs, with slightly more advanced grain formation in the

OTC first layer. However, the presence of porosity was more noticeable in the wall produced by Fronius in all macrographs, being the process that presented less porosity the ColdArc, from EWM. The last layer had a lamellar structure formation for all the processes. In the thermally affected zone, OTC presented the smaller grains and Fronius the largest, but in the area just after the fusion line in the first layer, Fronius has the smaller grain formation, almost no noticeable, followed by OTC and the very advanced grain formation of EWM.

6 Discussion

6.1 Welds comparation

The results presented by the three different processes in the additive manufacturing of the walls were a reflection of the results shown in the 1st phase. Fronius CMT managed to better control the temperature of the wall, having the fastest cooling, as shown in the comparison for the area 1 in Figure 40 and also visible in the area 2, Figure 41. The result was consistent with the theoretical heat input calculation and also with the macrograph, which showed that CMT had the lowest heat input among the three processes and also the lowest power transfer to the workpiece.

OTC Synchrofeed had the lowest temperature peaks in the four different areas, although had a cooling curve similar to EWM ColdArc. The temperature reduction of the wall produced by Synchrofeed does not follow the same behavior as the other two processes. It did not reduce the wall temperature to the same level when the 2º area was reached. This behavior can be related to the wall geometry. As EWM ColdArc generated the thicker wall between the three processes. According with the thermal conduction equation, the larger is the transversal area of the body, the higher is the thermal conductivity. Therefore, in theory, the wall produced by EWM ColdArc is better at dissipating heat. This could explain why OTC Synchrofeed, a process that has less heat input, also has the same decrease in the cooling curve. The lower temperature peaks of OTC show a better heat control. However the thinner thickness does not allow the heat to decrease as fast as the wall made by EWM ColdArc. In this case, there is a balance between the amount of heat introduced and the amount of heat that the body is able to dissipate.

Can be noticed the amount of silicate formed in the walls, more precisely in the picture of the top layer. The amount of silica solidification in the walls produced by Fronius CMT and EWM ColdArc is greater than the silica in the wall produced by OTC Synchrofeed. Since the shielding gas and wire used were the same for all processes, the power control is the possible reason for this silicate formation seen. The main voltage of the processes are close to each other, but

not the current. This can be related with the melt pool grown, what allows the melt metal contact with the atmosfere. Therefore, the high current of the processes is one deduction of why OTC Synchrofeed is better at controlling silicate formation.

In fact, controlling the size of the molten metal also allows the formation of more continuous weld beads. EWM ColdArc was the process that suffered most from dilution and wall deformation. This because it was the process that had the hottest melt pool. In the electrical measurement throughout the AM process, Fronius CMT still had a higher current than OTC Synchrofeed, but significantly lower than EWM ColdArc. This can be related to the more continuous thickness produced by the two retractable wire processes compared to EWM ColdArc.

This relation of thickness continuity and melt pool geometry control end up by affect the efficiency of the AM process. This one can be measured by the buy-to-fly ratio [31]. This represents the relationship between the mass of the part produced by AM and the mass of the part after post-processing, representing the material lost in the process. As showed in the walls, this deformations and dilutions need more post processing to give to the part the shape sought, turning all the process more expensive.

The OTC hardness showed a faster decrease in the first layers. Lower hardness is characteristic of larger grains [32]. OTC Synchrofeed maintained the lowest temperatures considerably higher than the other two processes, which could generate the grain coalecense and the reduction of hardness. However, the hardness of the three walls stabilized at the same value throughout the wall body and had the same behavior in the last layers.

The macrographs of the four different areas showed similar results among each other and also similar to those presented by the literature [10, 11]. The micrograph of the first layer showed finer grains due to the thermal shock. This was caused by the contact with the cold substrate. The middle layer showed coated grains, since this is the area that experienced a higher temperature gradient. The top layer showed lamellar formation due to the highest thermal shock in the wall [10]. The last layer does not experiment any more heating, therefore the grains have no excitation by a new temperature gradient and do not coalesce.

7 Conclusion

The results of the additive manufacturing processes confirmed the expectations and objectives of the work. Different short circuit process variations have different impacts on the heat input and thermal behavior of the part built.

The processes using the retractable wire feed technique were significantly better at controlling the peak temperatures and also the temperature decreasement. Fronius CMT, as expected from the results in the 1st phase, was the process that led to better control the temperature, had its cooling earlier and used fewer layers to produce the same wall height.

OTC Synchrofeed proved to be more suitable for the additive manufacturing process due to its arc and melt pool stability. The wall produced had straight growth and continuous thickness, with a better buy-to-fly ratio. Also, the stability of the arc and the use of lower power in the welding process allow the silicate production on the wall to be controlled.

EWM ColdArc achieved the highest temperatures of the three processes, which led to dilution of the wall. For the selected metrics, the ColdArc process could not produce a wall with the expected thickness. One option to generate the same geometry production would be to control the melt pool geometry. It could be done by giving more cooling time between layers and allow the wall to reduce more the temperature, mantaining the weld less wet. Another option would be to change the parameters throughout the wall bild to change the melt pool behavior.

The temperature difference in each wall did not have much influence in the hardness of the bodies. They maintained the same hardness curve behavior, stabilizing around 150 HV. The differences in the mechanical properties could not be observed deeply in the hardness test and micrographs. Therefore, further tests would be necessary to study the mechanical influence of heat in the bodies.

8 References

[1] I. 17296-3:2014(E), Additive manufacturing — General principles — Main characteristics and corresponding test methods, ISO, 2014.

[2] Z. Feng, Processes and mechanisms of welding residual stress distortion, Parkway, NW: Woodhead Publishing Limited and CRC Press LLC, 2005.

[3] P. Kah, Advancements in Intelligent Gas Metal Arc Welding Systems, Elsevier, 2021.

[4] K. K. a. H. Chung, „Wire melting rate of alternating current gas metal arc welding," *The International Journal of Advanced Manufacturing Technology,* Bd. 90, pp. 1253-1263, 2017.

[5] J. Norrish, Advanced Welding Processes, 2006.

[6] D. F. D. H. a. R. R. A. Joseph, „Influence of GMAW-P current waveforms onheat input and weld bead shape," *Science and Technology of Welding and Joining,* Bd. 10, Nr. 3, pp. 311-318, 2005.

[7] M. G. Y. A. J. R. a. J. P. B. Philipp Henckell, „Reduction of Energy Input in Wire Arc Additive Manufacturing (WAAM) with Gas Metal Arc Welding (GMAW)," *MDPI,* Bd. 13, 2020.

[8] G. W. a. G. Z. Dongqing Yang, „Thermal analysis for single-pass multi-layer GMAW based additive manufacturing using infrared thermography," *Journal of Materials Processing Technology,* Bd. 244, pp. 215-224, 2017.

[9] H. P. J. V. a. V. K. P. Rakesh Chaudhari, „Parametric Study and Investigations of Bead Geometries of GMAW-Based Wire–Arc Additive Manufacturing of 316L Stainless Steels," *MDPI,* Bd. 12, 2022.

[10] A. A. G. C. A. S. F. M. G. V. M. D. L. B. F. M. C. M. a. A. S. Mariacira Liberinia, „Selection of optimal process parameters for wire arc additive manufacturing," *Procedia CIRP,* Bd. 62, pp. 470-474, 2017.

[11] A. M. A. K. D. a. S. K. Vishal Kumar, „Parametric study and characterization of wire arc additive manufactured steel structures," *The International Journal of Advanced Manufacturing Technology,* Bd. 115, p. 1723–1733, 2021.

[12] R. W. M. Jr., Principlesof Welding - Processes, Physics, Chemestry and Metallurgy, Weinheim: WILEY-VCH Verlag GmbH & Co. KGaA, 1999.

[13] „What is Arc Welding – Methods and Advantages – Definition," Material Properties, [Online]. Available: https://material-properties.org/what-is-arc-welding-methods-and-advantages-definition/.

[14] S. P. a. S. K. Sahoo, „Gas metal arc welding based additive manufacturing—a review," *CIRP Journal of Manufacturing Science and Technology,* Bd. 33, pp. 398-442, 2021.

[15] J. Grill, „Weld guru," 22 08 2023. [Online]. Available: https://weldguru.com/mig-welding/. [Zugriff am 04 10 2023].

[16] D. Dzelnitzki, „ Increasing the deposition volume or the welding speed? - Advantages of heavy-duty MAG welding," *EWM Hightec Welding,* 2000.

[17] J. N. a. D. Cuiuri, „The controlled short circuit GMAW process: A tutorial," *Journal of Manufacturing Processes,* Bd. 16, pp. 86-92, 2014.

[18] S. F. Goecke, „Low Energy Arc Joining Process for Materials Sensitive to Heat," *EWM Hightec Welding GmbH,* 2005.

[19] S. J. H. E. K.-A. U. Ersoy, „Observation of Arc Start Instability and Spatter Generation in GMAW," *Welding Journal,* Bd. 87, pp. 51-56, 2008.

[20] R. S. a. J. M. P. Kah, „Advanced gas metal arc welding processes," *The International Journal of Advanced Manufacturing Technology,* Bd. 67, pp. 655-674, 2013.

[21] L. Eletric, „Surface Tension Transfer (STT) - Lincoln Eletric," Lincoln Eletric, [Online]. Available: https://www.lincolnelectric.com/assets/us/en/literature/nx220.pdf. [Zugriff am 16 10 2023].

[22] H. W. a. G. S. Gerhard Posch, „Innovative GMAW solutions for high-alloyed and nickelbase overlays," in *OPE 2013 - Kalpakkam*, Mamallapuram, India, 2013.

[23] O. D. E. GmbH, „OTC MIG/MAG Synchrofeed," OTC DAIHEN EUROPE GmbH, [Online]. Available: https://otc-daihen.com/welding/welding-process/migmag/processes/synchrofeed.html#SynchroFeed-Evolution. [Zugriff am 10 10 2023].

[24] G. D. G. G. L. G. a. W. Y. Y. Swee Leong Sing, „Standards for metal additive manufacturing: Quality and quality control procedures," *Quality Analysis of Additively Manufactured Metals,* pp. 3-24, 2023.

[25] Y. B. Elif Karayel, „Additive manufacturing method and different welding applications," *Elsevier,* Bd. 9(5), pp. 11424-11438, 2020.

[26] Q. L. Nguyen, „Tool Path Planning for Wire-Arc Additive Manufacturing Processes," Brandenburgischen Technischen Universität Cottbus–Senftenberg, 2022.

[27] T. N.-P. a. K. Dilger, „Sources and Consequences of Residual Stresses due to Welding," *Materials Science Forum,* Bde. %1 von %2783-786, pp. 2777-2785, 2014.

[28] O. L. L. V. a. A. S. Luisa Quintino, „Heat input in full penetration welds in gas metal arc welding (GMAW)," *The International Journal of Advanced Manufacturing Technology,* Bd. 68, p. 2833–2840, 2013.

[29] H. D. H. A. a. L. O. Vilarinho, „Development and assessment of calorimeters using liquid nitrogen and continuous flow (water) for heat input measurement," *Soldagem & Inspeção,* Bd. 3, Nr. 17, pp. 236-250, 2012.

[30] E. M. S. S. L. E. M. a. F. B. R. Derrien, „Silicate Island Formation in Gas Metal Arc Welding," *Welding Journal,* Nr. 100, pp. 13-26, 2021.

[31] A. S. a. K. S. Gulnaaz Rasiya, „Additive Manufacturing - A Review," *Elsevier,* Nr. 47, pp. 6896-6901, 2021.

[32] J. M. Jr., „The influence of grain size on the mechanical properties of steel," *Lawrence Berkeley National Laboratory,* 2001.

[33] V. P. Américo Scotti, Soldagem MIG/MAG: melhor entendimento, melhor desempenho, São Paulo: Artliber editora, 2008.

[34] F. L. d. S. e. Silva, „Manufatura aditia de paredes inclinadas utilizando o processo CMT advanced e alumínio como material de adição," Federal University of Santa Catarina, Florianópolis, 2019.

[35] F. R. T. L. J. d. S. D. B. d. A. R. P. R. a. A. S. Fernando Matos Scotti, „Thermal management in WAAM through the CMT Advanced process and an active cooling technique," *Journal of Manufacturing Processes,* Bd. 57, pp. 23-35, 2020.

[36] D. C. K. M. J. K. a. S. R. Hyoung Jin Park, „The arc phenomenon by the characteristic of EN ratio in AC pulse GMAW," *The International Journal of Advanced Manufacturing Technology,* Bd. 66, pp. 867-875, 2013.

[37] C. Marques, „Análise de técnicas e efeitos físicos da alimentação dinâmica do arame no processo de soldagem MIG/MAG com vistas ao desenvolvimento de um sistema flexível nacional," Federal University of Santa Catarina, Florianópolis, 2017.

[38] J. Talkington, „Variable polarity Gas Metal Arc Welding," Graduate School of The Ohio State University, 1998.

[39] „Merkle.at," Merkle GmbH, [Online]. Available: https://www.merkle.at/technologie/merkle-schweissverfahren/coldmig/. [Zugriff am 09 10 2023].

[40] A. A. S. S. J. X. Z. J. L. L. X. G. M. D. G. Karan S. Derekar, „Effect of pulsed metal inert gas (pulsed-MIG) and cold metal transfer (CMT) techniques on hydrogen dissolution in wire arc additive manufacturing (WAAM) of aluminium," *The International Journal of Advanced Manufacturing Technology,* Bd. 107, pp. 311-331, 2020.

[41] M. a. M. P. o. T.-W. 3. S. S. U. S.-C.-W. A. M. Forming Process, „Wei Wu, Jiaxiang Xue, Leilei Wang, Zhanhui Zhang, Yu Hu and Changwen Dong," *MDPI,* 2019.

9 Attachment

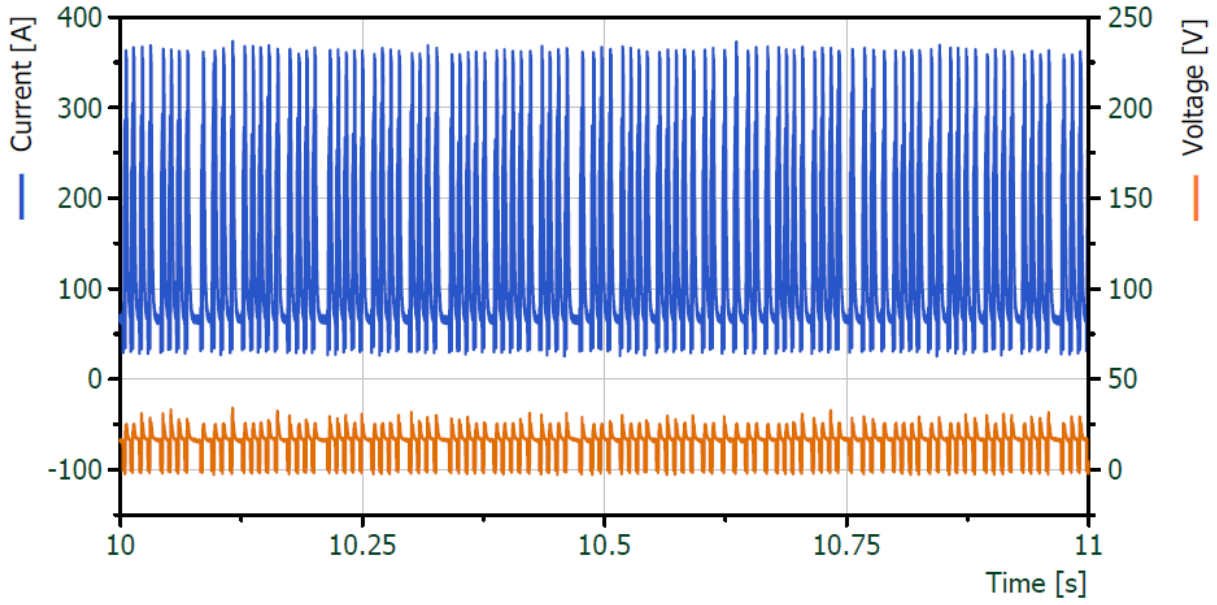

Figure 46. Lincoln STT process electrical measurement in 1 second interval.

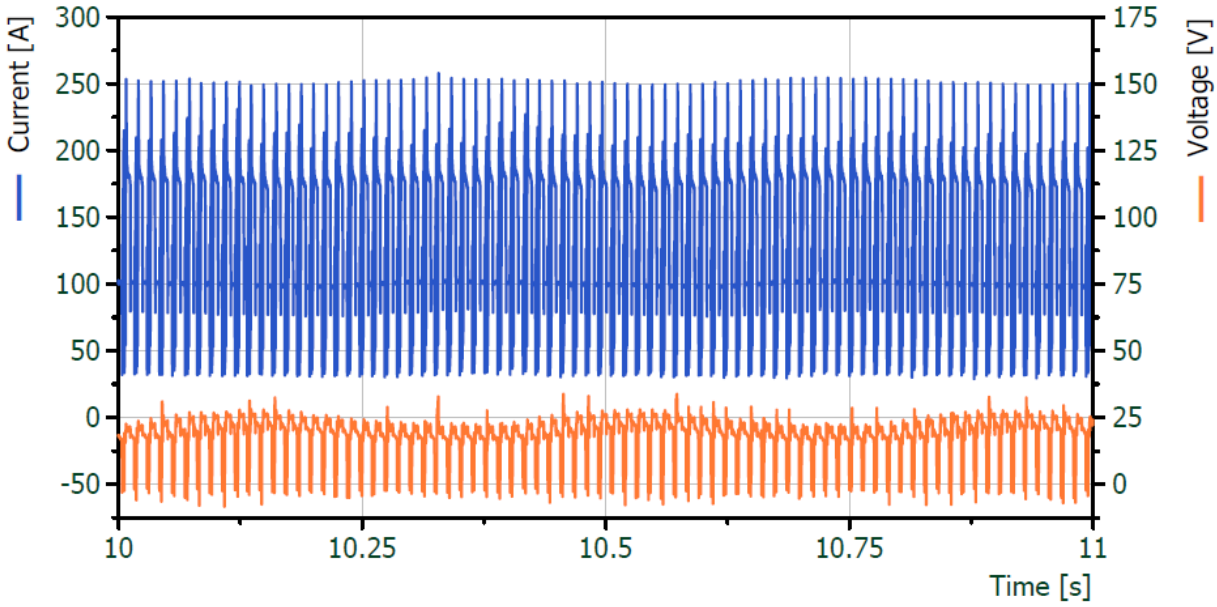

Figure 47. OTC Synchrofeed process electrical measurement in 1 second interval.

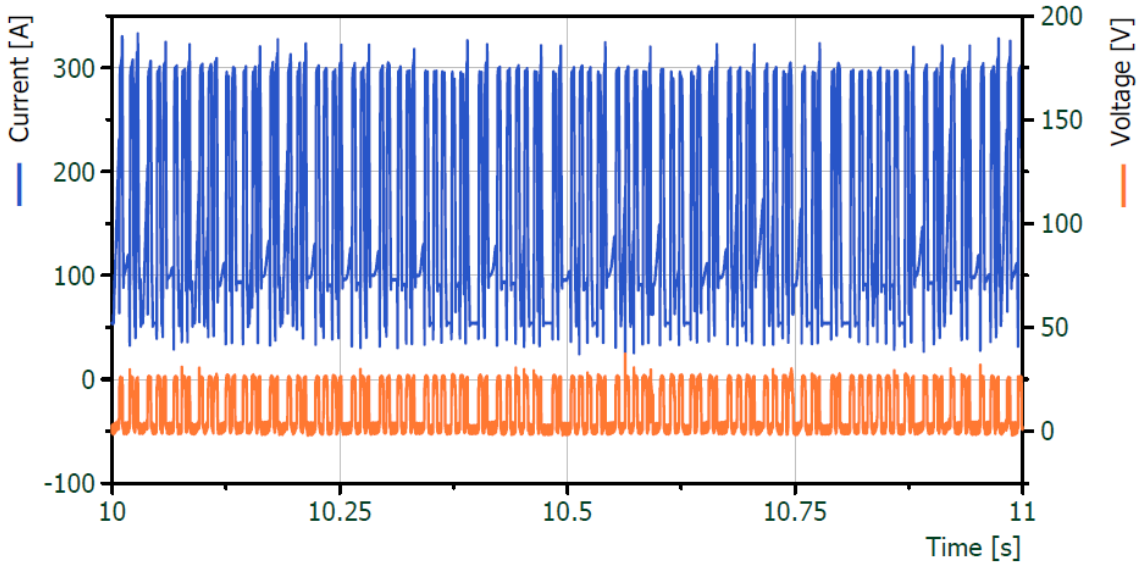

Figure 48. Fronius CMT process electrical measurement in 1 second interval.

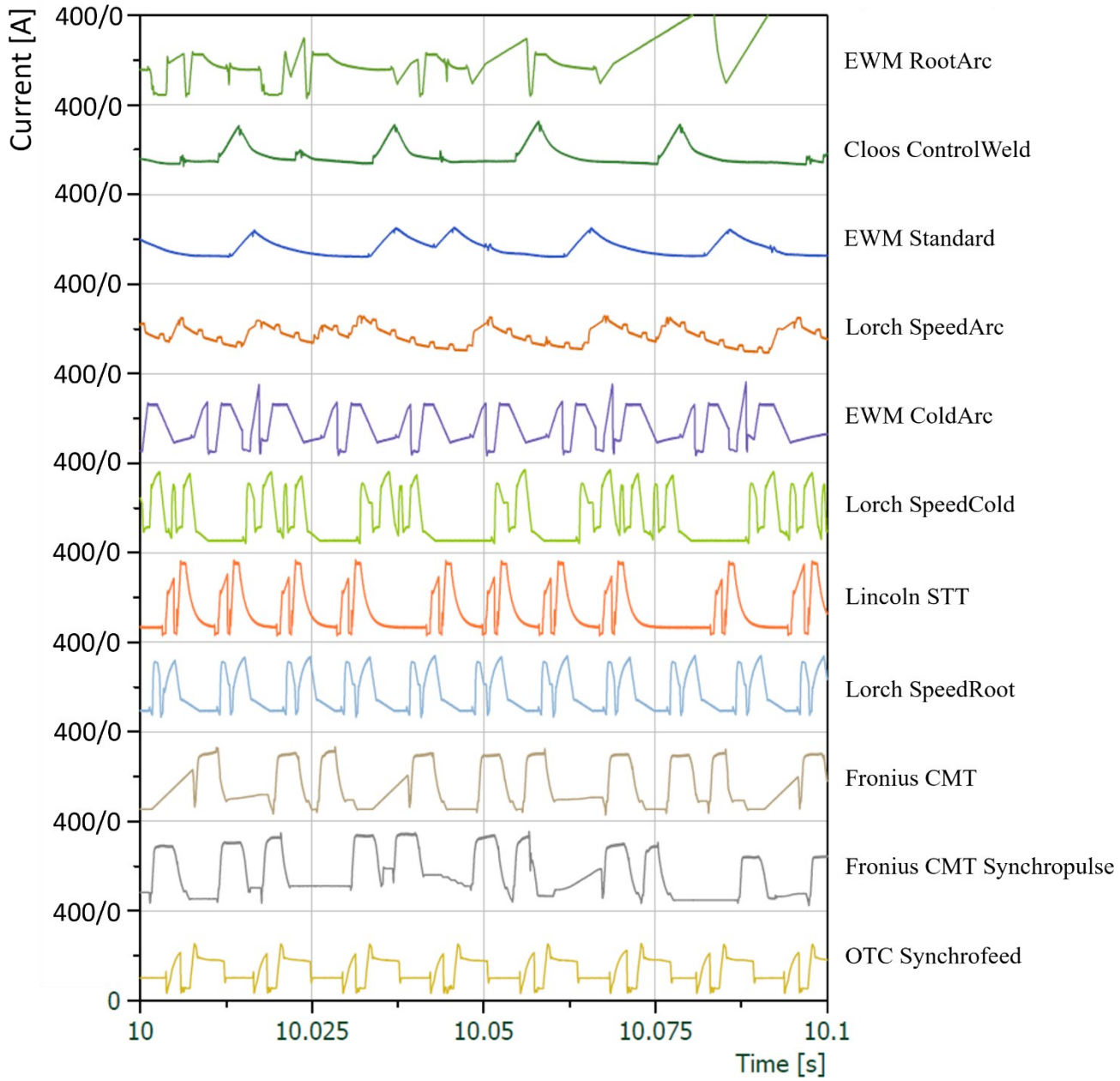

Figure 49. Comparation between electrical wave from each process from 0 to 400 A in 0,1 second.